Dissertation

HOCl-HDL-mediated Induction of HO-1 in human Endothelial Cells

submitted by

Mag.ª rer. nat. Christine Rossmann

for the Academic Degree of
Doctor of Philosophy (Ph.D.)

at the

Medical University of Graz,
Center for Molecular Medicine,
Institute of Molecular Biology and Biochemistry

under supervision of

Ao. Univ. Prof. Dr. Ernst Malle

September, 2011

Declaration

I hereby declare that this thesis is my own original work and that I have fully acknowledged by name all of those individuals and organizations that have contributed to the research for this thesis. Due acknowledgement has been made in the text to all other material used. Throughout this thesis and in all related publications I followed the guidelines of “Good Scientific Practice”.

September, 2011

Acknowledgements

My special thanks go to Prof. Ernst Malle for giving me the opportunity to carry out my thesis in his group. Thank you, Ernst, for the guidance through my PhD, for all the discussions and the continuous support during the last years.

I am thankful to the PhD Faculty and the Medical University of Graz for the financial support of my work.

I would like to thank my Thesis Committee Members, Prof. Gerald Höfler and Prof. Werner Windischhofer for their suggestions and support. Special thanks go to Werner for the constructive collaboration and lively discussions during our Lab meetings.

I am thankful to: Prof. Wolfgang Sattler for critically reading and improving my paper, Prof. Astrid Hammer for the great confocal laser-scanning microscopy, Dr. Daniela Jud for the assistance with Real-time RT-PCR, as well as Margit Rehn and Prof. Kurt Schmidt for the help with the eNOS activity assay.

I would like to show my gratitude to all members of the Institute of Molecular Biology and Biochemistry for the friendly atmosphere and their support. I am thankful to my colleagues Alenka, Anamaria, Gunther, Monika, Natascha, Kerstin, Evelyn, Karin, Ali, Chintan, Alexander, and especially Michaela and Sandra for experimental support, scientific discussions, exchange of ideas and great off-work activities.

I am grateful to my parents, to Patrick and my friends for the mental support and encouragement during all the years.

Abstract

The phagocytic enzyme myeloperoxidase (MPO) is the prime enzyme that generates hypochlorous acid (HOCl) from H_2O_2 in the presence of physiological chloride concentrations. Modification of the anti-atherogenic high-density lipoprotein (HDL) by HOCl, added as reagent or generated enzymatically by the MPO-H_2O_2-chloride-system, generates a pro-atherogenic lipoprotein particle. HOCl-HDL exhibits an impaired capacity during "reverse cholesterol transport" and represents a high uptake form for macrophages. MPO colocalizes with HOCl-modified HDL/apolipoprotein A-I in human atherosclerotic lesions and on endothelial cells lining the blood vessel. Furthermore, HOCl-HDL impairs expression and activity of vasculoprotective endothelial nitric oxide synthase (eNOS). The induction of heme oxygenase-1 (HO-1) and its products is considered a protection mechanism in endothelial cells in response to oxidative stress and endothelial dysfunction. The present study aimed at identifying the underlying pathways of HO-1 induction by HOCl-HDL in human endothelial EA.hy926 cells.

Our observations revealed that HDL modified by HOCl added as reagent or generated enzymatically, induced (i) phosphorylation of p42/44 and p38 mitogen-activated protein kinases (MAPKs), (ii) expression of transcription factor early-growth response-1 (Egr-1), and (iii) HO-1. Furthermore, HOCl-HDL treatment induced nuclear translocation of Egr-1 and enhanced Egr-1 DNA-binding activity. Inhibition of p42/44 MAPK decreased HOCl-HDL-mediated expression and nuclear translocation of Egr-1 as well as expression of HO-1. Knockdown of Egr-1 via RNA interference resulted in a decrease in Egr-1 nuclear translocation and a reduction of HO-1 on mRNA and protein level in response to HOCl-HDL. Moreover, inhibition of phosphatidyl-inositol-3-kinase decreased HOCl-HDL-induced HO-1 expression on protein level. Although HOCl-HDL caused a decrease in eNOS mRNA level, no reduction in HOCl-HDL-mediated eNOS protein expression or eNOS activity was observed. Furthermore, HOCl-HDL treatment did not cause any anti-proliferative effects, nor induced apoptosis in human endothelial cells.

The present study demonstrates that HO-1 is induced in response to HOCl-HDL via activation of p42/44 MAPK and transcription factor Egr-1 or alternatively via activation of phosphatidyl-inositol-3-kinase, thus proposing two novel rescue mechanisms in endothelial cells.

Zusammenfassung

Myeloperoxidase (MPO), ein von Phagozyten exprimiertes Protein, kann hypochlorige Säure (HOCl) aus H_2O_2 und Chloridionen bilden. Das anti-atherogene „high-density lipoprotein“ (HDL) wird durch Modifikation mit HOCl in ein pro-atherogenes Lipoprotein umgewandelt. Dieses modifizierte Lipoprotein weist eine verminderte Kapazität im „reversen Cholesterintransport“ auf und wird von Makrophagen aufgenommen. Die Modifikation von HDL durch HOCl erfolgt einerseits durch Zugabe des Reagens, oder durch den enzymatischen Weg durch die MPO. MPO ist gemeinsam mit HOCl-modifiziertem HDL und seinem Haupt-Apolipoprotein A-I in humanen atherosclerotischen Läsionen und auf Endothelzellen lokalisiert. HOCl-HDL vermindert die Expression und Aktivität der endothelialen Stickstoffmonoxid-synthase (eNOS). Die Induktion der Hämoxygenase-1 (HO-1) und ihrer Produkte wird als möglicher Schutzmechanismus in Endothelzellen angesehen, durch welchen oxidativer Stress und endotheliale Dysfunktionen kompensiert werden können. Das Ziel der vorliegenden Studie war die Aktivierung der HO-1 in HOCl-HDL-behandelten humanen Endothelzellen (EA.hy926) zu untersuchen.

Unsere Beobachtungen zeigten, dass sowohl MPO- als auch HOCl-modifiziertes HDL eine Aktivierung von p42/44 und p38 MAPKs (Mitogen-aktivierte Proteinkinasen) bewirkten und zu einer vermehrten Expression des Transkriptionsfaktors Egr-1 (early-growth response-1) und der HO-1 führten. Weiters induzierte HOCl-HDL die Translokation von Egr-1 in den Zellkern und erhöhte die Egr-1 DNA-Bindeaktivität. Die Hemmung von p42/44 MAPK verminderte sowohl die Expression und Kerntranslokation von Egr-1 sowie die Expression von HO-1 in HOCl-HDL-behandelten Zellen. Eine Hemmung der Egr-1 Expression mittels RNA-Interferenz verminderte die HOCl-HDL-induzierte Translokation von Egr-1 und die Expression von HO-1. Die Hemmung der Phosphatidyl-inositol-3-kinase führte zu einer Abnahme der HOCl-HDL-induzierten HO-1 Proteinexpression. Obwohl HOCl-HDL eine reduzierte eNOS mRNA Expression bewirkte, konnte weder eine Verminderung der eNOS Aktivität noch der eNOS Proteinexpression beobachtet werden. Weiters

bewirkte die Inkubation von Endothelzellen mit HOCl-HDL weder anti-proliferative Effekte noch Apoptose.

Mit vorliegender Studie konnte gezeigt werden, dass in die HOCl-HDL-induzierte Aktivierung von HO-1 in humanen Endothelzellen sowohl p42/44 MAPK, der Transkriptionsfaktor Egr-1, als auch die Phosphatidyl-inositol-3-kinase involviert sind.

Table of Contents

Abbreviations

ABC	ATP-binding cassette transporter
ANOVA	analysis of variance
AP-1	activating protein-1
apoA-I	apolipoprotein A-I
APS	ammonium persulfate
ARE	antioxidant response element
BSA	bovine serum albumin
CBP	CREB-binding protein
cGMP	cyclic guanosine monophosphate
CO	carbon monoxide
Cul3/Rbx1	cullin 3/ring box 1
DMEM	Dulbecco's Modified Eagle Medium
DMSO	dimethyl sulfoxid
dNTP	deoxynucleoside triphosphate
DTT	dithiothreithol
Egr-1	early growth response-1
EMSA	Electrophoretic Mobility Shift Assay
eNOS	endothelial nitric oxide synthase
ERK1/2	extracellular signal-regulated kinase 1/2
FCS	fetal calf serum
GAPDH	glyceraldehyde-3-phosphate dehydrogenase
H_2O_2	hydrogen peroxide
HAT	hypoxanthine, aminopterin and thymidine
HDL	high-density lipoprotein
HO	heme oxygenase
HOCl	hypochlorous acid
HSE	heat shock element
Hsp32	heat shock protein 32
HUVEC	human umbilical vein endothelial cell
ICAM-1	intercellular adhesion molecule-1

IDL	intermediate-density lipoprotein
SAPK/JNK	stress-activated protein kinase/c-jun-NH_2-terminal kinase
Keap1	Kelch-like ECH-associating protein 1, INrf2
LDL	low-density lipoprotein
MAPK	mitogen-activated protein kinase
MAPKK	MAPK kinase
MAPKKK	MAPK kinase kinase
MCP-1	monocyte chemoattractant protein-1
MPO	myeloperoxidase
MTT	3-(4,5-dimethylthiazol-2-yl)-2,5-diphenyltetrazolium)
NAB	NGFI-A-binding protein
NADPH	nicotinamide adenine dinucleotide phosphate
NFAT	nuclear factor of activated T cells
NGFI-A	nerve growth factor-induced-A
NO	nitric oxide
Nrf2	nuclear factor E2-related factor 2
oxLDL	oxidized LDL
p38 MAPK	p38 mitogen activated protein kinase
p42/44 MAPK	p42/44 mitogen activated protein kinase
PARP	poly(ADP-ribose) polymerase
PBS	phosphate-buffered saline
PCAM-1	platelet-endothelial cell adhesion molecule-1
PI3K	phosphatidyl-inositol-3-kinase
PKC	protein kinase C
PLC	phospholipase C
Poly(dI:dC)•(dI:dC)	poly(deoxyinosinic deoxycytidylic) acid
pp38 MAPK	phospho-p38 mitogen activated protein kinase
pp42/44 MAPK	phospho-p42/44 mitogen activated protein kinase
P/S	Penicillin-Streptomycin
ROS	reactive oxygen species
SDS	sodium dodecyl sulfate

siRNA	small interfering RNA
SP1	specificity protein-1
SR-BI	scavenger receptor class B, type I
TBE	Tris borate-EDTA buffer
TBS-T	Tris-buffered saline Tween-20
TE buffer	Tris-EDTA buffer
TEMED	N,N,N’,N’-tetramethylethylenediamine
VCAM-1	vascular cell adhesion molecule-1
VLDL	very low density lipoprotein

1. Introduction

1.1 Atherosclerosis

According to recent reports of the World Health Organization, cardiovascular diseases represent the major cause of death in Western societies and become more and more important in low- and middle-income countries. Cardiovascular diseases are mainly caused by atherosclerosis, a progressive disease that is characterized by the accumulation of lipids and fibrous elements in the large arteries (Lusis, 2000; Stary *et al.*, 1995). One of the initiating events in the development of atherosclerosis is the accumulation of oxidized lipoproteins in the subendothelial space that further leads to inflammation and the recruitment of monocytes to the endothelium (Navab *et al.*, 1995). Monocytes migrate into the intima of the artery and differentiate into macrophage cells, which take up modified lipoproteins and develop into foam cells (Gerrity, 1981; Libby, 2002) (Figure 1).

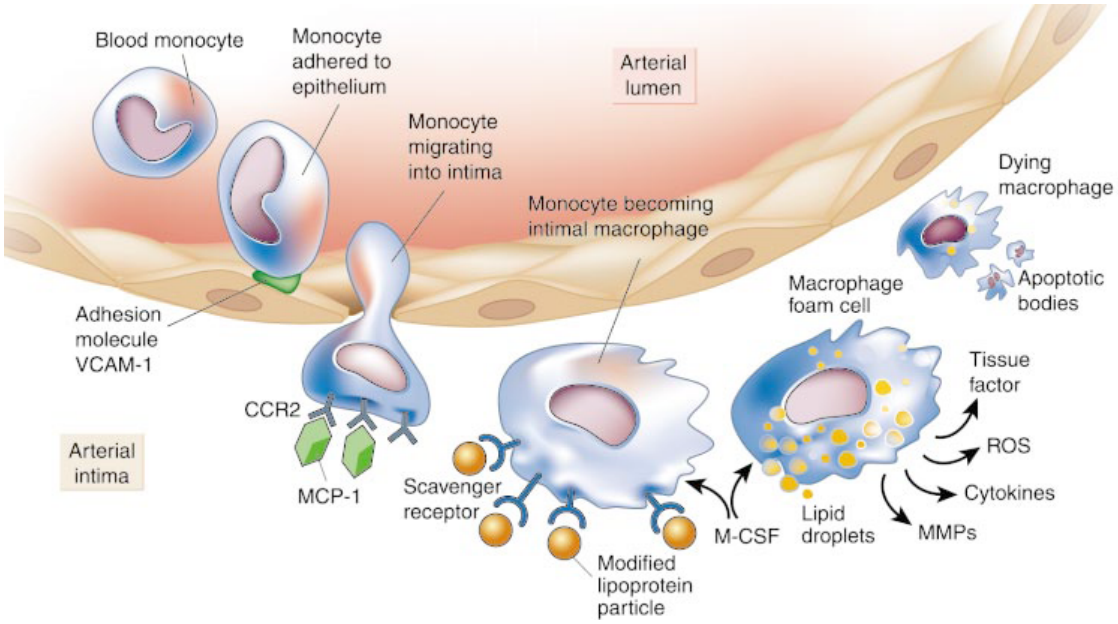

Figure 1: *Development of an early atherosclerotic lesion (Libby, 2002).* Activated endothelial cells express adhesion molecules such as VCAM-1 (vascular cell adhesion molecule-1) where circulating monocytes can adhere. After migration of monocytes into the intima and binding of monocyte chemoattractant protein-1 (MCP-1), they differentiate into macrophages. Macrophages take up modified lipoproteins via scavenger receptors and develop into foam cells that secrete pro-inflammatory agents to further induce inflammation within the atherosclerotic lesion. Debris of dead macrophages are constituents of the “necrotic core” of advanced lesions.

This early lesion (fatty streak) might then progress into a fibrous plaque that is additionally characterized by the accumulation of extracellular lipids, smooth muscle cells and extracellular matrix components (Lusis, 2000). The accumulating smooth muscle cells and the extracellular matrix are components of the “fibrous cap” that surround the “necrotic core” consisting of extracellular lipid, necrotic debris and cholesterol crystals (Spagnoli *et al.*, 2007). Rupture of a plaque results in contact of blood with the thrombogenic necrotic core, which leads to thrombosis and furthermore might cause clinical complications such as stroke or myocardial infarction (Spagnoli *et al.*, 2007).

1.2 Lipoproteins

Cholesterol is a precursor of steroid hormones and bile acids and an important component of cell membranes, which can be obtained either from the diet or can be synthesized mainly by the liver and the intestine. Although cholesterol biosynthesis might occur in all somatic cells, the predominant part of cholesterol catabolism takes place in the liver where cholesterol is converted to bile acids (Yokoyama, 2006). Lipoprotein particles, consisting of a core of hydrophobic lipids surrounded by polar lipids and apolipoproteins, enable the transport of hydrophobic cholesterol and triacylglycerol in the circulation (Berg *et al.*, 2002). Chylomicrons transport dietary triacylglyerol and cholesterol from the intestine to the periphery where triacylglycerol is released through hydrolysis by lipoprotein lipase. The cholesterol-rich chylomicron remnants are then transported to and are taken up by the liver. Newly synthesized triacylglycerol and cholesterol are transported as very low-density lipoproteins (VLDL) from the liver to peripheral tissues. Triacylglyerol is released and the remaining particles (intermediate-density lipoproteins, IDL) are either transported back to the liver or converted into low-density lipoproteins (LDL) (Berg *et al.*, 2002). LDL provides extrahepatic tissues with cholesterol, whereas high-density lipoproteins (HDL) remove excess cholesterol from somatic cells and transport it back to the liver.

1.2.1 Native HDL

HDL comprises various apolipoproteins (such as apoA-I, the major apolipoprotein, as well as apoA-II, apoC, apoE, apoD and apoA-IV) and lipids (like phospholipids, cholesterol, triacylglycerol and cholesterol esters) (Davidson *et al.*, 2007). Clinical studies demonstrated a strong correlation between low plasma HDL levels and the risk for atherosclerosis development and progression (Gordon *et al.*, 1989). Furthermore it was reported that HDL exhibits various anti-atherogenic and anti-inflammatory properties and therefore increasing HDL cholesterol by therapeutical intervention is considered as an anti-atherosclerotic approach (Kontush *et al.*, 2006; Linsel-Nitschke *et al.*, 2005). The most important anti-atherogenic function of HDL, however, is its role in "reverse cholesterol transport" to ensure cholesterol homeostasis (von Eckardstein *et al.*, 2001). Cholesterol efflux from cells to plasma HDL is a complex and highly regulated process mediated by four major pathways: (i) aqueous diffusion, (ii) binding of HDL to scavenger receptor class B, type I (SR-BI), (iii) interaction of HDL with the ATP-binding cassette transporter G1 (ABCG1) or (iv) binding of HDL to ABCA1 (Rothblat *et al.*, 2010). HDL then transports free cholesterol, which becomes esterified, to the liver, where it delivers cholesterol and cholesterol ester to hepatocytes by binding to SR-BI (Zannis *et al.*, 2006). In the liver cholesterol is used for the assembly of lipoproteins or the synthesis of bile acids and vitamin D (von Eckardstein *et al.*, 2001).

1.2.2 HOCl-modified HDL

Myeloperoxidase (MPO) is a marker for coronary artery disease in humans and its reaction products are reported to transform the anti-atherogenic HDL particle into a pro-atherogenic and pro-inflammatory lipoprotein particle (Fogelman, 2004; Zhang *et al.*, 2001b). MPO is a component of the innate immune response and is present in the azurophil granules of neutrophils and monocytes, where it accounts for approximately five and one percent of total cell protein content (Klebanoff, 2005). The main reaction catalyzed by MPO is the generation of hypochlorous acid (HOCl) from hydrogen peroxide (H_2O_2) in

the presence of physiological chloride concentrations (Winterbourn *et al.*, 2000).

HOCl acts as an oxidant and is reported to generate aldehydes, advanced glycation end products, protein/lipid adducts, protein crosslinks and chloramines that are present in inflammatory diseases like atherosclerosis and glomerulosclerosis (Malle *et al.*, 2006). Chlorine gas, which is formed under acidic conditions from HOCl may additionally produce 3-chlorotyrosine and 3,5-dichlorotyrosine; both chlorinated components are considered as biomarkers for stable chlorinated molecules occurring in human atherosclerotic lesions (Malle *et al.*, 2006).

It was previously demonstrated that enzymatically active MPO was detected in human atherosclerotic lesions (Daugherty *et al.*, 1994) and that MPO binds to apoA-I on the HDL particle in atherosclerotic lesions (Zheng *et al.*, 2004). Furthermore it was reported that HOCl-modified epitopes colocalize with apoA-I in human atherosclerotic lesions and on endothelial cells (Bergt *et al.*, 2004; Malle *et al.*, 2006; Marsche *et al.*, 2002). Zheng and colleagues (Zheng *et al.*, 2004) reported that MPO-generated oxidants like nitrotyrosine and 3-chlorotyrosine were detected in apoA-I isolated from human atherosclerotic lesions. Modified HDL is regarded as a clinically relevant marker for atherosclerotic disease, because it is able to transcend the endothelium and to re-enter circulation due to its low particle diameter (Malle *et al.*, 2006).

Within the HDL particle apoA-I represents the major site for HOCl-mediated protein modification, followed by other apolipoproteins as well as HDL-associated enzymes (Malle *et al.*, 2006). The amino acids most sensitive for HOCl-mediated modification are cysteine, methionine, and tyrosine followed by phenylalanine, lysine, histidine, and arginine. It was shown previously that all three methionine residues in apoA-I were oxidized and that two phenylalanine residues were chlorinated by HOCl within the apoA-I particle (Malle *et al.*, 2006). Additionally it was reported that the chlorination of tyrosine residues might occur via chloramine formation of adjacent lysine or histidine residues (Malle *et al.*, 2006). Furthermore, unsaturated fatty acid residues of the phospholipid and cholesterylester fraction of HDL represent targets for HOCl-mediated modification. It was further reported that modification of unsaturated

fatty acids by HOCl is not likely to occur under *in vivo* conditions (HOCl:HDL molar ratios of 30:1 to 50:1) but was detected *in vitro* at molar ratios $\geq$ 100:1 (Bergt *et al.*, 1999). Contrary, HOCl-mediated attack of HDL-associated plasmalogens (ether-phospholipids) leading to the formation of lysophosphatidylcholine and α-chlorinated fatty aldehydes (e.g. 2-chlorohexadecanal), takes place at lower HOCl:HDL molar ratios (Malle *et al.*, 2006; Marsche *et al.*, 2004). Thukkani and colleagues (Thukkani *et al.*, 2003) reported that both 2-chlorohexadecanal and lysophosphatidylcholine were present in human atherosclerotic lesions.

Marsche and colleagues (Marsche *et al.*, 2004) previously demonstrated that treatment of endothelial cells with HOCl-HDL led to an impaired expression and activity of vasculoprotective endothelial nitric oxide synthase (eNOS). Additionally, it was shown that HOCl-modified HDL exhibits an impaired capacity in reverse cholesterol transport by influencing SR-BI- and ABCA1-mediated cholesterol efflux (Malle *et al.*, 2006). HOCl-HDL binds with higher affinity to SR-BI compared to native HDL and is able to displace native HDL from SR-BI (Marsche *et al.*, 2002). Additionally it was reported that modification of HDL by reagent HOCl causes a loss of its ability to accept and to deliver cholesterol via SR-BI (Malle *et al.*, 2006). ABCA1 transports cholesterol to lipid-free or lipid-poor apoA-I to form nascent HDL in liver and peripheral cells, whereas ABCA1-mediated cholesterol efflux is impaired when apoA-I is modified by HOCl (Malle *et al.*, 2006). Furthermore HOCl-modified HDL represents a high uptake form for macrophages that may develop into foam cells (Panzenboeck *et al.*, 1997).

1.3 Heme oxygenases

Heme oxygenases (HOs) catalyze the rate-limiting step of heme degradation in mammals by conversion of heme into biliverdin, carbon monoxide (CO) and free iron (Fe^{2+}) (Figure 2). Biliverdin is subsequently converted into bilirubin via biliverdin reductase and the free iron is promptly sequestered into ferritin (Tenhunen *et al.*, 1969; Tenhunen *et al.*, 1968).

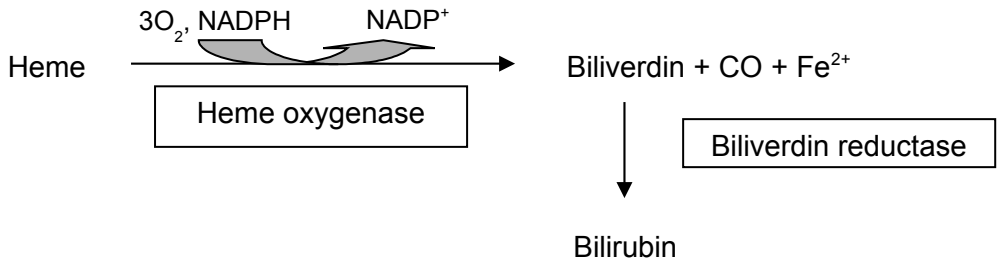

Figure 2: *Scheme of heme degradation.* Heme oxygenases degrade heme into biliverdin, CO and free iron. The reaction requires three mol of oxygen and the cofactor NADPH, which is converted into $NADP^+$. Biliverdin is converted into bilirubin via biliverdin reductase. This scheme was adapted from (Ryter *et al.*, 2006).

1.3.1 HO Isoenzymes

Two isoenzymes of HO (HO-1 and HO-2) and one pseudogene (HO-3) have been identified in humans so far: Distinct genes are encoding for HO-1 and HO-2, which share about 43% homology in the primary structure (Loboda *et al.*, 2008). The inducible isoform HO-1 has a molecular mass of 32 kDa and is expressed at a high level in spleen and specifically in reticuloendothelial cells of the liver and bone marrow, where degradation of red blood cells occurs (Ryter *et al.*, 2006). Contrary, HO-1 expression is very low under basal conditions in tissues that are not directly involved in hemoglobin or erythrocyte metabolism, but can increase by various stimuli including heme, metalloporphyrins and oxidative stress (Abraham *et al.*, 2008; Ryter *et al.*, 2006). In contrast, HO-2 has a molecular mass of 34 kDa and is constitutively expressed in tissues like brain, central nervous system, liver, kidney, gut, vasculature and testes, the latter exhibiting highest HO-2 expression (Abraham *et al.*, 2008; Ryter *et al.*, 2006). HO-3 was detected only in rats and initially thought to encode a 33 kDa HO-3 protein in various organs (McCoubrey *et al.*, 1997). It was shown recently, however, that there is no functional HO-3 gene in the rat and that the observed transcript should be regarded as pseudogene derived from HO-2 (Hayashi *et al.*, 2004).

1.3.2 Regulation of HO-1

Human HO-1 was previously classified as heat shock protein 32 (Hsp32) because of the presence of a potential heat shock element (HSE) within the human HO-1 promoter region (Yoshida *et al.*, 1988), similar to the HSE located in the rat HO-1 gene (Muller *et al.*, 1987). It was shown, however, that the human HSE is not functional and that transcriptional HO-1 induction by hyperthermia seems to be restricted to rodents (Shibahara *et al.*, 1989). Aside from HSE many transcription factor consensus-binding sites within the HO-1 promoter region were reported, such as: cadmium-responsive element, antioxidant response element (ARE), SMAD-binding element, consensus binding sites for activating protein-1 (AP-1), specificity protein-1 (Sp1), early growth response-1 (Egr-1), nuclear factor-κB and AP-2 (Loboda *et al.*, 2008; Ryter *et al.*, 2006).

Induction of stress-responsive HO-1 is regarded as an important cytoprotective pathway to cope with oxidative stress and endothelial dysfunction. Many reports show that HO-1 is induced by various stimuli like oxidized lipids, copper-oxidized LDL, heavy metal salts, metalloporphyrins, antioxidants, cytokines, growth factors, gases or reactive oxygen species (ROS) (Loboda *et al.*, 2008; Ryter *et al.*, 2006).

Multiple signaling pathways may be involved in the regulation of HO-1 expression, such as protein kinase C (PKC), phosphatidyl-inositol-3-kinase (PI3K), stress-activated protein kinase/c-jun-NH_2-terminal kinase (SAPK/JNK), p38 and p42/44 mitogen-activated protein kinases (MAPKs) (Anwar *et al.*, 2005; Lin *et al.*, 2007; Martin *et al.*, 2004).

1.3.3 Role of HO-1 in Atherosclerosis

Evidence exists that HO-1 plays a protective role in atherosclerosis by the conversion of the pro-oxidative heme into anti-oxidative bile pigments (biliverdin and bilirubin) and CO (Morita, 2005). Data obtained from isolated endothelial cells of human atherosclerotic arterial specimen revealed high expression and activity of HO-1 in advanced lesions compared to early lesions or healthy arteries (Morsi *et al.*, 2006). Additionally it was reported that

expression of HO-1 occurs in endothelium, foam cells and macrophages of thickened intima in lesions from both humans and apoE-deficient mice (Wang *et al.*, 1998). Studies using hypercholesterolemic rabbits, fed a high-cholesterol diet, revealed colocalization of HO-1 with bilirubin in foam cells (Nakayama *et al.*, 2001). Treatment of cells with copper-oxidized LDL potently induced HO-1 expression in human umbilical vein endothelial cells (HUVECs) (Agarwal *et al.*, 1996), whereas treatment with native LDL failed to induce HO-1 expression.

Experiments with various animal models further strengthened the hypothesis that HO-1 might play a protective role in the development of atherosclerosis. By using Watanabe heritable hyperlipidemic rabbits fed a high-fat diet, Ishikawa and colleagues (Ishikawa *et al.*, 2001a) demonstrated that inhibition of HO-1 by Sn-protophorphyrin IX led to more pronounced atherosclerotic lesions compared to control animals. Comparable results were obtained in mice deficient in HO-1 and apoE ($HO\text{-}1^{-/-}apoE^{-/-}$). These mice exhibited more pronounced atherosclerotic lesion formation compared to $HO\text{-}1^{+/+}apoE^{-/-}$ mice (Yet *et al.*, 2003). Furthermore it was reported that peritoneal macrophages isolated from $HO\text{-}1^{-/-}$ and $HO\text{-}1^{-/+}$ mice exhibited elevated ROS generation, accelerated levels of proinflammatory cytokines and increased copper-oxidized LDL-induced foam cell formation compared to $HO\text{-}1^{+/+}$ macrophages (Orozco *et al.*, 2007). Cheng and colleagues (Cheng *et al.*, 2009) further demonstrated that induction of HO-1 by cobalt protoporphyrin detained atherosclerotic lesion progression into a vulnerable plaque, whereas inhibition of HO-1 by zinc protoporphyrin worsened plaque formation. To investigate whether HO-1 gene transfer might resemble a future therapy to alleviate atherosclerotic lesion progression, Juan and colleagues (Juan *et al.*, 2001) delivered the human HO-1 gene into the left ventricles of $apoE^{-/-}$ mice using adenovirus-mediated gene transfer. These authors (Juan *et al.*, 2001) observed strong expression of human HO-1 in the endothelium and atherosclerotic lesions as well as smaller lesions and less iron deposition in the aortic tissue after adenoviral gene transfer.

1.3.3.1 Biliverdin, Bilirubin and Atherosclerosis

The HO-1 reaction product biliverdin is subsequently converted to bilirubin via biliverdin reductase (Tenhunen *et al.*, 1969). Bilirubin is then conjugated by UDP-glucuronyl transferase and excreted into the bile (Abraham *et al.*, 2008). Although biliverdin and bilirubin are reported to be toxic at high concentrations in neonates, bilirubin is regarded as endogenous antioxidant because of its ability to scavenge reactive oxygen and nitrogen species and to inhibit oxidation of LDL lipids (Ryter *et al.*, 2006; Stocker *et al.*, 1987). It was further demonstrated that bilirubin inhibited the activation of NADPH oxidase, thereby reducing the amount of generated superoxide anion (Kwak *et al.*, 1991). Furthermore it was reported that treatment of high-fat fed LDL receptor$^{-/-}$ mice with bilirubin improved impaired vascular relaxation (Kawamura *et al.*, 2005). It was shown previously that bilirubin exhibited anti-proliferative effects in smooth muscle cells (Ollinger *et al.*, 2005) and that high-normal levels of bilirubin were associated with reduced atherosclerosis (Ollinger *et al.*, 2007). Clark and colleagues (Clark *et al.*, 2000) demonstrated that exogenously applied bilirubin decreased infarct size and mitochondrial damage and restored myocardial function in a model of ischemia-reperfusion injury in rat hearts.

1.3.3.2 CO and Atherosclerosis

CO was regarded previously solely as a toxic air pollutant, that exhibited a stronger affinity to hemoglobin than oxygen (Abraham *et al.*, 2008). Displacement of oxygen by CO leads to a shift of the oxygen dissociation curve and results in tissue hypoxia (Ryter *et al.*, 2004). Despite the occurring toxic effects after exposure to high concentrations of CO, physiological levels of CO exhibit vasodilatory, anti-apoptotic and anti-inflammatory effects (Kirkby *et al.*, 2006; Morita, 2005). Comparable to the vasodilator NO, CO exerts vasodilatory effects through cyclic guanosine monophosphate (cGMP)-dependent smooth muscle relaxation (Kajimura *et al.*, 2002; Kirkby *et al.*, 2006). CO, however, was less potent than NO in inducing cGMP formation via soluble guanylate cyclase (Abraham *et al.*, 2008). CO-mediated vasorelaxant effects are reported to occur also via cGMP-independent stimulation of potassium channels (Ryter *et al.*,

2006). Furthermore CO is reported to exert cytoprotective effects via the MAPK signaling pathway. Amersi and colleagues (Amersi *et al.*, 2002) demonstrated that exogenously applied CO prevented hepatic ischemia-reperfusion injury via p38 MAPK signaling. Exogenously applied CO exerts both anti-apoptotic (Zhang *et al.*, 2003) and anti-inflammatory (Otterbein *et al.*, 2003) effects mediated by the p38 MAPK signaling pathway in lung injury.

1.3.3.3 Iron and Atherosclerosis

In the plasma, iron is bound to transferrin and taken up by cells via receptor-mediated endocytosis (Abraham *et al.*, 2008). Iron is then released from transferrin by a decrease in endosomal pH and passes through the endosomal membrane to enter the cytosol of the cell (Ponka *et al.*, 1998). Although iron is an essential component of various iron-containing enzymes and proteins, an excess of intracellular free iron is reported to lead to ROS formation by the Fenton reaction via generation of hydroxyl radical and peroxide radical (Abraham *et al.*, 2008). To antagonize iron-mediated ROS formation and cytotoxic effects, free intracellular iron is promptly sequestered by ferritin. Expression of ferritin is increased by the up-regulation of HO-1 as well as by elevated levels of free iron (Balla *et al.*, 1992; Eisenstein *et al.*, 1991).

1.4 Nuclear factor E2-related factor 2

The stress-responsive transcription factor Nrf2 (nuclear factor E2-related factor 2) is ubiquitously expressed and regulates the expression of defense genes encoding antioxidant proteins including HO-1, NAD(P)H:quinine oxidoreductase 1 and γ–glutamylcysteine synthetase (Moi *et al.*, 1994; Nguyen *et al.*, 2003). Nrf2 is a basic leucine zipper transcription factor that binds to ARE sequences within the promoter region of target genes in response to various stimuli such as antioxidants, xenobiotics, metals and UV irradiation (Kaspar *et al.*, 2009). Under basal conditions Nrf2 is bound to the cytosolic protein Keap1 (Kelch-like ECH-associating protein 1, INrf2) and retained in the cytosol (Itoh *et al.*, 1999; Kaspar *et al.*, 2009). Keap1, however, functions as adapter for the

cullin 3/ring box 1 (Cul3/Rbx1) E3 ubiquitin ligase complex (Kaspar *et al.*, 2009). This complex is responsible for the ubiquitination and degradation of Nrf2 through the 26S proteasome (Kaspar *et al.*, 2009). In response to oxidative stress, the Nrf2-Keap1 complex is activated by oxidative modification of Keap1 and/or phosphorylation of Nrf2, which results in the release of Nrf2 from Keap1 (Kaspar *et al.*, 2009). Nrf2 is stabilized, translocates to the nucleus, where it forms heterodimers with small Maf and Jun proteins, and binds to ARE to induce transcription (Itoh *et al.*, 1997; Venugopal *et al.*, 1998).

Various signaling pathways such as the MAPK cascades, the PI3K and PKC are reported to be involved in the activation of Nrf2-ARE-mediated transcription (Nguyen *et al.*, 2003). Furthermore it was demonstrated that copper-oxidized LDL induced expression of HO-1 via MAPKs and Nrf2 in human aortic smooth muscle cells (Anwar *et al.*, 2005) as well as via enhanced ROS levels and Nrf2 in murine macrophages (Calay *et al.*, 2010).

1.5 Egr-1

The zinc finger transcription factor Egr-1 (also known as NGFI-A (nerve growth factor-induced-A), zif268, Krox-24 or TIS8) belongs to the family of immediate-early genes (Khachigian, 2006). Egr-1 is reported to regulate the transcription of various genes implicated in the development of atherosclerosis such as transcription factors, growth factors, adhesion molecules, cytokines and HO-1 in response to extracellular stimuli including shear stress, angiotensin II and tissue injury (Blaschke *et al.*, 2004; Yang *et al.*, 2001). McCaffrey and colleagues (McCaffrey *et al.*, 2000) further reported that high levels of Egr-1 and Egr-1-inducible genes are expressed in human and mouse atherosclerotic lesions. The DNA-binding domain of Egr-1 consists of three zinc fingers that bind to GC-rich sequences in the promoter region of target genes (Silverman *et al.*, 1999). It was demonstrated previously that Egr-1 exhibits similar consensus binding sites as transcription factors Sp1 and Wilms tumor suppressor and that these transcription factors can displace one another (Silverman *et al.*, 1999). Furthermore it is reported that both coactivators and corepressors such as Sp1,

NFAT (nuclear factor of activated T cells), CBP (CREB-binding protein), NAB1 and NAB2 (NGFI-A-binding protein) might influence Egr-1-mediated transcription (Blaschke *et al.*, 2004; Khachigian, 2006).

It was shown previously that Egr-1 expression was induced by copper-oxidized LDL in human monocytes (Stoyanova *et al.*, 2001) and rat smooth muscle cells (Cui *et al.*, 1999). Furthermore it was reported that phosphorylation of SAPK/JNK, p38 and p42/44 MAPKs led to Egr-1 expression (Day *et al.*, 1999; Guha *et al.*, 2001; Lim *et al.*, 1998) and that HO-1 expression was mediated by Egr-1 (Chen *et al.*, 2010; Yang *et al.*, 2001).

1.6 Aim of the Study

Evidence exists that inducible HO-1 and its products function as adaptive molecules against oxidative insults and that expression of HO-1 may be considered a novel therapeutic target for cardiovascular disease (Loboda *et al.*, 2008). Furthermore, oxidative stress leads to more pronounced endothelial cell injury in humans deficient in HO-1 compared to healthy controls (Yachie *et al.*, 1999). Immunohistochemical experiments revealed expression of MPO, HOCl-modified epitopes and HO-1 within and around endothelial cells in human atherosclerotic lesions (Malle *et al.*, 2000; Wang *et al.*, 1998). Therefore, the present study aimed at investigating the signaling pathways involved in HOCl-HDL-mediated induction of HO-1 expression in EA.hy926 human endothelial cells.

Aim (i) To identify intracellular signaling pathways (e.g. MAPKs, phospholipase C (PLC) and PI3K) involved in the activation of HO-1 via HOCl-HDL

Aim (ii) To understand the involvement of transcription factors (e.g. Egr-1 and Nrf2) in HOCl-HDL-mediated activation of HO-1

Aim (iii) To investigate the functional correlation between HO-1 and eNOS

Aim (iv) To determine apoptotic and anti-proliferative effects in HOCl-HDL-treated cells

2. Materials and Methods

2.1 Materials

2.1.1 Cell Culture Materials

Cell culture flasks, dishes and microtiterplates were purchased from Greiner Bio-One (Frickenhausen, Germany). Lab-Tek chamber slides were obtained from Thermo Fisher Scientific (Rochester, NY, USA) and FCS (fetal calf serum) was from PAA (Linz, Austria). Dulbecco`s Modified Eagle Medium (DMEM), Penicillin-Streptomycin (P/S), Trypsin and HAT (hypoxanthine, aminopterin and thymidine) Supplement were from Gibco Invitrogen (Lofer, Austria).

2.1.2 Materials for Preparation and Modification of (Lipo)proteins

Plasma of healthy, normolipidemic patients was kindly provided by Drs. Sipurzynski and Vadon (Department of Blood Group Serology and Transfusion Medicine, Medical University of Graz, Austria). Beckman LE-80K Ultracentrifuge Optima, 50.2 Ti Rotor and Quick-Seal® centrifuge tubes were obtained from Beckman Coulter Inc. (Fullerton, CA, USA). Rotilabo®-syringe filters (pore size 0.22 µm) were purchased from Carl Roth GmbH (Karlsruhe, Germany). PD-10 Desalting Columns were from Amersham Biosciences (Buckinghamshire, UK). NaOCl, KBr and essentially fatty acid free bovine serum albumin (BSA) were from Sigma-Aldrich (Saint Louis, MO, USA). BSA was from Serva (Heidelberg, Germany). MPO was from Planta Natural Products (Vienna, Austria).

2.1.3 Inhibitors and Reagents for MTT-Assay

The inhibitors for the MAPK kinase (MAPKK) MEK1 (PD98059) and for p38 MAPK (SB203580) and staurosporine were from Merck Biosciences (Darmstadt, Germany). The PI3K inhibitor LY294002 was from Santa Cruz Biotechnology, Inc. (Santa Cruz, CA, USA). The inhibitor for PLC U73122, MTT (3-[4,5-Dimethylthiazol-2-yl]-2,5-diphenyltetrazolium bromide; Thiazolyl blue), Actinomycin D and HCl were purchased from Sigma-Aldrich (Saint Louis, MO,

USA). Isopropanol was from Carl Roth GmbH (Karlsruhe, Germany).

2.1.4 Materials for RNA isolation, Reverse Transcription and Real-time-PCR

QIAshredder and RNeasy Mini Kit were from QIAGEN (Hilden, Germany). β-Mercaptoethanol was from Merck Biosciences (Darmstadt, Germany). DNase I, SuperScript® II Reverse Transcriptase and RNaseOUT™ Recombinant Ribonuclease Inhibitor were from Invitrogen (Lofer, Austria). Random hexamer primers were from Applied Biosystems Inc. (Foster City, CA, USA) and dNTP Mix was from Fermentas GmbH (St. Leon-Rot, Germany). QuantiTect Primer Assays and QuantiFast SYBR Green PCR Kit were from QIAGEN (Hilden, Germany). LightCycler® 480 and LightCycler® 480 multiwell plates were from Roche Applied Science (Vienna, Austria).

2.1.5 Materials for Isolation of cytosolic and nuclear Proteins

HEPES, $MgCl_2$, NP-40 and EDTA were from Sigma-Aldrich (Saint Louis, MO, USA). Complete Mini protease inhibitor cocktail tablets were from Roche Applied Science (Vienna, Austria). KCl, NaCl and glycerol were from Carl Roth GmbH (Karlsruhe, Germany). Dithiothreitol (DTT) was from Invitrogen (Lofer, Austria).

2.1.6 Materials for Protein Isolation and Western Blot Experiments

Complete Mini protease inhibitor cocktail tablets were used to inhibit protein degradation. Super Signal West Pico Chemiluminescent substrate, NE-PER nuclear and cytoplasmic protein extraction kit and BCA™ Protein Assay kit were from Pierce Biotechnology, Inc. (Rockford, IL, USA). Immobilon™ Western Chemiluminescent HRP Substrate was from Millipore Corporation (Billerica, MA, USA). NuPAGE® 4-12% Bis-Tris Gels, NuPAGE® MOPS SDS Running Buffer and SeeBlue® Plus prestained standard were from Invitrogen (Lofer, Austria). Nitrocellulose blotting membrane (0.45 µm pore size) was from Sartorius AG (Goettingen, Germany) and Hyperfilm™ MP was from GE Healthcare (Vienna, Austria). Ponceau S Solution, bromphenol blue, HEPES,

EDTA, $Na_4P_2O_7$, Na_3VO_4 and Triton® X-100 were from Sigma-Aldrich (Saint Louis, MO, USA). NaCl, Tris(hydroxymethyl)aminomethane, sodium dodecyl sulfate (SDS) and glycerol were from Carl Roth GmbH (Karlsruhe, Germany). NaF was from Fluka GmbH (Buchs, Switzerland) and β-Mercaptoethanol was from Merck Biosciences (Darmstadt, Germany).

2.1.7 Antibodies

2.1.7.1 Primary Antibodies

Antibodies for MAPKs

Mouse monoclonal pp44/42 MAPK (Erk1/2) antibody and rabbit polyclonal pp38 MAPK antibody recognized pp42/44 (42 and 44 kDa) and pp38 MAPK (38 kDa) and were from Cell Signaling Technology, Inc. (Danvers, MA, USA).

Antibodies for Egr-1 and Nrf2

Rabbit polyclonal Egr-1 antibody (clone C19) and rabbit polyclonal Nrf2 antibody (clone C-20) were from Santa Cruz Biotechnology, Inc. (Santa Cruz, CA, USA) and recognized the respective proteins at 75-80 kDa (Egr-1) and 57 kDa (Nrf2).

Antibodies for HO-1 and eNOS

Rabbit polyclonal HO-1 antibody (Hsp32) recognized HO-1 (32 kDa), was from Assay Designs, Inc. (Ann Arbor, MI, USA). Rabbit polyclonal eNOS/NOS Type III antibody was from BD Biosciences (San Jose, CA, USA) and detects eNOS at 130-140 kDa.

Antibodies for Observation of Apoptosis

Rabbit polyclonal Caspase-3 antibody from Cell Signaling Technology, Inc. (Danvers, MA, USA) was used to detect full-length caspase-3 (35 kDa) and the cleaved Caspase-3 fragment (17 kDa). Mouse monoclonal Poly(ADP-ribose) polymerase (PARP) antibody (clone C-2-10) was from Enzo Life Sciences International, Inc. (Plymouth Meeting, PA, USA) and recognizes full-

length PARP (116 kDa) and the apoptosis-related cleaved fragment (85 kDa). Additional necrosis-related PARP-fragments might be observed at 50 kDa, 62 kDa and 74 kDa.

Antibodies for Normalization of Protein Content

Mouse monoclonal β-Actin antibody (clone C4) was used to detect the corresponding protein as a cytosolic loading control at a molecular weight of 43 kDa. Rabbit polyclonal Lamin A/C antibody (clone H-110) was used to detect the corresponding 69 kDa protein as nuclear loading control. β-Actin and Lamin antibodies were from Santa Cruz Biotechnology, Inc. (Santa Cruz, CA, USA).

2.1.7.2 Secondary Antibodies

Cy-3 labeled goat anti-rabbit antibody was from Jackson ImmunoResearch Laboratories, Inc. (West Grove, PA, USA). Peroxidase-conjugated goat anti-rabbit IgG was from Pierce Biotechnology, Inc. (Rockford, IL, USA). Peroxidase-conjugated goat anti-mouse IgG was from Rockland Immunochemicals, Inc. (Gilbertsville, PA, USA).

2.1.8 Materials for Electrophoretic Mobility Shift Assay (EMSA)

Super Signal West Pico Chemiluminescent substrate, NE-PER nuclear and cytoplasmic protein extraction kit and BCA™ Protein Assay kit were from Pierce Biotechnology, Inc. (Rockford, IL, USA). Complete Mini protease inhibitor cocktail tablets were used to avoid protein degradation. Oligonucleotide sequences of the Egr-1 consensus binding site, offered by Santa Cruz Biotechnology, Inc. (Santa Cruz, CA, USA) were synthesized by TibMolBiol (Berlin, Germany). PCR-buffer (10-fold) and $MgCl_2$ were from Solis Biodyne (Tartu, Estonia). Tris borate-EDTA buffer solution (TBE, 5-fold) was from Eppendorf AG (Hamburg, Germany). Acrylamid/bis-acrylamide (w/w ratio of 19:1), TEMED, bromphenol blue, EDTA and ammonium persulfate (APS) were from Sigma-Aldrich (Saint Louis, MO, USA). DTT was from Invitrogen (Lofer, Austria). Glycerol, NaCl and Tris-(hydroxymethyl)-aminomethan were from Carl Roth GmbH (Karlsruhe, Germany). Hyperfilm™ MP and [γ-^{32}P]ATP (3000

Ci/mmol) were from GE Healthcare (Vienna, Austria). T4 polynucleotide kinase was from Fermentas GmbH (St. Leon-Rot, Germany) and Micro Bio-Spin™ Chromatography Columns were from Bio-Rad Laboratories, Inc. (Vienna, Austria). Poly[d(I-C)] was from Roche Applied Science (Vienna, Austria) and BSA was from New England Biolabs, Inc. (Ipswich, MA, USA). Rabbit polyclonal Egr-1 antibody (clone C19; TransCruz reagent for Gel Supershift and ChIP applications) was from Santa Cruz Biotechnology, Inc. (Santa Cruz, CA, USA).

2.1.9 Materials for Immunocytochemistry

DakoCytomation Antibody Diluent with Background Reducing Components was from Dako, Inc. (Carpinteria, CA, USA). Aceton was from Carl Roth GmbH (Karlsruhe, Germany). Hoechst 33258 and formaldehyde were from Sigma-Aldrich (Saint Louis, MO, USA). Moviol was from Merck Chemicals, Ltd. (Nottingham, UK). The Leica SP2 confocal laser-scanning microscope was from Leica Lasertechnik GmbH (Heidelberg, Germany).

2.1.10 Materials for Transfection

Oligofectamine and Lipofectamine RNAiMAX were from Invitrogen (Lofer, Austria). Egr-1 siRNA and scrambled control siRNA were from Santa Cruz Biotechnology, Inc. (Santa Cruz, CA, USA).

2.1.11 Materials for eNOS Activity Assay

Histamine, ionomycine, DMSO, $CaCl_2$, $MgCl_2$, EGTA, HCl, sodium acetate and L-citrulline were from Sigma-Aldrich (Saint Louis, MO, USA). L-[2,3-^{3}H]arginine hydrochloride (40-60 Ci/mmol) was from American Radiolabeled Chemicals (St. Louis, MO, USA). Ultima Gold™ liquid scintillation cocktail was from PerkinElmer (Waltham, MA, USA).

2.2 Methods

2.2.1 Cell Culture

Human EA.hy926 endothelial cells were grown in DMEM with 4.5 g/l glucose, 3.97 mM L-glutamine and 1 mM sodium pyruvate supplemented with 10% (v/v) FCS, 1% (v/v) P/S, 1 x HAT Supplement at 37°C in a humidified atmosphere (5% CO_2).

2.2.2 Preparation of human Lipoproteins

LDL (density = 1.035 – 1.065 g/ml) and HDL (subclass 3, density = 1.125 – 1.21 g/ml) were isolated from the plasma of healthy, normolipidemic patients by discontinuous density ultracentrifugation and stored at 4°C until usage (Malle *et al.*, 1995b; Malle *et al.*, 1994). In brief, KBr was used to adjust a density of 1.063 g/ml after addition of a point of a spatula of EDTA and sodium azide to fresh plasma. After centrifugation at 48,000 rpm for 24 h (10°C) the LDL fraction was recovered from the upper part and the HDL fraction was recovered from the lower part of the centrifuge tubes. Then LDL was dialysed against isotonic saline solution (0.15 M NaCl) for 30 min, a density of 1.027 g/ml was adjusted and the LDL was centrifuged for 24 h at 48,000 rpm (15°C) to remove the VLDL fraction. Next, a density of 1.63 g/ml was adjusted using NaCl, the LDL fraction was covered with isotonic saline solution and centrifuged for 24 h at 40,000 rpm (15°C). The LDL was recovered from the middle of the centrifuge tube and sterilized by filtration through a Rotilabo®-syringe filter and stored at 4°C until usage. To further purify HDL, KBr was added to the HDL fraction to adjust a density of 1.125 g/ml and HDL was centrifuged at 45,000 rpm for 24 h (10°C.) HDL was recovered from the lower part of the centrifuge tubes and a density of 1.21 g/ml was adjusted using KBr. After centrifugation at 40,000 rpm for 48 h (10°C) HDL_3 was recovered as supernatant. HDL_3 fraction was again centrifuged at 45000 rpm for 24 h (10°C) after adjusting density to 1.21 g/ml. The supernatant comprised the HDL_3 fraction that was sterilized by filtration through a Rotilabo®-syringe filter and stored at 4°C.

The protein concentration of isolated HDL and LDL was determined by the Lowry method, using BSA as a standard (Lowry *et al.*, 1951). Native lipoproteins were desalted using PD-10 desalting columns prior to modification.

2.2.3 HOCl Modification of (Lipo)proteins

Modification of HDL by reagent NaOCl was performed as described (Marsche *et al.*, 2002; Panzenboeck *et al.*, 1997). Briefly, 2.5 or 1 mg of HDL/ml of phosphate-buffered saline (PBS) (10 mM, pH 7.4) was modified at pH 7.4 by a single addition of NaOCl solution. Incubation of HDL and BSA with a final HOCl concentration in between 0.2 and 1.6 mM resulted in an oxidant: (lipo)protein molar ratio in between 25:1 and 200:1 (Malle *et al.*, 1995a; Marsche *et al.*, 2001). Modification of LDL by reagent NaOCl was performed as previously described (Malle *et al.*, 1995a). Briefly, 1 mg of LDL/ml of PBS was modified by the single addition of NaOCl solution and incubation for 60 min (4°C). Treatment of LDL with a final HOCl concentration in between 0.2 and 1.6 mM resulted in an oxidant:lipoprotein molar ratio in between 100:1 and 800:1. HOCl-modified (lipo)protein solutions were stored at 4°C und used between 12 and 24 h after preparation.

2.2.4 Modification of HDL by MPO

HDL was modified by the MPO-H_2O_2-chloride system as described by Panzenboeck et al (Panzenboeck *et al.*, 1997), but slightly modified (approx. oxidant:lipoprotein molar ratio of 25:1). Briefly, 1 mg of HDL/ml of PBS was modified at pH 7.4 and 37°C by alternate additions of H_2O_2 and MPO; in some experiments ascorbate was added (final concentrations: 440 µM H_2O_2, 8 µg/ml MPO and 14 µM ascorbate). The reaction mixture was stored at 4°C and used between 12 and 24 h after preparation.

2.2.5 Stimulation of Cells

2.2.5.1 Study of MAPK Activation

To study phosphorylation of p42/44 and p38 MAPK, cells were seeded in 6 well dishes and grown until reaching confluence. Medium was changed to

complete medium without FCS and HAT supplement 16 h prior to stimulation with 100 µg/ml HOCl-HDL, MPO-HDL or MPO-ascorbate HDL for 5 min. To investigate time-dependent phosphorylation of respective MAPKs, cells were stimulated with 100 µg/ml HOCl-HDL or native HDL for 1 up to 15 min. To determine concentration-dependent activation of MAPKs, cells were incubated with HOCl-HDL or native HDL (10 up to 200 µg/ml) for 5 min. To block MAPK activation cells were incubated with 25 µM of a p42/44 MAPK kinase inhibitor (PD98059) or with 10 µM of a p38 MAPK inhibitor (SB203580) for 30 min prior to stimulation of cells with 100 µg/ml of HOCl-HDL for 5 min. In all studies native HDL was used as a control.

2.2.5.2 Study of Egr-1 and Nrf2 Expression

Cells were grown in 6 well dishes until reaching confluence and 16 h prior to stimulation of cells, medium was changed to complete medium without FCS and HAT supplement. To study Egr-1 and Nrf2 expression on protein level, cells were incubated with 100 µg/ml of HOCl-HDL, MPO-HDL or MPO-ascorbate-HDL for 1.5 h. To determine time-dependent induction of transcription factors cells were stimulated with 100 µg/ml HOCl-HDL for 0.5 up to 4 h, whereas cells were incubated with 10 up to 200 µg/ml HOCl-HDL for 1.5 h to analyze concentration-dependent Egr-1 and Nrf2 activation. To determine the role of involved signaling pathways, cells were pre-incubated with respective inhibitors for MAPKs (25 µM PD98059 and 10 µM SB203580) for 30 min, for PI3K (25 µM LY294002) for 15 min or for PLC (10 µM U73122) for 10 min followed by stimulation with 100 µg/ml HOCl-HDL for 1.5 h. To investigate Er-1 and Nrf2 mRNA expression, cells were pre-incubated with PD98059, SB203580, LY294002 or U73122 respectively and pre-incubated and non-preincubated cells were then stimulated with 100 µg/ml HOCl-HDL for 0.5 up to 6 h. In all experiments native HDL was used as a control.

2.2.5.3 Study of Egr-1 DNA-binding Activity

Cells were seeded in dishes with a diameter of 6 cm and grown until reaching confluence. Medium was changed to complete medium without FCS

and HAT supplement 16 h prior to incubation of cells with 100 µg/ml of HOCl-HDL for 0.5 up to 6 h.

2.2.5.4 Study of Egr-1 nuclear Translocation

To study Egr-1 nuclear translocation via Western Blotting technique, cells were grown in dishes with 6 cm of diameter until reaching confluence. Medium was changed to complete medium without FCS and HAT supplement 16 h prior to stimulation of cells with 100 µg/ml HOCl-HDL for 0.5 up to 4 h. To investigate the involvement of upstream signaling pathways, cells were incubated with inhibitors (30 min 25 µM PD98059, 30 min 10 µM SB203580, 15 min 25 µM LY294002 or 10min 10 µM U73122) prior to stimulation with 100 µg/ml HOCl-HDL for 1 h. To study nuclear translocation via Immunofluorescence, cells were seeded in Lab-Tek chamber slides and grown until reaching 40% confluence. Then medium was changed to complete medium without FCS and HAT supplement, and after 16 h cells were incubated with 100 µg/ml HOCl-HDL for 1 h. In all experiments native HDL was used as a control.

2.2.5.5 Study of HO-1 Expression

Cells were seeded in 6 well dishes and grown until reaching confluence. Medium was changed to complete medium without FCS and HAT supplement and after 16 h cells were incubated with 100 µg/ml of HOCl-HDL, MPO-HDL or MPO-ascorbate-HDL for 12 h to follow HO-1 protein expression. Time- and concentration-dependent activation of HO-1 was followed by incubation with HOCl-HDL or native HDL for 4 up to 24 h or with increasing concentrations of HOCl-HDL or native HDL (10-200 µg/ml) for 12 h, respectively. To further observe the ability of various HOCl-modified (lipo)proteins to induce HO-1 protein expression, cells were incubated with 100 µg/ml of HOCl-HDL (50:1-200:1), HOCl-LDL (100:1-400:1), HOCl-BSA (25:1-100:1) or with HOCl-BSA (fatty acid-free; 50:1-100:1) for 12 h. To investigate the involvement of upstream signaling pathways in HO-1 induction, cells were incubated with PD98059 (30 min), SB203580 (30 min), LY294002 (15 min) or U73122 (10 min) prior to stimulation with HOCl-HDL for 12 h. To determine HO-1 expression on mRNA

level, cells were pre-incubated with PD98059, SB203580, LY294002, U73122 or with 2 µg/ml of Actinomycin D for 30 min prior to stimulation with HOCl-HDL for 0.5 up to 8 h. In all experiments native HDL was used as a control.

2.2.5.6 Study of eNOS Expression and Activity

Cells were cultured in 6 well dishes and grown until reaching confluence. 16 h prior to incubation of cells with 100 µg/ml HOCl-HDL or native HDL for 0.5 up to 24 h to assess eNOS mRNA expression or for 12 up to 24 h to determine eNOS protein expression, medium was changed to complete medium without FCS and HAT supplement. To investigate eNOS activity, cells were cultured in 6-well plates, medium was changed to complete medium without FCS and HAT supplement and after 16 h, cells were incubated with 100 µg/ml native- or HOCl-HDL for 16 and 24 h.

2.2.5.7 Study of Apoptosis and Cell Viability

To study apoptotic marker proteins caspase-3 and PARP via Western Blot analysis, cells were seeded in 6 well dishes and grown until reaching confluence. Medium was changed to complete medium without FCS and HAT supplement 16 h prior to incubation with 100 µg/ml HOCl-HDL or 1 µM staurosporine for 12 up to 24 h. To investigate cell viability via MTT Assay, the cells were cultured in 12-well dishes until reaching 50% confluence. After changing the medium to complete medium without FCS and HAT and incubation for 16 h, cells were incubated with 100 µg/ml of HOCl-HDL for 18 and 26 h. In all experiments native HDL was used as a control.

2.2.6 Western Blot Analysis

Cells were lysed on ice in 100 µl lysis buffer (50 mM HEPES, 150 mM NaCl, 1 mM EDTA, 10 mM $Na_4P_2O_7$, 2 mM Na_3VO_4, 10 mM NaF, 1% (v/v) Triton X-100, 10% (v/v) glycerol and Complete Mini protease inhibitor cocktail tablets; pH 7.4) for 10 min. Cell lysates were scraped and centrifuged at 21,000 *g* for 10 min (4°C) to remove cell debris. Protein concentration was determined using the Lowry method as previously described (Lowry *et al.*, 1951). Three-fold reducing

sample buffer (8% (w/v) SDS, 18% (v/v) glycerin, 114 mM Tris pH 6.8, 0.04% (w/v) bromphenol-blue and 5% (v/v) β-Mercaptoethanol) was added to equal amounts (50 to 100 µg) of total cell protein lysates, and heated for 5 min at 95°C. Samples were subjected to electrophoresis on NuPAGE® 4-12% Bis-Tris Gels in NuPAGE® MOPS SDS Running Buffer for 30 min at 50 V followed by 1 h at 150 V. Then proteins were blotted to nitrocellulose membranes in blotting-buffer (10 mM Tris-HCl, 39 mM glycine, 0.27 mM EDTA, 1.5 mM NaN_3) supplemented with 20 % (v/v) methanol for 40 min at 200 mA. Membranes were stained with Ponceau S solution to confirm transfer of proteins, washed 3 times with TBS-T washing buffer (150 mM NaCl, 10 mM Tris pH 7.4, 0.4 mM Tween-20) and blocked with 5% (w/v) non-fat milk in TBS-T washing buffer pH 7.4 for 30 min. Afterwards membranes were incubated with the respective primary antibodies (Table 1) diluted in 5% (w/v) BSA in TBS-T washing buffer at 4°C overnight, that are recognizing the respective human epitopes.

Table 1: *Primary antibodies for Western blotting experiments*

primary antibodies	dilution
mouse monoclonal pp44/42 MAPK (Erk1/2)	1:1000
rabbit polyclonal pp38 MAPK	1:1000
rabbit polyclonal Egr-1 (C19)	1:1000
rabbit polyclonal Nrf2 (C-20)	1:1000
rabbit polyclonal HO-1 (Hsp32)	1:1000
rabbit polyclonal eNOS	1:5000
rabbit polyclonal Caspase-3	1:1000
mouse monoclonal PARP (C-2-10)	1:1000
mouse monoclonal β-Actin (C4)	1:1000
rabbit polyclonal Lamin A/C (H-110)	1:1000

Membranes were washed 3 times for 10 min with TBS-T washing buffer and were incubated with the following secondary antibodies diluted in blocking solution for 2 h at 25°C: peroxidase-conjugated goat anti-rabbit IgG (1:50,000) and peroxidase-conjugated goat anti-mouse IgG (1:50,000). Membranes were washed 3 times for 10 min with TBS-T washing buffer and immunoreactive bands were visualized using Super Signal West Pico Chemiluminescent substrate or Immobilon™ Western Chemiluminescent HRP Substrate and

Hyperfilm™ MP. To reprobe membranes with another set of antibodies, membranes were stripped with stripping buffer (1 M NaCl, 0.1 M glycine, pH 2.15) twice for 10 min (25°C).

2.2.7 RNA Isolation and Real-time RT-PCR

2.2.7.1 Isolation of total RNA, DNase I Digestion and Reverse Transcription

Total RNA was isolated using QIAshredder and RNeasy Mini Kit according to manufacturers instructions. Total RNA (1 µg) was subjected to DNase I digestion to convert single- and double-stranded DNA into oligodeoxy-ribonucleotides prior to reverse transcription using random hexamer primers. In brief, 1 µg of total RNA was digested with 1 µl 10-fold DNase I Reaction Buffer, 1 µl DNase I (1 U/µl) and RNase-free water in a total of 10 µl for 15 min at 25°C. DNase I was inactivated by the addition of 1 µl of 25 mM EDTA and incubation for 10 min at 65°C. DNase I-digested RNA (1 µg) was reverse transcribed using SuperScript® II Reverse Transcriptase. Briefly, 1 µg RNA, 0.6 µl of 25 µM Random Hexamers and 1.8 µl RNase-free water were incubated for 5 min at 65°C and 10 min at 25°C prior to the addition of 4 µl of 5-fold First-Strand Buffer, 2 µl of 0.1 M DTT, 0.625 µl of 20 mM dNTPs, 0.5 µl of 40 U/µl RNaseOUT™ and 0.5 µl of 200 U/µl SuperScript® II Reverse Transcriptase. The reaction mixture was incubated for 90 min at 70°C and subsequently for 15 min at 70°C and cDNAs were stored at -20°C until usage.

2.2.7.2 Real-time PCR

Six ng of cDNA was used as template for each Real-time PCR. Gene expression was determined by quantitative Real-time PCR using the LightCycler® 480 system and the QuantiFast SYBR Green PCR Kit. QuantiTect Primer Assays were used to determine gene expression of Egr-1 (Hs_Egr1_2_SG), HO-1 (Hs_HMOX1_1_SG), eNOS (Hs_NOS3_1_SG) and GAPDH (glyceraldehyde-3-phosphate dehydrogenase; Hs_GAPDH_2_SG), respectively. For detection of Nrf2 gene expression following primer pair was used: forward 5'-TAC TCC CAG GTT GCC CAC A–3' and reverse 5'-CAT CTA

CAA ACG GGA ATG TCT GC–3'. Fold change in gene expression levels of the target gene compared to the housekeeping gene GAPDH was calculated by the $2^{-\Delta\Delta CT}$ method.

2.2.8 EMSA

2.2.8.1 Isolation of nuclear Protein Extracts

Cells were scraped in PBS, centrifuged at 500 *g* for 3 min (4°C) and nuclear proteins were isolated using NE-PER extraction reagents according to the manufacturer's suggestions. In brief, protease inhibitor tablets were added to buffers CER1 and NER, supplied by the NE-PER kit, and to obtain non-denatured, active proteins all steps were carried out at 4°C. After addition of 200 µl of CER1 buffer to the pelleted cells, vortexing for 15 sec, and 10 min incubation, 11 µl of CER2 buffer (supplied by the NE-PER kit) was added to disrupt cell membranes and to release the cytoplasmic contents. The mixture was vortexed for 5 sec, incubated for 1 min, vortexed for 5 sec and centrifuged for 5 min at 16,000 *g* to separate the cytoplasmic extracts from the intact nuclei. The supernatant containing the cytoplasmic fraction was removed and stored at -70°C, whereas the pelleted nuclei were lysed by addition of 100 µl of NER buffer and incubation for 40 min interrupted by 15 sec of vortexing every 10 min. The mixture was centrifuged for 10 min at 16,000 *g* and the supernatant containing the nuclear fraction was stored at -70°C. Nuclear protein concentration was determined using the BCA™ Protein Assay kit.

2.2.8.2 Annealing of Egr-1 Probe

Oligonucleotide sequences representing the Egr-1 consensus binding site were: 5'-GGA TCC AGC GGG GGC GAG CGG GGG CGA–3' and 3'-CCT AGG TCG CCC CCG CTC GCC CCC GCT–5'. Complementary oligonucleotides were annealed by incubating the reaction mixture (20 µl of each oligonucleotide (1.75 pmol/µl), 5 µl 10x PCR-buffer, 1.88 µl of 25 mM $MgCl_2$ and 3 µl H_2O) for 5 min at 95°C and then cooling down to 25°C.

2.2.8.3 Radioactive Labeling of Egr-1 Probe

Egr-1 oligonucleotides were labeled with [γ-^{32}P]-ATP using T4 polynucleotide kinase. Briefly, 5 µl of 0.7 pmol/µl Egr-1 probe, 1 µl 10x T4 polynucleotide kinase buffer, 2.2 µl [γ-^{32}P]-ATP (3000 Ci/mmol, 10 mCi/ml), 0.8 µl nuclease-free water and 1 µl T4 polynucleotide kinase (5-10 U/µl) were incubated for 10 min at 37°C. Labeling reaction was stopped by the addition of 1 µl 0.5 M EDTA and 89 µl of TE buffer. Unincorporated radioactivity was removed using Micro BioSpin 6 columns according to manufacturers instructions. Labeled Egr-1 probe was stored at 4°C until usage.

2.2.8.4 EMSA Binding Reaction and Electrophoresis of DNA-Protein-Complexes

Five µg of nuclear protein extracts were incubated with the binding buffer containing 10 mM Tris pH 7.5, 50 mM NaCl, 1 mM DTT, 0.1 mM EDTA, 5% glycerol (v/v), 0.25 µg Poly[d(I-C)] and 5 µg BSA for 10 min. After addition of 1 µl of labeled oligonucleotide to each sample EMSA binding reaction took place for 20 min. Supershift experiments were performed as previously described (Faour *et al.*, 2005; Zhang *et al.*, 2007), but slightly modified. In brief, nuclear protein extracts were either incubated with the binding buffer and an anti-Egr-1 antibody for 10 min prior to incubation with the probe for 20 min or nuclear extracts were incubated with the binding buffer for 10 min, followed by incubation with the probe for 20 min and incubation with the antibody for 15 min. All incubation steps were carried out at 25°C. A 20-fold molar excess of nonradiolabeled oligonucleotides was added to the samples prior to the addition of labeled probe for competition experiments. Glycerol was added to a final concentration of 20% (v/v) and samples were subjected to polyacrylamide gel electrophoresis (3.9% (w/v) polyacrylamide gel; acrylamide:bisacrylamide, 29:1) in 0.25% (w/v) Tris boric acid buffer at 120 V (25°C) for 3.5 h. The gel was dried under vacuum at 80°C for 1.5 h and then exposed to Hyperfilm™ MP for 12 to 24 h.

2.2.9 Isolation of cytosolic and nuclear Proteins

For translocation experiments, nuclear and cytosolic proteins were isolated using a modification of the method of Dignam (Dignam *et al.*, 1983; Solan *et al.*, 2002). Briefly, cells were washed twice with ice-cold PBS and once with cold buffer A (10 mM Hepes pH 7.9, 1.5 mM $MgCl_2$, 10 mM KCl, 1 mM DTT and Complete Mini protease inhibitor cocktail tablets). Cells were lysed in buffer A including 0.1% (v/v) Nonidet P-40 for 10 min on ice, centrifuged at 4500 *g* for 10 min (4°C) and the supernatant, containing the cytosolic fraction, was stored at -70°C. The nuclear pellet was washed once in PBS, once in buffer A and lysed in buffer C (20 mM Hepes pH 7.9, 0.42 M NaCl, 1.5 mM $MgCl_2$, 0.2 mM EDTA, 1 mM DTT, 25% (v/v) glycerol and Complete Mini protease inhibitor cocktail tablets) for 30 min on ice. Samples were centrifuged at 21,000 *g* for 20 min (4°C) and the supernatant, containing the nuclear fraction, was stored at -70°C.

2.2.10 Immunofluorescence and Confocal Laser-scanning Microscopy

Lab-Tek chamber slides were washed with PBS, fixed with 3.7% (v/v) formaldehyde for 20 min and re-hydrated in PBS. After incubation with cold (-20°C) acetone for 3 min (4°C), slides were again re-hydrated in PBS and blocked with DakoCytomation Antibody Diluent with Background Reducing Components for 45 min at 25°C. Slides were then incubated with a rabbit anti-Egr-1 (C19) as a primary antibody diluted with Antibody Diluent 1:50 for 45 min (25°C), washed with PBS and incubated with a Cy-3 labeled goat anti-rabbit as a secondary antibody (1:250) for 45 min (25°C). After rinsing in PBS for 15 min at 25°C, Hoechst 33258 was added to the slides for 15 min to counterstain nuclei. Slides were washed with PBS and mounted with Moviol. Slides were analyzed on a confocal laser-scanning microscope using the 405 nm laser line for the excitation of Hoechst and the 543 nm line for Cy-3. Detection settings were: 420-470 nm for Hoechst Stain and 590-670 nm for Cy-3. Control experiments were performed by omitting the primary antibody.

2.2.11 siRNA Transfection

2.2.11.1 siRNA Transfection and Analysis of Egr-1 and HO-1 Expression on mRNA and Protein Level using Lipofectamine RNAiMax

Cells were cultured in 6-well plates and grown until reaching 50% confluence. Prior to the transfection, cells were washed once with transfection medium (DMEM 4.5 g/l glucose without FCS, HAT supplement and P/S) and then 800 µl of transfection medium was added to the cells. Egr-1 siRNA (50 nM) or scrambled control siRNA (50 nM) were diluted in transfection medium to give a total of 100 µl. Four µl of Lipofectamine RNAiMAX transfection reagent were mixed with 96 µl of transfection medium and were incubated for 10 min at 25°C. The diluted siRNA duplex was then combined with the diluted Lipofectamine RNAiMAX, mixed and incubated for 20 min (25°C). The transfection complex (200 µl) was added to the respective cells and transfection took place while 6 h incubation time at 37°C in a humidified atmosphere (5% CO_2). The transfection complex was removed and 4 ml of post-transfection medium (DMEM 4.5 g/l glucose with 10% (v/v) FCS, 1 x HAT supplement) was added to the cells. Medium was changed to complete medium without FCS and HAT 30 h after transfection and 16 h prior to incubation with 100 µg/ml HOCl-HDL for 1 or 4 h to determine mRNA expression of Egr-1 or HO-1 and for 1.5 or 12 h to assess protein expression levels of Egr-1 and HO-1, respectively.

2.2.11.2 siRNA Transfection and Determination of Egr-1 nuclear Translocation using Oligofectamine

Cells were seeded in 6-well plates and maintained in complete medium until they reached 50% confluence. After washing the cells once with transfection medium (DMEM 4.5 g/l glucose, without FCS, HAT supplement and Penicillin-Streptomycin) 800 µl of transfection medium was added to the cells. Four µl of the transfection reagent Oligofectamine were combined with 21 µl of transfection medium and incubated for 10 min (25°C). Egr-1 siRNA (100 nM) or scrambled control siRNA (100 nM), respectively, were mixed with transfection medium and then the siRNA duplexes (175 µl) were mixed with the Oligofectamine solution (25 µl) and incubated for 20 min at 25°C. Afterwards,

200 µl of transfection complex was added to the cells and they were incubated for 5 h at 37°C in a humidified atmosphere (5% CO_2). Then 3 ml of post-transfection medium (DMEM 4.5 g/l glucose containing as many FCS and HAT supplement that the final volume of 4 ml medium is supplemented with 10% (v/v) FCS and 1 x HAT) were added and after 48 h medium was changed to complete medium without FCS and HAT supplement for another 16 h. Cells were incubated with 100 µg/ml HOCl-HDL for 1 h and nuclear and cytosolic extracts were prepared using a modification of the method of Dignam et al (Dignam *et al.*, 1983; Solan *et al.*, 2002).

2.2.12 eNOS Activity Assay

The eNOS activity assay was performed as described (Schmidt *et al.*, 2010; Schmidt *et al.*, 1999), but slightly modified. After washing the cells twice with incubation buffer (50 mM Tris pH 7.4, 3 mM $CaCl_2$, 1 mM $MgCl_2$), reactions were started by the addition of 50 µl L-[2,3-^{3}H]arginine (~10^6 dpm) to 850 µl incubation buffer and where indicated additionally with 100 µl 10 µM ionomycine, 1 mM histamine or H_2O. After 5 min incubation time at 37°C, the reaction was terminated by aspiration of the reaction mixture and washing the cells twice with cold (4°C) washing buffer (50 mM Tris pH 7.4, 1 mM $MgCl_2$, 100 µM EGTA). Cells were lysed in 1 ml HCl (10 mM) for 30 min at 25°C and then aliquots (100 µl) were removed for determination of incorporated radioactivity. To the remaining samples (900 µl), 100 µl sodium acetate buffer (200 mM sodium acetate, 10 mM L-citrulline, pH 12.6) was added (final pH ~ 5.0). Each of the samples (1 ml) was loaded on a cation-exchange chromatography column to separate L-[^{3}H]citrulline from L-[^{3}H]arginine. Radioactivity was determined using a liquid-scintillation-counter and the Ultima Gold™ liquid scintillation cocktail. Values are expressed as percentage conversion of incorporated L-[^{3}H]arginine into L-[^{3}H]citrulline.

2.2.13 MTT Assay

The medium was removed and cells were washed twice with PBS prior to addition of 0.5 mg/ml of MTT diluted in complete medium without FCS and HAT)

to each well. After 2 h incubation time, MTT was removed, acidic isopropanol (0.04 M HCl in absolute isopropanol) was added to lyse the cells and dishes were shaken for 3 min to dissolve the built formazan crystals. The supernatant, containing the formazan, was removed, centrifuged for 2 min at 13000 rpm and MTT reduction was measured spectrophotometrically at 570 nm. The measured values at 570 nm were corrected for background absorbance at 630 nm.

2.2.14 Statistical Analysis

Statistical analysis was performed for Real-time PCR and densitometric evaluation of immunoreactive bands. Data are expressed as means ± SD. One-way ANOVA including Bonferroni posttest was performed by using Prism 5 software (Graphpad Software, La Jolla, CA, USA). Means were considered as significantly different at $p < 0.05$.

2.2.15 Densitometric Evaluation of Immunoreactive Bands

Immunoreactive bands were scanned and the intensity of Western blot bands was determined using ImageJ 1.40g software from Wayne Rasband of the National Institutes of Health (Bethesda, MD, USA). The relative intensity of each band was calculated by dividing the absolute intensity of each sample band by the absolute intensity of the respective loading control band. Relative intensities were normalized to the level in non-stimulated control cells.

3. Results

3.1 HDL and HOCl-HDL-mediated Activation of MAPKs

3.1.1 Time- and concentration-dependent Activation of MAPKs by HDL

Previous reports showed that native HDL is able to promote activation of p38 MAPK in HUVECs (Norata *et al.*, 2004b). We here demonstrate that native HDL induces phosphorylation of p42/44 and p38 MAPKs in a time- (1-15 min) and concentration-dependent (10-200 µg/ml) manner in human EA.hy926 endothelial cells (**Fig. 3A** and B, Supplement Fig. I). Maximum phosphorylation was observed after 5 to 10 minutes incubation time at a concentration of 100 µg/ml.

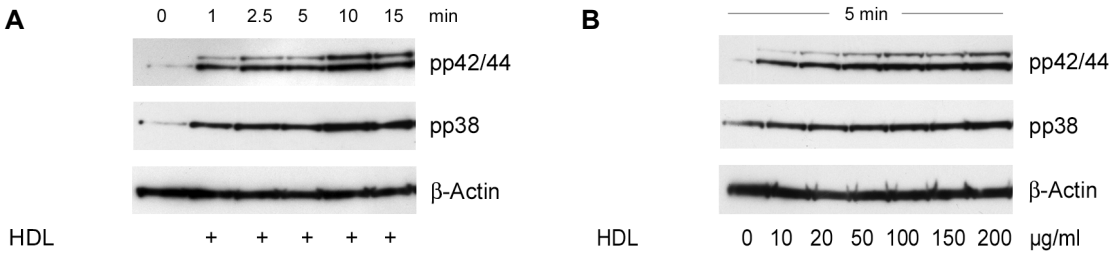

Figure 3: *Western blot analysis of HDL-induced MAPK activation in EA.hy926 cells.* **A** Cells were incubated with 100 µg/ml HDL for indicated times (1-15 min). **B** Cells were incubated with indicated concentrations of HDL (10–200 µg/ml) for 5 min. **A-B** Cells were lysed and equal amounts of proteins were subjected to Western blot analysis for pp42/44 and pp38 MAPKs. β-Actin was used as a loading control. Lane 1 (**A**) represents non-stimulated cells. One representative experiment out of three is shown.

3.1.2 Time- and concentration-dependent Activation of MAPKs by HOCl-HDL

Norata and colleagues (Norata *et al.*, 2004a) reported that copper-oxidized HDL induced phosphorylation of p38 MAPK in HUVECs. We investigated in a next series of experiments, time- and concentration-dependent activation of MAPKs in HOCl-HDL-treated human EA.hy926 endothelial cells. Western blot experiments revealed that incubation of cells with HOCl-HDL

enhanced phosphorylation of p42/44 and p38 MAPKs in a time- (1–15 min) and concentration-dependent (10–200 µg/ml) manner compared to non-stimulated cells (**Fig. 4A** and B, Supplement Figure II). Stimulation of cells with native HDL led to increased phosphorylation of MAPKs compared to non-stimulated cells, but was less pronounced compared to HOCl-HDL-treated cells. Maximum phosphorylation was observed between 5 and 10 min incubation time at a concentration of 100 µg/ml.

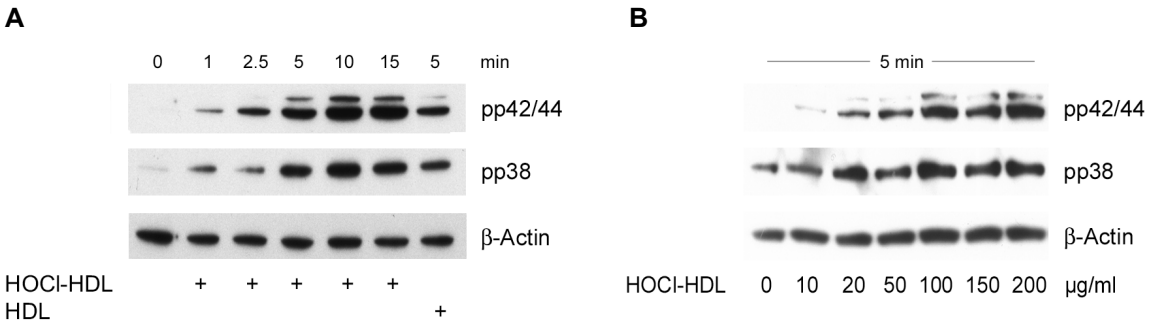

Figure 4: *Western blot analysis of HOCl-HDL-induced MAPK activation in EA.hy926 cells.* **A** Cells were incubated with 100 µg/ml HOCl-HDL or HDL for indicated time points (1-15 min). **B** Cells were incubated with indicated concentrations of HOCl-HDL (10–200 µg/ml) for 5 min. **A-B** Cells were lysed and equal amounts of proteins were subjected to Western blot analysis for pp42/44 and pp38 MAPKs. β-Actin was used as a loading control. Lane 1 (**A**) represents non-stimulated cells. One representative experiment out of three is shown.

3.1.3 Effect of MAPK Inhibitors on HOCl-HDL-mediated Activation of MAPKs

To investigate the ability of MAPK inhibitors to block the respective MAPK, cells were incubated with PD98059 (inhibitor for p42/44 MAPK kinase) or with SB203580 (inhibitor for p38 MAPK) prior to stimulation with HOCl-HDL for 5 min. Preincubation of cells with PD98059 completely abolished HOCl-HDL-induced phosphorylation of p42/44 MAPK (**Fig. 5,** Supplement Figure III). Incubation of cells with SB203580, however, did not impair phosphorylation of p38 MAPK but even enhanced immunoreactive p42/44 MAPK signal.

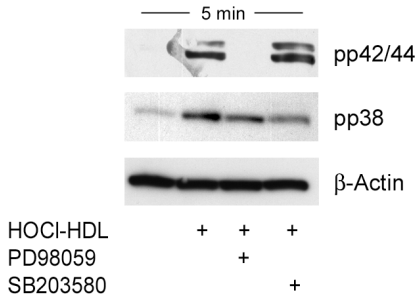

Figure 5: *Western blot analysis of HOCl-HDL-induced MAPK activation in EA.hy926 cells in the absence or presence of MAPK inhibitors.* Cells were incubated for 30 min with 25 µM PD98059 (p42/44 MAPK kinase inhibitor) or 10 µM SB203580 (p38 MAPK inhibitor) prior to stimulation with 100 µg/ml HOCl-HDL for 5 min. Cells were lysed and equal amounts of proteins were subjected to Western blot analysis for pp42/44 and pp38 MAPKs. β-Actin was used as a loading control. Lane 1 represents non-stimulated cells. One representative experiment out of three is shown.

3.1.4. Chlorinated HDL-mediated Activation of MAPKs

Next, we investigated, whether and to what extent MPO-modified HDL, as occurring under *in vivo* conditions, is able to induce phosphorylation of p42/44 and p38 MAPKs. Incubation of cells with native HDL or HDL modified by HOCl, added as reagent (HOCl-HDL) or generated enzymatically by the MPO-H_2O_2-chloride system in the absence (MPO-HDL) or presence of ascorbate (an enhancer of chlorination reaction of MPO (Marquez *et al.*, 1990); MPO-Asc-HDL), increased phosphorylation of p42/44 and p38 MAPK compared to non-stimulated cells (**Fig. 6**).

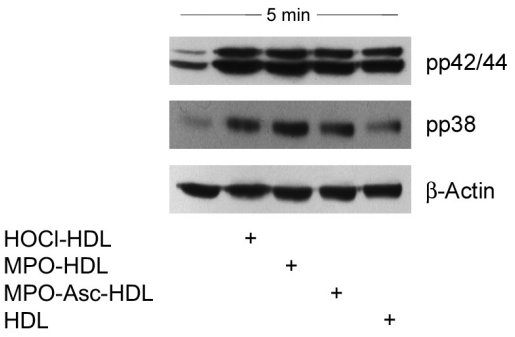

Figure 6: *Western blot analysis of HOCl-HDL- and MPO-HDL-induced MAPK activation in EA.hy926 cells.* Cells were incubated with 100 µg/ml HOCl-HDL (oxidant : lipoprotein molar ratio of 200:1), HDL, MPO-HDL or MPO-Asc-HDL for 5 min. Cells were lysed and equal amounts of proteins were subjected to Western blot analysis for pp42/44 and pp38 MAPKs. β-Actin was used as a loading control. Lane 1 represents non-stimulated cells. One representative experiment out of three is shown.

3.2 HOCl-HDL-mediated Activation of Transcription Factors

3.2.1 Time- and concentration-dependent Protein Expression of Egr-1/Nrf2 by HOCl-HDL

Another set of experiments was aimed to identify transcription factors involved in the activation pathway of HO-1 EA.hy926 cells treated with HOCl-HDL. It is reported that Egr-1 plays a role in the development of atherosclerosis (Khachigian, 2006) and that Nrf2 is involved in the induction of antioxidant defense genes in vascular atherosclerotic disease (Nguyen *et al.*, 2003). Additionally it was shown that Egr-1 and Nrf2 might be involved in the activation mechanism of HO-1 under various stimuli (Anwar *et al.*, 2005; Chen *et al.*, 2010; Nguyen *et al.*, 2003; Yang *et al.*, 2001).

We performed Western blot experiments to follow time- and concentration-dependent activation of transcription factors Egr-1 and Nrf2. Treatment of cells with HOCl-HDL caused a time- (0.5–4 h) and concentration-dependent (10–200 µg/ml) induction of Egr-1 expression compared to non-stimulated cells (**Fig. 7A** and B, Supplement Figure IV). Maximum induction of Egr-1 protein by HOCl-HDL was observed between 1 and 1.5 h and at a concentration of 200 µg/ml.

The stimulation with native HDL caused only a slight activation of Egr-1. Nrf2, however, remained constitutively expressed when cells were treated with native or modified HDL.

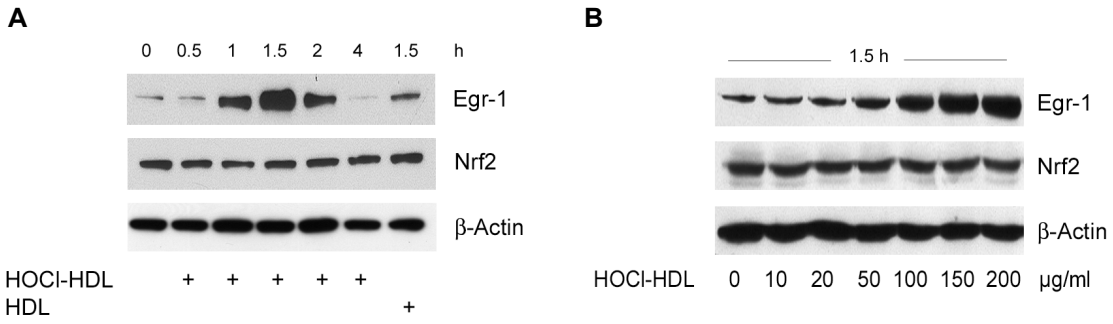

Figure 7: *Western blot analysis of HOCl-HDL-induced Egr-1 and Nrf2 expression in EA.hy926 cells.* **A** Cells were incubated with 100 µg/ml HOCl-HDL or HDL for indicated time points (0.5–4 h). **B** Cells were incubated with indicated concentrations of HOCl-HDL (10–200 µg/ml) for 1.5 h. **A-B** Cells were lysed and equal amounts of proteins were subjected to Western blot analysis for Egr-1 and Nrf2. β-Actin was used as a loading control. Lane 1 (**A**) represents non-stimulated cells. One representative experiment out of three is shown.

3.2.2 Chlorinated-HDL-mediated Protein Expression of Egr-1/Nrf2

Next, cells were treated with HDL modified by reagent HOCl or by the MPO-H_2O_2-chloride system in the absence or presence of ascorbate for 1.5 h. Incubation of cells with modified HDL (HOCl-HDL, MPO-HDL, MPO-Asc-HDL) led to a pronounced Egr-1 protein expression compared to non-stimulated cells (**Fig. 8**). Stimulation of cells with native HDL led only to a slight induction of Egr-1 protein expression. Nrf2 was constitutively expressed and the immunoreactive signal remained unaffected by the presence of native and modified HDL.

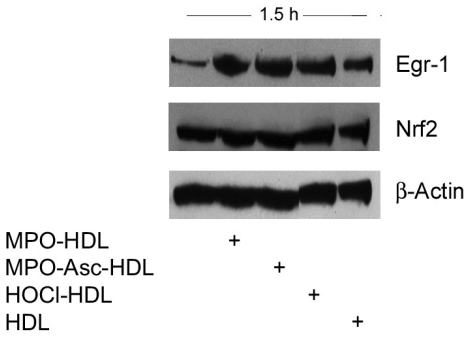

Figure 8: *Western blot analysis of HOCl-HDL- and MPO-HDL-induced Egr-1 and Nrf2 expression in EA.hy926 cells.* Cells were incubated with 100 µg/ml HOCl-HDL, HDL, MPO-HDL or MPO-Asc-HDL for 1.5 h. Cells were lysed and equal amounts of proteins were subjected to Western blot analysis for Egr-1 and Nrf2. β-Actin was used as a loading control. Lane 1 represents non-stimulated cells. One representative experiment out of three is shown.

3.2.3 Effect of MAPK Inhibitors on HOCl-HDL-mediated Protein Expression of Egr-1/Nrf2

To investigate, whether expression of Egr-1 is dependent on activation of the MAPK signaling, cells were incubated with respective pharmacological inhibitors prior to stimulation with HOCl-HDL. Incubation of cells with the p42/44 MAPK kinase inhibitor (PD98059) completely abolished HOCl-HDL-mediated Egr-1 protein expression. Preincubation of cells with the p38 MAPK inhibitor SB203580 further increased Egr-1 expression compared to HOCl-HDL-treated cells (**Fig. 9**). Concordant with data from Figures 7 and 8, HOCl-HDL did not affect expression of Nrf2 on the protein level.

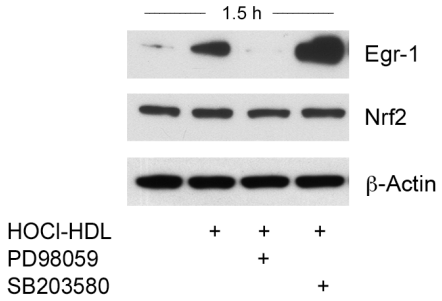

Figure 9: *Western blot analysis of HOCl-HDL-induced Egr-1 and Nrf2 expression in EA.hy926 cells in the absence or presence of MAPK inhibitors.* Cells were incubated for 30 min with 25 µM PD98059 or 10 µM SB203580 prior to stimulation with 100 µg/ml HOCl-HDL for 1.5 h. Cells were lysed and equal amounts of proteins were subjected to Western blot analysis for Egr-1 and Nrf2. β-Actin was used as a loading control. Lane 1 represents non-stimulated cells. One representative experiment out of three is shown.

3.2.4 Effect of PI3K and PLC Inhibitors on HOCl-HDL-mediated Protein Expression of Egr-1/Nrf2

The next set of experiments aimed to investigate the involvement of PI3K and PLC in the activation of Egr-1 and Nrf2 by HOCl-HDL. Western blot experiments revealed that blocking of PLC (U73122) had no effect on HOCl-HDL-mediated Egr-1 expression. However, inhibition of PI3K by LY294002 increased HOCl-HDL mediated Egr-1 protein expression (**Fig. 10**). In contrast to Egr-1, Nrf2 was constitutively expressed.

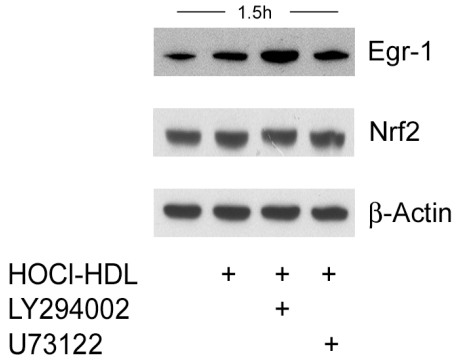

Figure 10: *Western blot analysis of HOCl-HDL-induced Egr-1 and Nrf2 expression in EA.hy926 cells in the absence or presence PI3K and PLC inhibitors.* Cells were incubated for 15 min with 25 µM LY294002 (PI3K inhibitor) or for 10 min with 10 µM U73122 (PLC inhibitor) prior to stimulation with 100 µg/ml HOCl-HDL for 1.5 h. Cells were lysed and equal amounts of proteins were subjected to Western blot analysis for Egr-1 and Nrf2. β-Actin was used as a loading control. Lane 1 represents non-stimulated cells. One representative experiment out of three is shown.

3.2.5 HOCl-HDL-mediated mRNA Expression of Egr-1/Nrf2 in the absence or presence of Pathway Inhibitors

Next, cells were stimulated with HOCl-HDL or native HDL in the absence or presence of specific pathway inhibitors and Real-time RT-PCR analysis was performed to investigate expression of transcription factors Egr-1 and Nrf2 on mRNA level. HOCl-HDL led to a time-dependent (0.5–6 h) increase in Egr-1 mRNA expression with a significant increase after 0.5 and 1 h compared to non-stimulated cells (**Fig. 11A**). Treatment of cells with PD98059 significantly reduced HOCl-HDL-mediated Egr-1 mRNA expression. Incubation of cells with U73122, however, had no effect on HOCl-HDL-mediated Egr-1 expression. Concordant with findings regarding Egr-1 protein expression, incubation of cells with SB203580 or LY294002 did not block but even potentiated HOCl-HDL-mediated Egr-1 mRNA expression. Consistent with data on Nrf2 protein expression, Nrf2 was constitutively expressed on mRNA level under HOCl-HDL stimulation (Fig. 11B).

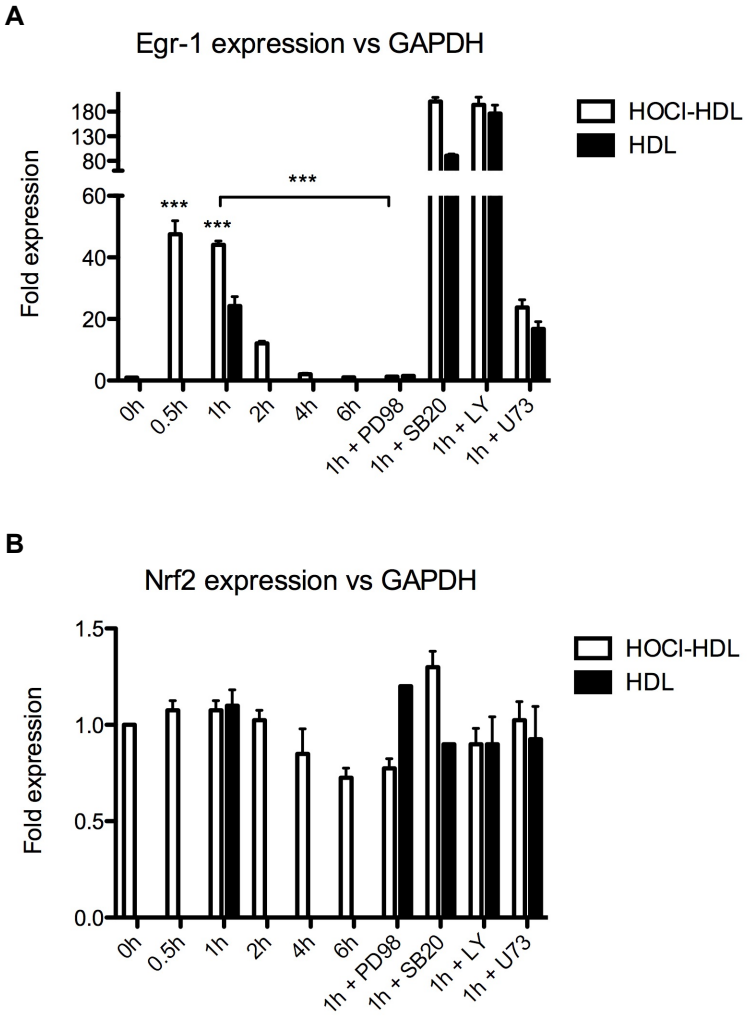

Figure 11: *Real-time RT-PCR of HOCl-HDL-stimulated Egr-1 and Nrf2 expression in EA.hy926 cells in absence or presence of pathway inhibitors.* **A-B** Cells were preincubated with 25 µM PD98059 (30 min), 10 µM SB203580 (30min), 25 µM LY294002 (15 min) or with 10 µM U73122 (10 min), respectively. Preincubated and non-preincubated cells were then stimulated with 100 µg/ml HOCl-HDL or HDL for indicated time points (0.5–6 h). RNA was isolated, treated with DNase, reverse transcribed and equal amounts of cDNA were subjected to Real-time-PCR for Egr-1 (**A**) and Nrf2 (**B**). Egr-1 and Nrf2 expression levels were normalized to GAPDH. One representative experiment out of three is shown. (*** $p<0.001$).

3.3 Nuclear Translocation of Egr-1

3.3.1 HOCl-HDL-mediated nuclear Translocation of Egr-1

To investigate the ability of transcription factors Egr-1 and Nrf2 to undergo nuclear translocation after HOCl-HDL stimulation, cytosolic and nuclear

protein extracts from endothelial cells were subjected to Western blot analysis. HOCl-HDL stimulation led to a maximum of Egr-1 protein expression in the cytosolic fraction after 1 h compared to non-stimulated cells (**Fig. 12A**). Egr-1 nuclear translocation was observed after 1-1.5 h of HOCl-HDL stimulation compared to non-stimulated cells (Fig. 12A). Incubation of cells with HOCl-HDL caused a time-dependent increase in the protein amount of nuclear Egr-1 with a maximum after 1 h compared non-stimulated cells (Fig. 12B). HDL caused a less pronounced nuclear translocation of Egr-1 compared to HOCl-HDL (Fig. 12B). Contrary to Egr-1, Nrf2 was constitutively expressed in the cytosolic fraction and did not undergo nuclear translocation by HOCl-HDL treatment (Fig. 12A-B).

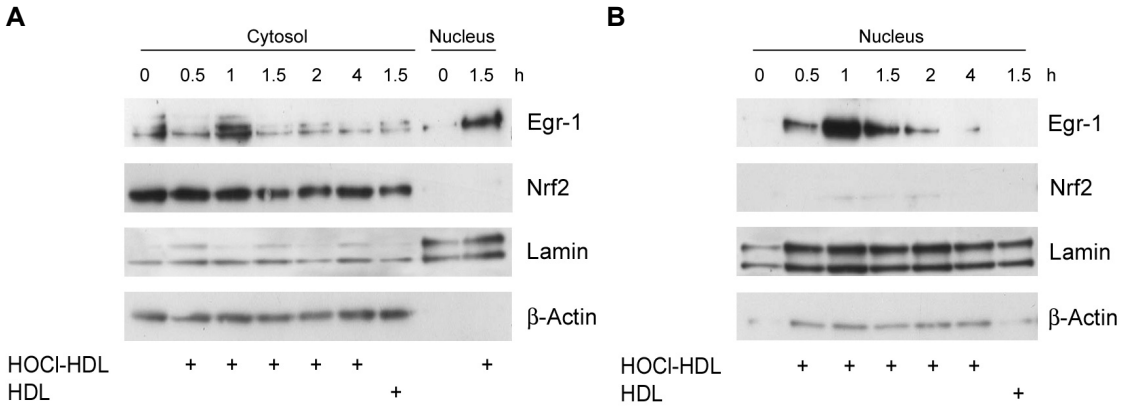

Figure 12: *HOCl-HDL-induced nuclear translocation of Egr-1 in EA.hy926 cells.* **A-B** Cells were incubated with 100 µg/ml HOCl-HDL or HDL for indicated times (0.5–4 h). Cells were lysed, nuclear and cytosolic extracts were isolated and equal amounts of proteins were subjected to Western blot analysis for Egr-1 and Nrf2. β-Actin was used as a cytosolic and Lamin as a nuclear loading control. Lanes 1 and 8 (**A**) and Lane 1 (**B**) represent non-stimulated cells. **A-B** One representative experiment out of three is shown.

Immunocytochemistry experiments confirmed increased nuclear translocation of Egr-1 in HOCl-HDL-treated cells compared to the cytosolic localization of Egr-1 in HDL- or non-stimulated cells (**Fig. 13**). Egr-1 staining is shown in red and nuclear counterstain (Hoechst) in blue. Control experiments (antibody control) were performed by omitting the primary antibody. (Microscopy was done with the help of Dr. Astrid Hammer, Medical University of Graz).

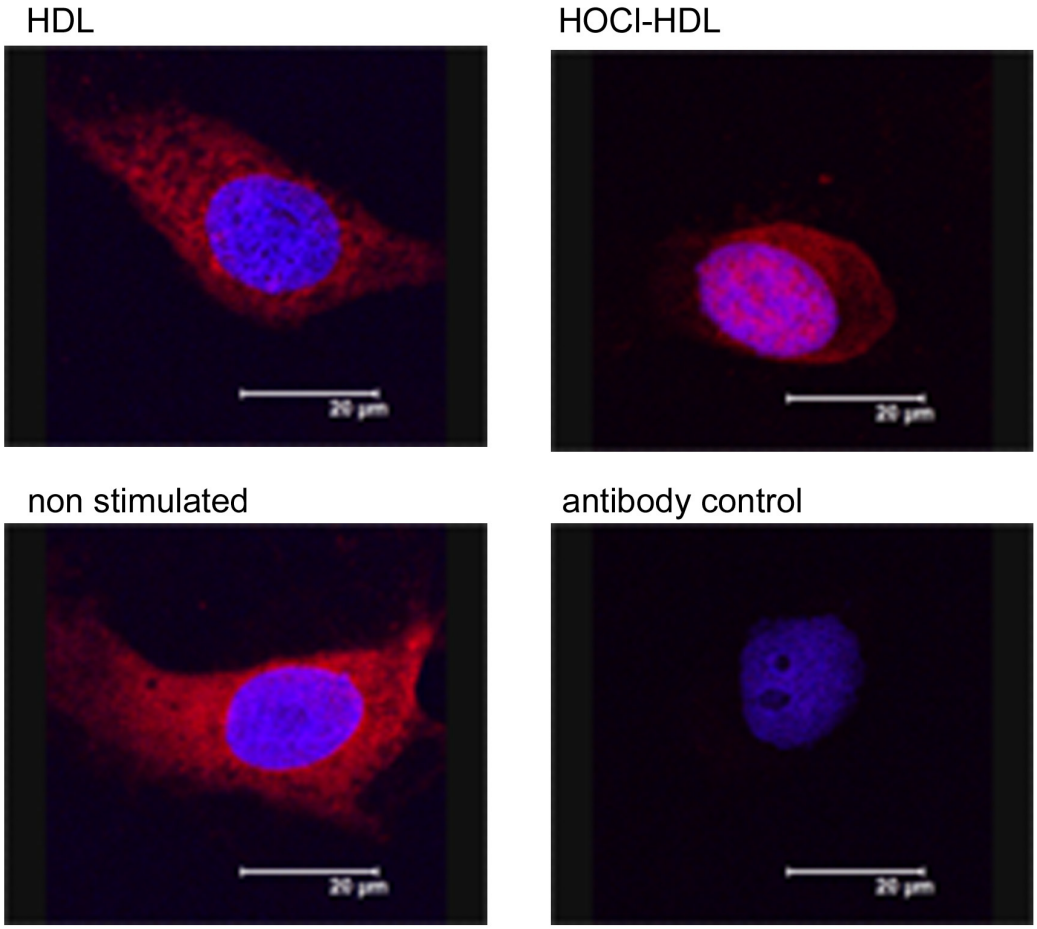

Figure 13: *Immunocytochemistry of HOCl-HDL-induced nuclear translocation of Egr-1 in EA.hy926 cells.* (Microscopy was done by Dr. Astrid Hammer, Institute of Cell Biology, Histology and Embryology, Center of Molecular Medicine, Medical University of Graz, Austria.). Cells were seeded in chamber slides and stimulated with 100 µg/ml HOCl-HDL or HDL for 1 h. Cells were incubated with primary rabbit anti-Egr-1 antibody and secondary Cy-3-labeled goat-anti-rabbit antibody (red). Nuclei were counterstained with Hoechst (blue). Control experiments were performed by omitting the primary antibody (antibody control). Slides were then analyzed on a confocal laser-scanning microscope. The bar represents 20 µm. One representative experiment out of three is shown.

3.3.2 HOCl-HDL-mediated nuclear Translocation of Egr-1 in the absence or presence of Pathway Inhibitors

Another set of experiments was performed to study the involvement of upstream signaling pathways in HOCl-HDL-mediated nuclear translocation of

Egr-1. Cells were incubated with respective inhibitors prior to stimulation with HOCl-HDL for 1 h; then nuclear and cytosolic protein extracts were prepared and subjected to Western Blot analysis. Treatment of cells with PD98059 and U73122 reduced HOCl-HDL-mediated nuclear Egr-1 protein amount to the level of non-stimulated cells (**Fig. 14**). In contrast, incubation of cells with SB203580 or LY294002 prior to stimulation with HOCl-HDL led to a slight increase in nuclear Egr-1 protein level. Nrf2, however, was constitutively expressed in the cytosolic fraction and did not undergo nuclear translocation by HOCl-HDL treatment.

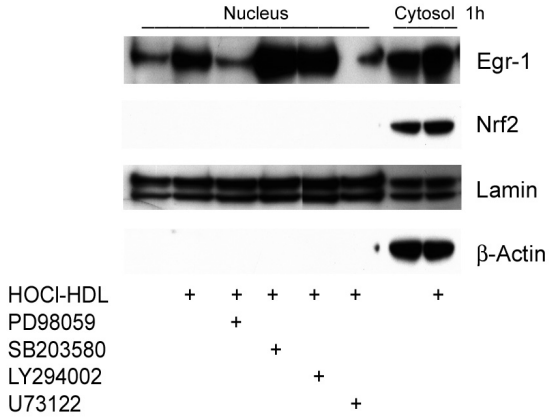

Figure 14: *HOCl-HDL-induced nuclear translocation of Egr-1 in the absence or presence of pathway inhibitors in EA.hy926 cells.* Cells were preincubated with 25 µM PD98059 for 30 min, 10 µM SB203580 for 30 min, 25 µM LY294002 for 15 min or with 10 µM U73122 for 10 min prior to stimulation with 100 µg/ml HOCl-HDL for 1 h. Cells were lysed, nuclear and cytosolic extracts were isolated and equal amounts of proteins were subjected to Western blot analysis for Egr-1 and Nrf2. β-Actin was used as a cytosolic and Lamin as a nuclear loading control. Lanes 1 and 7 represent non-stimulated cells. One representative experiment out of two is shown.

3.3.3 HOCl-HDL-induced Egr-1 DNA-binding Activity

Results from a Blast search of the -2000 nucleotide region of the human HO-1 gene against consensus DNA-binding sequences of known transcription factors using the software Genomatix MatInspektor (Genomatix Software GmbH, Munich, Germany) showed consensus DNA-binding sites for Egr-1 within the HO-1 promoter.

To determine whether HOCl-HDL stimulation induced binding of the transcription factor Egr-1 to its consensus DNA-binding element in the promoter region of target genes, EMSA experiments were performed. HOCl-HDL stimulation caused a time-dependent (0.5–3 h) increase in Egr-1 DNA-binding activity with a maximum at 0.5 h compared to non-stimulated cells. Competition experiments with an excess of non-radiolabeled probe were performed to confirm that the EMSA band is specific for Egr-1 (**Fig. 15**).

In a next set of experiments we performed supershift assays to further confirm that the EMSA band is specific for Egr-1. According to previous reports we either incubated the nuclear protein extracts with the anti-Egr-1 antibody prior to addition of the radioactive labeled probe (Faour *et al.*, 2005), or incubated the extracts with the probe followed by incubation with the anti-Egr-1 antibody (Zhang *et al.*, 2007). Unfortunately we were not able to observe any supershifted bands using the anti-Egr-1 antibody in all of the conditions tested (**Fig. 16**).

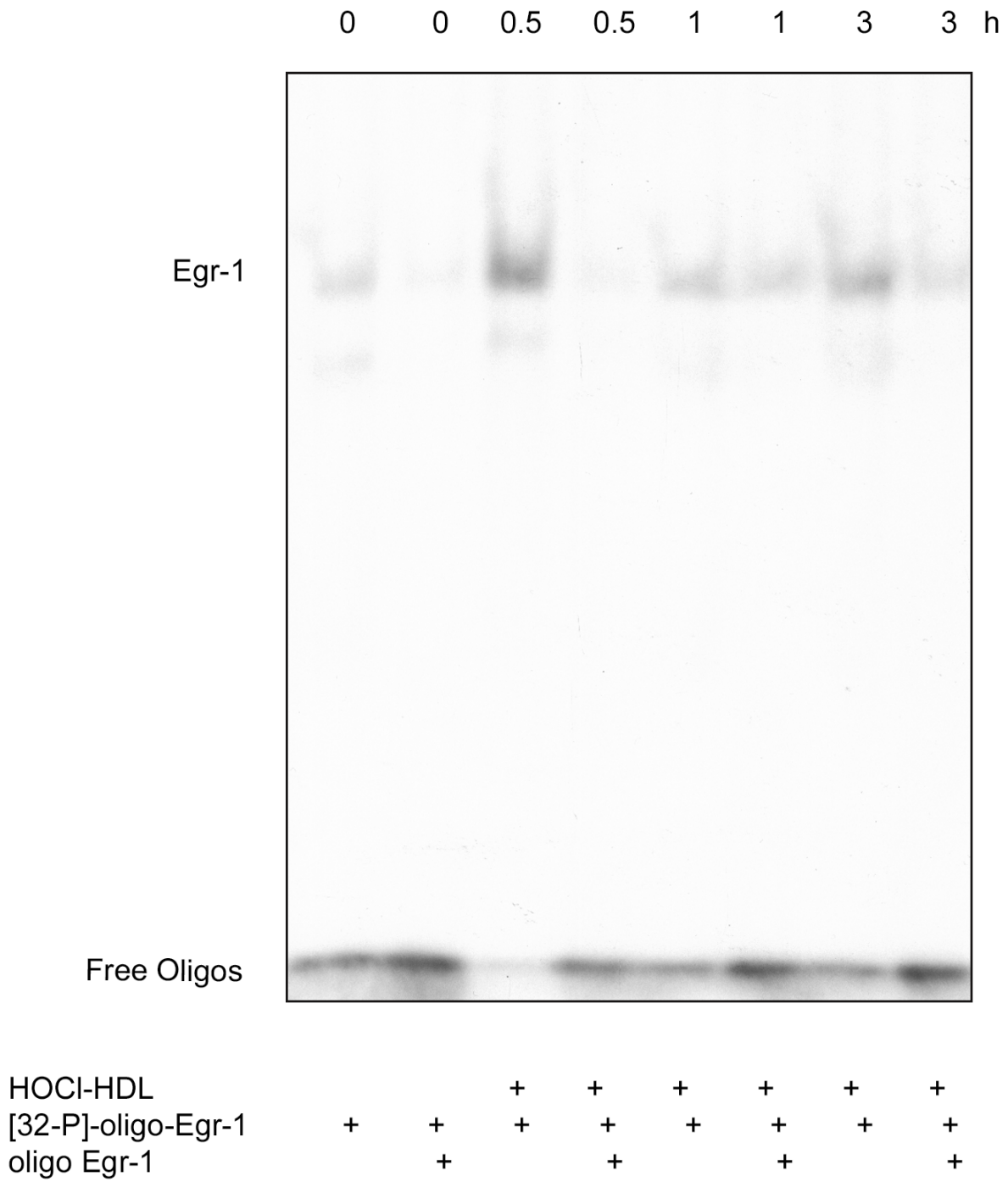

Figure 15: *HOCl-HDL-induced Egr-1 DNA-binding activity in EA.hy926 cells.* Cells were stimulated with 100 µg/ml HOCl-HDL for indicated times (0.5–3 h), nuclear extracts were isolated and incubated with radioactive labeled oligonucleotides of the Egr-1 consensus binding site ([32-P]-oligo-Egr-1). For competition experiments extracts were preincubated with a 20-fold molar excess of unlabeled oligonucleotides (oligo Egr-1) specific for Egr-1. Lanes 1 and 2 represent non-stimulated cells. One representative experiment out of three is shown.

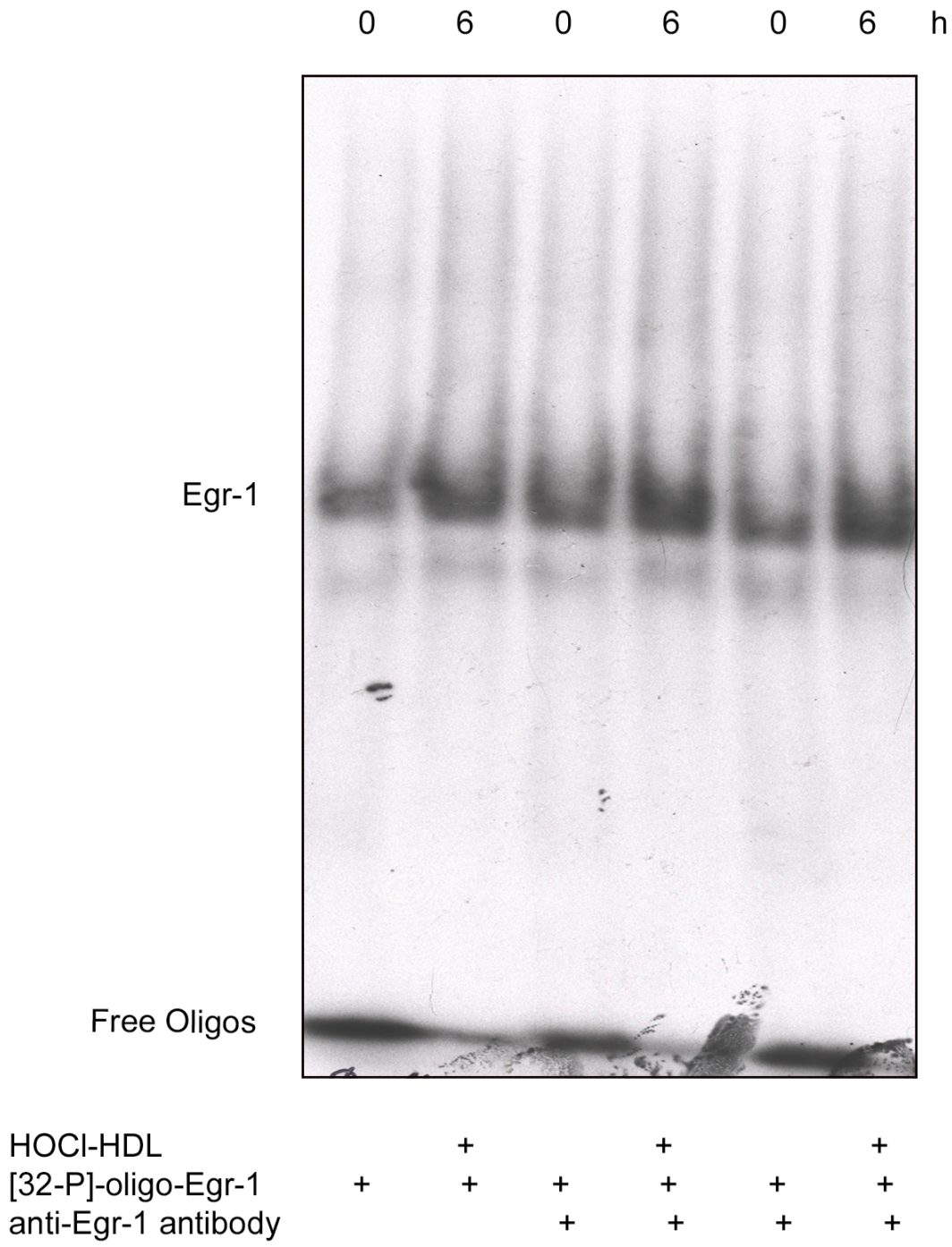

Figure 16: *HOCl-HDL-induced Egr-1 DNA-binding activity in the absence or presence of anti-Egr-1 antibody in EA.hy926 cells.* Cells were stimulated with 100 µg/ml HOCl-HDL for 6 h, nuclear extracts were isolated and incubated with radioactive labeled oligonucleotides of the Egr-1 consensus binding site ([32-P]-oligo-Egr-1). For supershift experiments extracts were incubated before (lanes 3 and 4) or after (lanes 5 and 6) the addition of radioactive labeled oligonucleotides with an anti-Egr-1 antibody. Lanes 1, 3 and 5 represent non-stimulated cells. One preliminary experiment is shown.

3.4 HDL- and HOCl-HDL-mediated Induction of HO-1

3.4.1 Time- and concentration-dependent Protein Expression of HO-1 by HDL

In a next series of experiments we wanted to investigate the ability of native HDL to induce protein expression of HO-1 in human EA.hy926 endothelial cells. Treatment of cells with native HDL led to a time- (4-24 h) and concentration-dependent (10-200 µg/ml) induction of HO-1 protein expression compared to non-stimulated cells (**Fig. 17A** and B). A more pronounced induction of HO-1 protein expression was observed when cells were treated with HOCl-HDL than with native HDL.

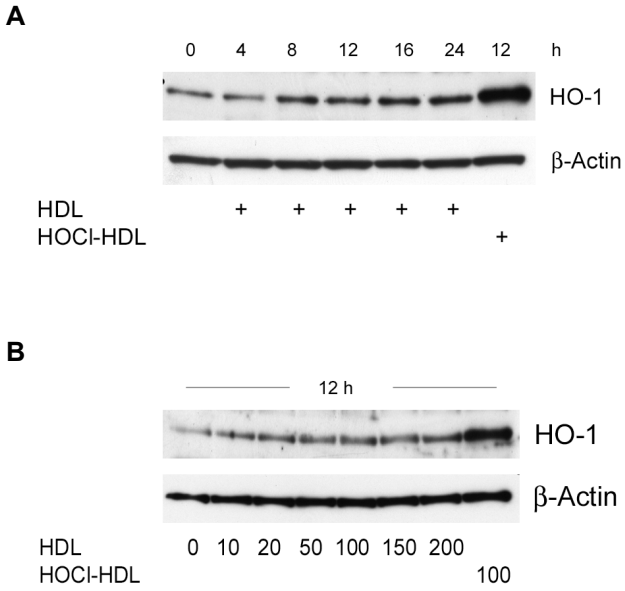

Figure 17: *Western blot analysis of HDL-induced HO-1 expression in EA.hy926 cells.* **A** Cells were incubated with 100 µg/ml HDL or HOCl-HDL for indicated times (4–24 h). **B** Cells were incubated with indicated concentrations of HDL or HOCl-HDL (10–200 µg/ml) for 12 h. **A-B** Cells were lysed and equal amounts of proteins were subjected to Western blot analysis for HO-1. β-Actin was used as a loading control. Lane 1 (**A**) represents non-stimulated cells. One representative experiment out of two is shown.

3.4.2 Time- and concentration-dependent Protein Expression of HO-1 by HOCl-HDL

To follow time- and concentration-dependent activation of HO-1 expression by HOCl-HDL, Western blot experiments were performed. HOCl-HDL treatment enhanced HO-1 protein expression in a time- (4–24 h) and

concentration-dependent (10–200 µg/ml) manner compared to HDL- and non-stimulated cells (**Fig. 18A** and B). Maximum of HO-1 protein expression was observed at 12 h and 200 µg/ml HOCl-HDL.

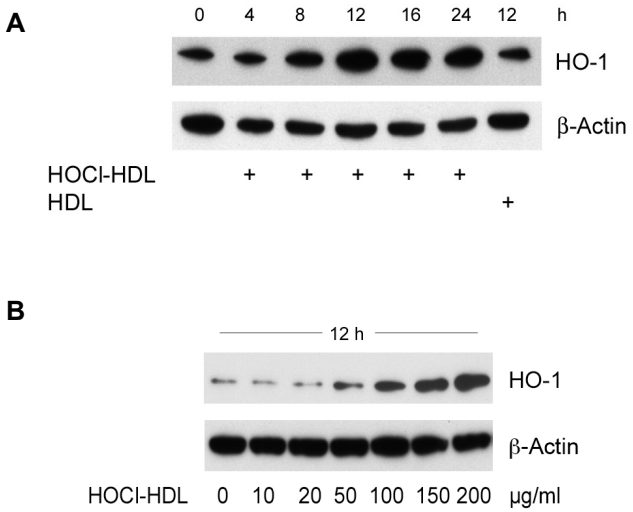

Figure 18: *Western blot analysis of HOCl-HDL-induced HO-1 expression in EA.hy926 cells.* **A** Cells were incubated with 100 µg/ml HOCl-HDL or HDL for indicated times (4–24 h). **B** Cells were incubated with indicated concentrations of HOCl-HDL (10–200 µg/ml) for 12 h. **A-B** Cells were lysed and equal amounts of proteins were subjected to Western blot analysis for HO-1. β-Actin was used as a loading control. Lane 1 (**A**) represents non-stimulated cells. One representative experiment out of three is shown.

3.4.3 Chlorinated-HDL-mediated Induction of HO-1 Protein Expression

The next set of experiments was performed to investigate whether HDL, modified by reagent HOCl or by the MPO-H_2O_2-chloride system, is able to alter protein expression of HO-1. Treatment of cells with modified HDL (MPO-HDL, MPO-Asc-HDL, HOCl-HDL) for 12 h increased HO-1 protein expression compared to non-stimulated cells (**Fig. 19**). Stimulation of cells with native HDL, however, caused only a slight induction of HO-1 expression when compared to non-stimulated cells.

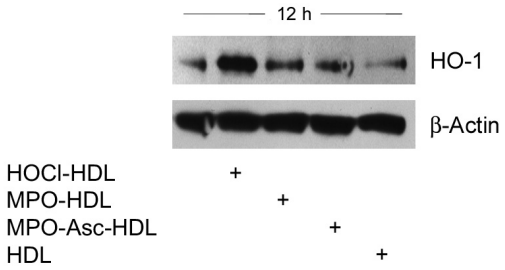

Figure 19: *Western blot analysis of HOCl-HDL- and MPO-HDL-induced HO-1 expression in EA.hy926 cells.* Cells were incubated with 100 µg/ml HOCl-HDL, HDL, MPO-HDL or MPO-Asc-HDL for 12 h. Cells were lysed and equal amounts of proteins were subjected to Western blot analysis for HO-1. β-Actin was used as a loading control. Lane 1 represents non-stimulated cells. One representative experiment out of three is shown.

3.4.4 HOCl-modified (Lipo)protein-mediated Induction of HO-1 Protein Expression

To investigate whether induction of HO-1 protein expression by HOCl-HDL is a specific HDL effect or achieved also by other HOCl-modified proteins we incubated EA.hy926 cells with different modifications of HOCl-modified BSA (normal and fatty acid-free), LDL and HDL for 12 h. HO-1 expression was increased with an increasing degree of HDL and LDL modification (**Fig. 20A**). HOCl-BSA tended to induce HO-1 expression with increasing oxidant:protein molar ratio (25:1 to 100:1), but this induction was less effective compared to HOCl-HDL (200:1) (Fig. 20B). No difference in the induction of HO-1 expression was observed in cells treated either with BSA or fatty acid-free BSA (Fig. 20B). The most pronounced HO-1 expression was observed with HOCl-HDL at an oxidant:lipoprotein molar ratio of 200:1 (Fig. 20A and B).

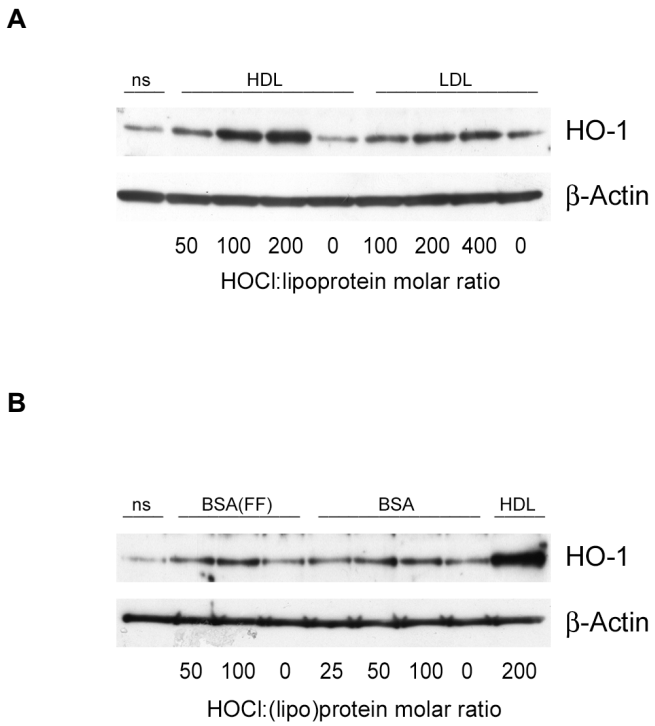

Figure 20: *Western Blot analysis of HO-1 expression induced by HOCl-modified (lipo)proteins in EA.hy926 cells.* **A-B** Cells were incubated with 100 µg/ml native and modified (lipo)proteins (at an indicated oxidant:(lipo)protein molar ratio, 25:1 to 400:1, FF=fatty acid-free) for 12 h. HOCl-HDL (200:1) was used as a positive control (**B**). Cells were lysed an equal amounts of proteins were subjected to Western blot analysis for HO-1. β-Actin was used as a loading control. Lane 1 represents non-stimulated cells (ns). One representative experiment out of three is shown.

3.4.5 Effect of MAPK Inhibitors on HOCl-HDL-mediated Protein Expression of HO-1

To study the involvement of MAPK signaling in the activation of HO-1, cells were incubated with respective inhibitors prior to stimulation with HOCl-HDL for 12 h. Treatment of cells with PD98059 reduced HOCl-HDL-induced HO-1 expression (**Fig. 21**). Although SB203580 promoted HOCl-HDL-mediated activation of p42/44 MAPK (Fig. 5) and expression of Egr-1 (Fig. 9 and 11A), protein expression of HO-1 was not induced compared to HOCl-HDL-stimulated cells (Fig. 21).

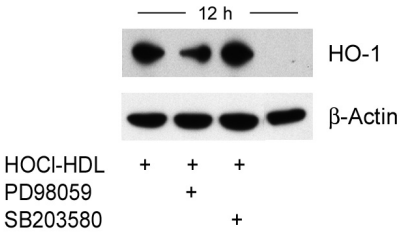

Figure 21: *Western blot analysis of HOCl-HDL-induced HO-1 expression in EA.hy926 cells in the absence or presence of MAPK inhibitors.* Cells were incubated for 30 min with 25 µM PD98059 or 10 µM SB203580 prior to stimulation with 100 µg/ml HOCl-HDL for 12 h. Cells were lysed and equal amounts of proteins were subjected to Western blot analysis for HO-1. β-Actin was used as a loading control. Lane 4 represents non-stimulated cells. One representative experiment out of three is shown.

3.4.6 Effect of PI3K and PLC Inhibitors on HOCl-HDL-mediated Protein Expression of HO-1

Another set of experiments was performed to assess the involvement of PI3K and PLC in the HOCl-HDL-mediated activation of HO-1 protein expression. Cells were incubated with inhibitors for PI3K or PLC prior to stimulation with HOCl-HDL for 12 h; then Western blot analysis was performed. Treatment of cells with LY294002 reduced HOCl-HDL-induced HO-1 expression (**Fig. 22**). Preincubation of cells with U73122, however, did not inhibit but even increased HOCl-HDL-induced HO-1 protein expression when compared to HOCl-HDL-treated cells.

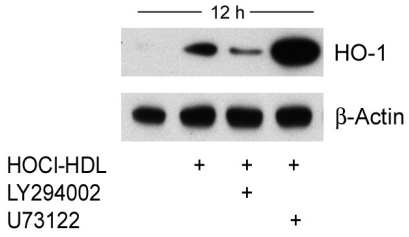

Figure 22: *Western blot analysis of HOCl-HDL-induced HO-1 expression in EA.hy926 cells in the absence or presence of PI3K and PLC inhibitors.* Cells were incubated for 15 min with 25 µM LY294002 or for 10 min with 10 µM U73122 prior to stimulation with 100 µg/ml HOCl-HDL for 12 h. Cells were lysed and equal amounts of proteins were subjected to Western blot analysis for HO-1. β-Actin was used as a loading control. Lane 1 represents non-stimulated cells. One representative experiment out of three is shown.

3.4.7 HOCl-HDL-mediated Induction of HO-1 mRNA Expression

To determine HOCl-HDL-mediated expression of HO-1 on mRNA level, cells were incubated with HOCl-HDL or HDL (0.5 and 6 h) in the absence or presence of pathway inhibitors. HOCl-HDL stimulation caused a slight increase in HO-1 mRNA expression with a maximum between 4 and 6 h; treatment of cells with native HDL had no effect when compared to non-stimulated cells (**Fig. 23A**). Pre-incubation of cells with PD98059, SB203580 or LY294002 exhibited no inhibitory effect on HOCl-HDL-induced HO-1 expression; however, incubation of cells with U73122 prior to HOCl-HDL treatment led to a further increase of HO-1 mRNA expression compared to HOCl-HDL-treated cells.

As we were not able to observe a significant increase in HO-1 mRNA expression in HOCl-HDL-treated cells between 0.5 to 6 h incubation time, cells were stimulated with HOCl-HDL or HDL up to 10 h in the absence or presence of MAPK inhibitors. HOCl-HDL treatment led to a significant elevation of HO-1 mRNA between 4 and 10 h compared to non-stimulated cells (Fig. 23B). HO-1 expression was significantly increased after 6 and 8 h of HOCl-HDL stimulation compared to native HDL-treated cells. Incubation of cells with PD98059 led to a slight reduction in HOCl-HDL-mediated (8 h) induction of HO-1, whereas SB203580 exhibited no effect.

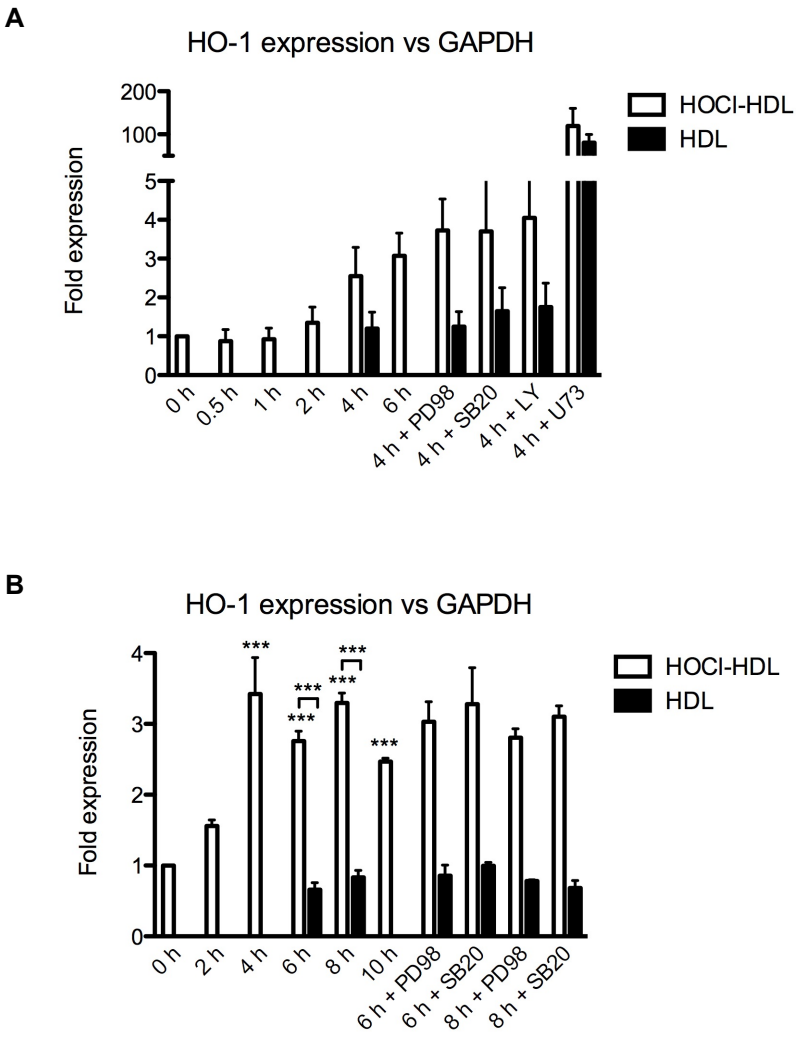

Figure 23: *Real-time RT-PCR of HOCl-HDL-stimulated HO-1 expression in the absence or presence of pathway inhibitors in EA.hy926 cells.* **A** Cells were stimulated with 100 µg/ml HOCl-HDL or HDL for indicated times (0.5–6 h) in the absence or presence of 25 µM PD98059 (30 min), 10 µM SB203580 (30 min), 25 µM LY294002 (15 min) or 10 µM U73122 (10 min). **B** Cells were treated with 25 µM PD98059 or 10 µM SB203580 for 30 min prior to stimulation with 100 µg/ml HOCl-HDL or HDL for indicated times (2–10 h). **A-B** RNA was isolated, treated with DNase, reverse transcribed and equal amounts of cDNA were subjected to Real-time-PCR. HO-1 expression was normalized to GAPDH. One representative experiment out of three is shown. (*** $p<0.001$).

To further verify HOCl-HDL-induced expression of HO-1 on mRNA level, cells were incubated with HOCl-HDL or additionally with Actinomycin D (an inhibitor of transcription) for indicated time points (0.5–6 h). Real-time RT-PCR results revealed a significant increase in HO-1 mRNA expression in HOCl-HDL-

treated cells between 2 and 6 h (**Fig. 24**). This increase in HOCl-HDL-mediated HO-1 mRNA expression (2-6 h) was significantly reduced in Actinomycin D-treated cells, indicating that the elevated mRNA level in HOCl-HDL treated cells was due to increased transcription of HO-1. (Real-time PCR of Fig. 24 was done with the help of Dr. Daniela Jud, Medical University of Graz).

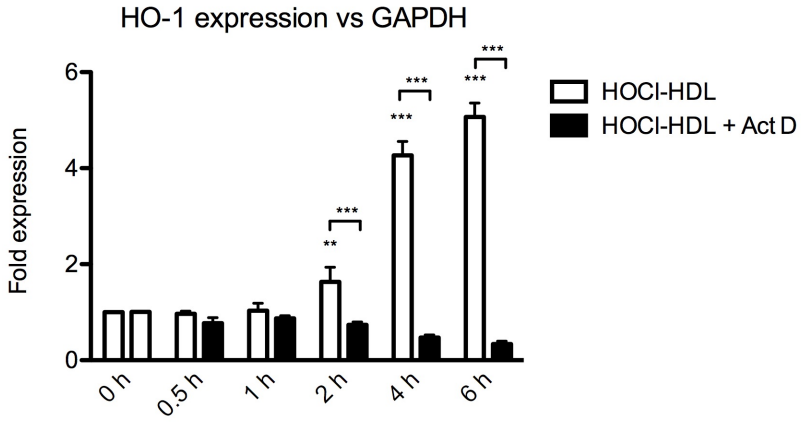

Figure 24: *Real-Time RT-PCR of HOCl-HDL-induced HO-1 activation in the absence or presence of an inhibitor of transcription in EA.hy926 cells.* Cells were preincubated for 30 min with 2 µg/ml Actinomycin D and stimulated with 100 µg/ml HOCl-HDL for indicated time points (0.5 – 6 h). RNA was isolated, treated with DNase, reverse transcribed and equal amounts of cDNA were subjected to Real-Time-PCR (Real-Time-PCR was done by Dr. Daniela Jud, Institute of Human Genetics, Medical University of Graz, Austria.). HO-1 expression was normalized to GAPDH. One representative experiment out of two is shown. (** $p<0.01$; *** $p<0.001$).

3.5 Involvement of Egr-1 in HOCl-HDL-mediated Activation of HO-1

To investigate, if transcription factor Egr-1 is directly involved in the HOCl-HDL-mediated activation pathway of HO-1, siRNA approach was used to knockdown Egr-1 expression. Real-time RT-PCR and Western blot experiments were performed to determine HOCl-HDL-induced Egr-1 and HO-1 expression levels of cells transfected with siRNA against Egr-1 compared to cells transfected with scrambled control siRNA.

3.5.1 Effect of Egr-1 Silencing on HOCl-HDL-mediated Induction of Egr-1/HO-1 mRNA Expression

The silencing efficiency of the specific Egr-1 siRNA had to be analyzed in HOCl-HDL-treated cells, because of the low mRNA and protein levels in non-stimulated cells. This is the reason for a reduced silencing efficiency of RNA interference under our experimental conditions.

HOCl-HDL treatment of cells caused an increase in Egr-1 mRNA expression when compared to non-stimulated cells (**Fig. 25A**). Incubation of cells with a scrambled control siRNA did not alter HOCl-HDL-mediated Egr-1 mRNA expression. Knockdown of Egr-1, using a siRNA specific for Egr-1, significantly decreased HOCl-HDL-mediated Egr-1 mRNA expression to about 55% compared to cells transfected with scrambled control siRNA (Fig. 25B).

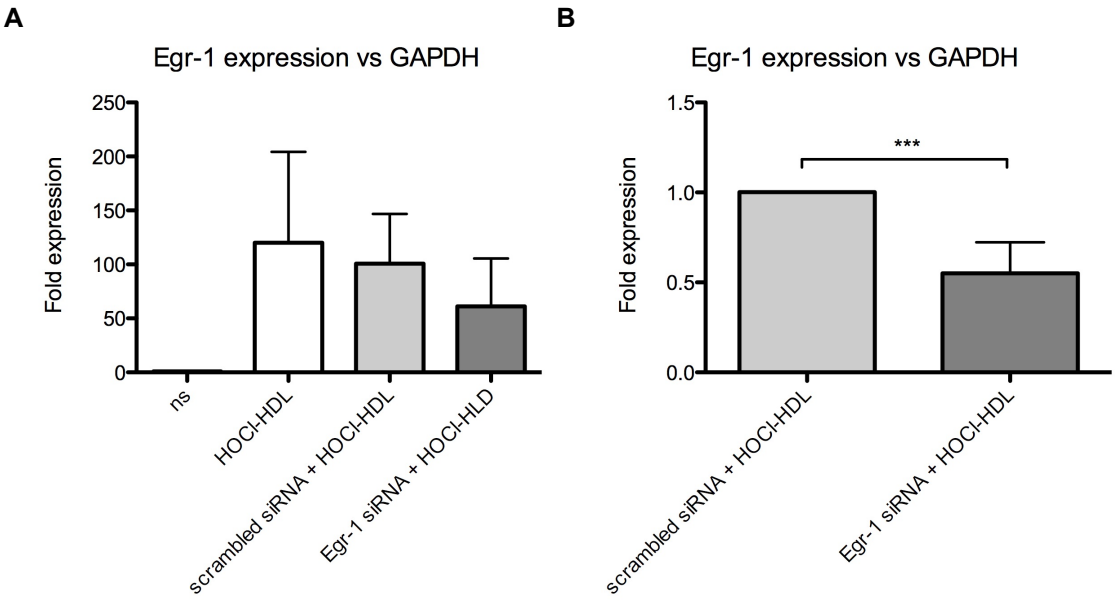

Figure 25: *Real-time RT-PCR of HOCl-HDL-stimulated Egr-1 expression in EA.hy926 cells treated with siRNA against Egr-1.* **A-B** Cells were transfected with 50 nM siRNA against Egr-1 or with scrambled control siRNA. 48 h after transfection, cells were stimulated with 100 µg/ml HOCl-HDL for 1 h to assess Egr-1 mRNA expression. RNA was isolated, treated with DNase and reverse transcribed and equal amounts of cDNA were subjected to Real-time-PCR. Egr-1 expression was normalized to GAPDH. ns (non-stimulated cells); One representative experiment out of three is shown. (*** $p<0.001$).

To follow the effect of Egr-1 silencing on HOCl-HDL-mediated expression of HO-1 on mRNA level, Real-time RT-PCR was performed. Treatment of cells with HOCl-HDL caused a significant increase in HO-1 mRNA expression compared to non-stimulated cells (**Fig. 26A**). Transfection of cells with a scrambled control siRNA led to no significant alteration in HOCl-HDL-mediated HO-1 mRNA expression when compared to non-transfected cells (Fig. 26A). Silencing of Egr-1, using Egr-1 siRNA, significantly decreased HOCl-HDL-mediated HO-1 mRNA expression to about 65% compared to control cells transfected with scrambled control siRNA (Fig. 26B).

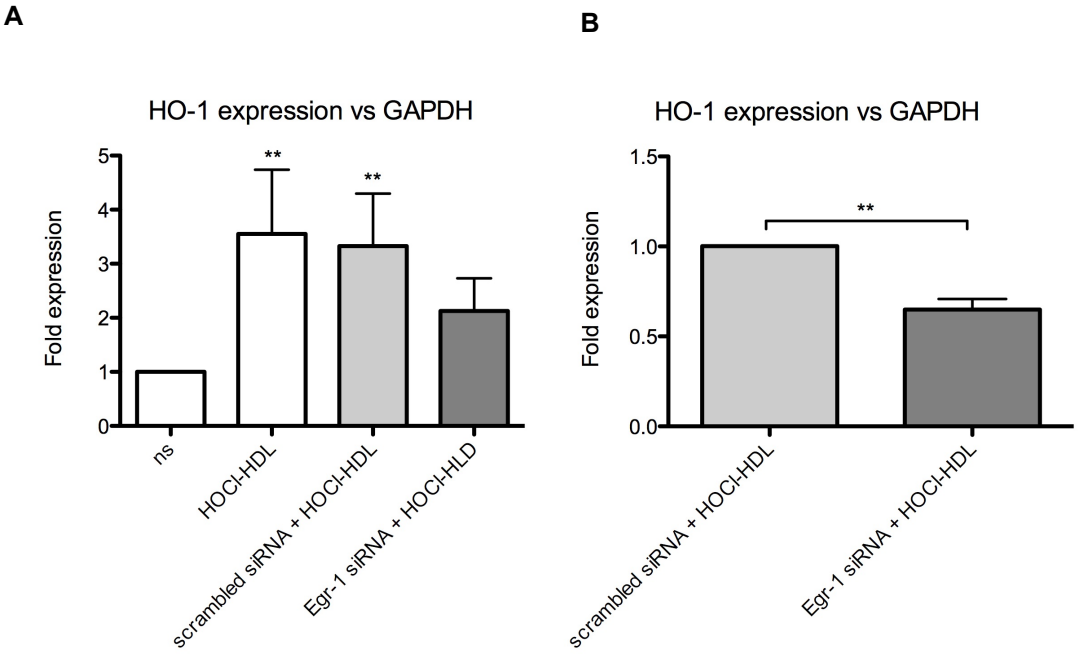

Figure 26: *Real-time RT-PCR of HOCl-HDL-stimulated HO-1 expression in EA.hy926 cells treated with siRNA against Egr-1.* **A-B** Cells were transfected with 50 nM siRNA against Egr-1 or with scrambled control siRNA. 48 h after transfection, cells were stimulated with 100 µg/ml HOCl-HDL for 4 h to assess HO-1 mRNA expression. RNA was isolated, treated with DNase and reverse transcribed. Equal amounts of cDNA were subjected to Real-time-PCR. HO-1 expression was normalized to GAPDH. ns (non-stimulated cells); One representative experiment out of three is shown. (** $p<0.01$).

3.5.2 Effect of Egr-1 Silencing on HOCl-HDL-mediated Induction of Egr-1/HO-1 Protein Expression

In a next series of experiments, cells were transfected with Egr-1 siRNA or with a scrambled control siRNA and HOCl-HDL-mediated expression of Egr-1 and HO-1 was investigated using Western blot experiments.

Incubation of cells with HOCl-HDL for 1.5 h increased Egr-1 protein expression compared to non-stimulated cells (**Fig. 27)**. Transfection of cells with scrambled control siRNA prior to stimulation with HOCl-HDL had no effect on HOCl-HDL-mediated induction of Egr-1. In line with data of Egr-1 mRNA expression (Fig. 25), knockdown of Egr-1 using RNA interference reduced HOCl-HDL-mediated Egr-1 protein expression to 65% compared to control cells transfected with a scrambled control siRNA.

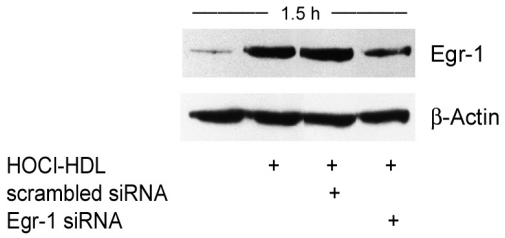

Figure 27: *Western blot analysis of HOCl-HDL-induced Egr-1 expression in EA.hy926 cells treated with siRNA against Egr-1.* Cells were transfected with 50 nM siRNA against Egr-1 or with scrambled control siRNA and after 48 h cells were stimulated with 100 µg/ml HOCl-HDL for 1.5 h. Cells were lysed and equal amounts of proteins were subjected to Western blot analysis for Egr-1. β-Actin was used as a loading control. Lane 1 represents non-stimulated cells. One representative experiment out of three is shown.

Next, the effect of Egr-1 silencing on HOCl-HDL-mediated HO-1 protein expression was investigated. Incubation of cells with HOCl-HDL for 12 h led to an increase in HO-1 expression compared to non-stimulated cells (**Fig. 28**). Treatment of cells with a scrambled control siRNA did not alter HOCl-HDL-mediated HO-1 expression when compared to HOCl-HDL-treated cells. Silencing of Egr-1 using siRNA approach reduced HOCl-HDL-mediated HO-1 protein expression to 45% compared to control cells transfected with a scrambled control siRNA.

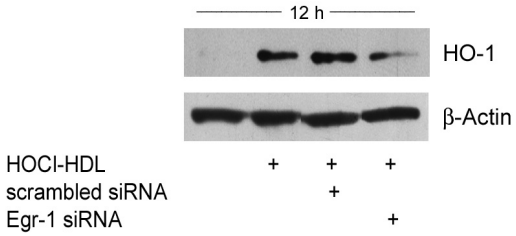

Figure 28: *Western blot analysis of HOCl-HDL-induced HO-1 expression in EA.hy926 cells treated with siRNA against Egr-1.* Cells were transfected with 50 nM siRNA against Egr-1 or with scrambled control siRNA and after 48 h cells were stimulated with 100 µg/ml HOCl-HDL for 12 h. Cells were lysed and equal amounts of proteins were subjected to Western blot analysis for HO-1. β-Actin was used as a loading control. Lane 1 represents non-stimulated cells. One representative experiment out of three is shown.

3.5.3 Effect of Egr-1 Silencing on HOCl-HDL-mediated nuclear Translocation of Egr-1

To examine HOCl-HDL-mediated nuclear translocation of Egr-1 in cells transfected with a siRNA specific for Egr-1, nuclear and cytosolic extracts were prepared and Western blot experiments were performed. Treatment of cells with HOCl-HDL for 1 h led to an increase in Egr-1 expression in the nucleus compared to non-stimulated cells, whereas cytosolic Egr-1 protein expression was only slightly enhanced (**Fig. 29**). The scrambled control siRNA had no effect on HOCl-HDL-mediated induction of nuclear Egr-1 expression. Knockdown of Egr-1 reduced HOCl-HDL-mediated nuclear expression of Egr-1 to 65% compared to cells transfected with a scrambled control siRNA. In line with previous findings (Fig. 12A, B and Fig. 14), expression of Nrf2 was not affected by HOCl-HDL incubation and was only observable in the cytosolic fraction (Fig. 29).

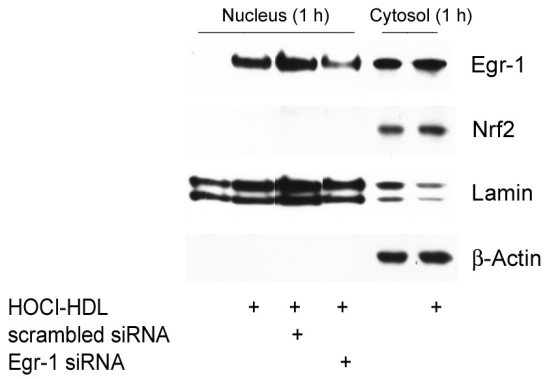

Figure 29: *Western blot analysis of HOCl-HDL-induced nuclear translocation of Egr-1 in EA.hy926 cells treated with siRNA against Egr-1.* Cells were transfected with 100 nM siRNA against Egr-1 or with scrambled control siRNA and after 48 h cells were stimulated with 100 µg/ml HOCl-HDL for 1 h. Cells were lysed, nuclear and cytosolic extracts were isolated and equal amounts of proteins were subjected to Western blot analysis for Egr-1 and Nrf2. β-Actin was used as a cytosolic and Lamin as a nuclear loading control. Lane 1 and 5 represent non-stimulated cells. One representative experiment out of three is shown.

3.6 HOCl-HDL-mediated Expression and Activity of eNOS

Previous reports suggested that stimulation of HUVECs with HOCl-modified lipoproteins might reduce expression and activity of vasculoprotective eNOS (Marsche *et al.*, 2004; Nuszkowski *et al.*, 2001). To reveal whether this is also true for EA.hy926 cells Real-time RT-PCR, Western blot experiments and eNOS activity assays were performed.

Treatment of cells with HOCl-HDL between 0.5 and 24 h led to no significant alteration in eNOS mRNA expression compared to non-stimulated cells (**Fig. 30**). HOCl-HDL treatment for 8 h significantly reduced eNOS mRNA expression compared to cells stimulated with native HDL.

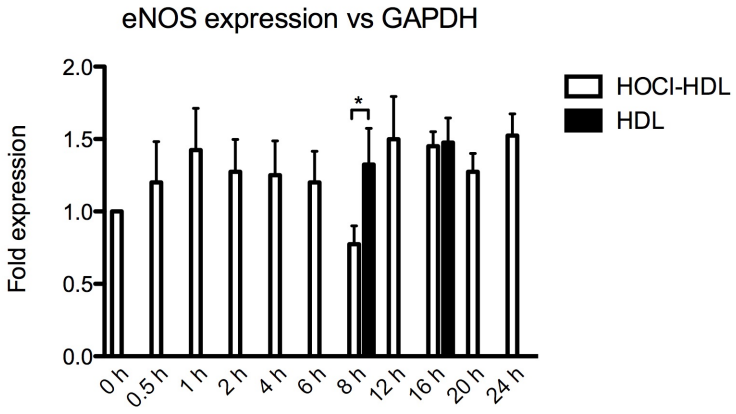

Figure 30: *Real-time RT-PCR of HOCl-HDL-stimulated eNOS expression in EA.hy926 cells.* Cells were incubated with 100 µg/ml HOCl-HDL or HDL for indicated time points (0.5–24 h). RNA was isolated, treated with DNase and reverse transcribed. Equal amounts of cDNA were subjected to Real-time-PCR. eNOS expression was normalized to GAPDH. One representative experiment out of two is shown. (* $p<0.05$).

To study HOCl-HDL-mediated eNOS protein expression in a time-dependent manner, cells were incubated for 12 up to 36 h with HOCl-HDL or native HDL. Concordant with data of previous experiments (Fig. 18 and 19) incubation of cells with HOCl-HDL for 12 h led to an increase in HO-1 protein expression compared to non-stimulated cells (**Fig. 31A** and B). Treatment of cells with HOCl-HDL, however, did not reduce but even slightly increased eNOS protein expression compared to HDL- or non-stimulated cells.

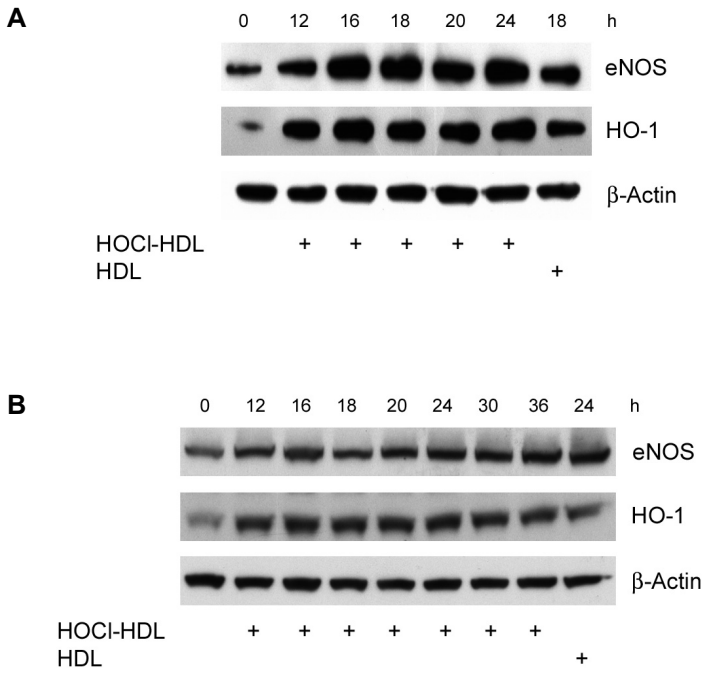

Figure 31: *Western blot analysis of HOCl-HDL-induced eNOS expression in EA.hy926 cells.* **A-B** Cells were incubated with 100 µg/ml HOCl-HDL or HDL for indicated time points (12–36 h). Cells were lysed and equal amounts of proteins were subjected to Western blot analysis for eNOS and HO-1. β-Actin was used as a loading control. Lane 1 represents non-stimulated cells. One representative experiment out of two is shown.

Next, we determined enzymatic activity of eNOS. This is reflected by the conversion of L-arginine into L-citrulline. Cells were treated with HOCl-HDL or native HDL for 16 and 24 h prior to stimulation with histamine or ionomycine. Agonist treatment (histamine or ionomycine) significantly induced eNOS activity in HOCl-HDL-, HDL- or non-stimulated cells compared to cells treated without any agonist (only H_2O) (**Fig. 32**). eNOS activity was not reduced in HOCl-HDL-treated cells compared to HDL- or non-stimulated cells.

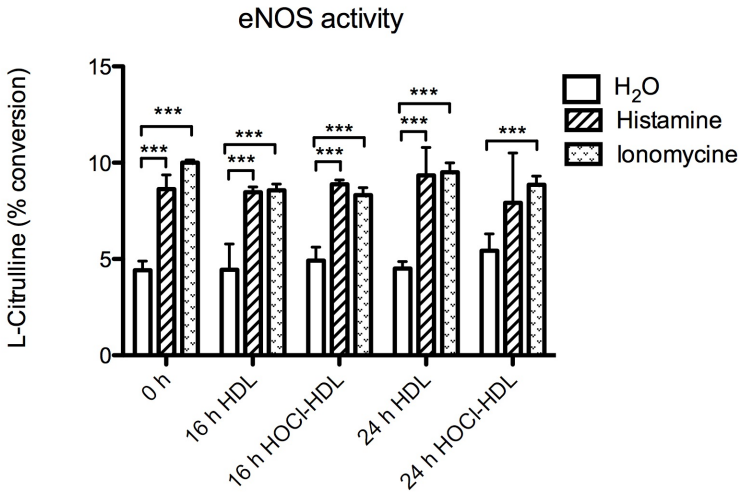

Figure 32: *eNOS activity assay in HOCl-HDL-stimulated EA.hy926 cells.* Cells were incubated with 100 µg/ml HOCl-HDL or HDL for indicated time points (16 and 24 h) and eNOS activity was induced by the addition of agonists histamine or ionomycine. eNOS activity is expressed as percent conversion of incorporated L-arginine into L-citrulline. One representative experiment out of two is shown. (*** $p<0.001$).

3.7 HOCl-HDL-mediated apoptotic and anti-proliferative Effects

3.7.1 Effect of HOCl-HDL on Protein Expression of apoptotic Marker Genes

To examine whether HOCl-HDL treatment induced apoptosis in EA.hy926 cells, Western blot experiments for apoptotic marker proteins were performed. Neither PARP nor Caspase 3 was cleaved by HOCl-HDL or native HDL when compared to staurosporine, used as a positive control (**Fig. 33**). Staurosporine-induced apoptosis was detected by the appearance of the apoptosis-related cleaved PARP fragment and by the reduced amount of the full-length Caspase 3.

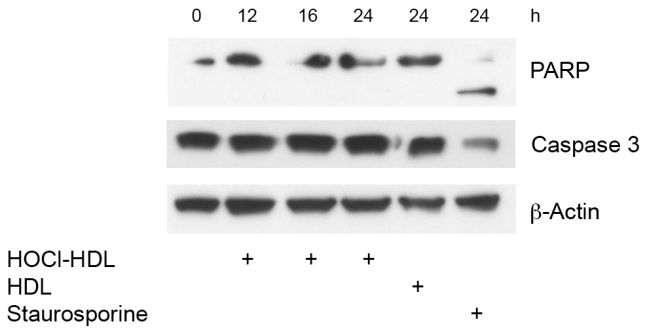

Figure 33: *Western blot analysis of HOCl-HDL-induced apoptosis in EA.hy926 cells.* Cells were incubated with 100 µg/ml HOCl-HDL or HDL for indicated time points (12–24 h). As a positive control 1 µM staurosporine was used for stimulation. Cells were lysed and equal amounts of proteins were subjected to Western blot analysis. PARP and Caspase 3 antibodies were used to determine HOCl-HDL-induced apoptosis. β-Actin was used as a loading control. Lane 1 represents non-stimulated cells. One representative experiment out of three is shown.

3.7.2 Effect of HOCl-HDL on Proliferation

Next, the MTT assay was performed to determine the proliferative potential of cells. Incubation of cells with HOCl-HDL or native HDL for 18 and 26 h prior to addition of MTT for 2 h did not lead to any anti-proliferative effects compared to native HDL- or non-stimulated cells (**Fig. 34**).

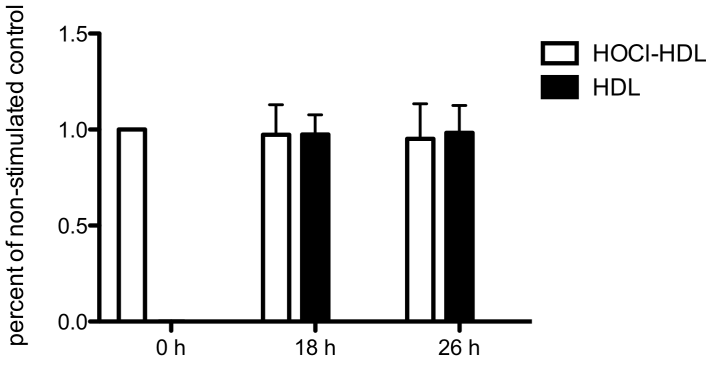

Figure 34: *MTT Assay of HOCl-HDL-treated EA.hy926 cells.* After treatment of cells with 100 µg/ml HOCl-HDL or HDL for indicated time points (18–26 h) cells were incubated with MTT for 2 h. Cells were lysed and their proliferative potential was assessed by the amount of built formazan. One representative experiment out of two is shown.

4. Discussion

Epidemiological studies demonstrate a direct correlation between high levels of plasma LDL and the risk for atherosclerosis development, whereas high levels of HDL are reported to exhibit anti-atherogenic effects (Stocker *et al.*, 2004b). Steinberg and colleagues (Steinberg *et al.*, 1989) were the first proposing the hypothesis that an *in vivo* occurring oxidative modification of LDL represents one of the initial steps in the development of atherosclerosis. Accordingly it was reported that modified LDL stimulates the expression and secretion of MCP-1 by endothelial and smooth muscle cells that further causes recruitment of monocytes into the subendothelial space (Stocker *et al.*, 2004b). Accumulating modified LDL within the subendothelial space leads then to the expression of scavenger receptors by macrophages, that facilitates the uptake of modified LDL and the development of foam cells (Stocker *et al.*, 2004b).

Although interest has focused upon LDL as a target for oxidative modification *in vivo* for a long time, accumulating articles report on HDL modification and the associated alterations in lipoprotein function (Nicholls *et al.*, 2005). Evidence exists that MPO-mediated loss of the atheroprotective functional properties of HDL might provide a novel mechanism linking inflammation and oxidative stress to the pathogenesis of atherosclerosis (Nicholls *et al.*, 2005). It was reported that apoA-I represents a selective target for MPO-mediated oxidation within human atherosclerotic plaques as well as in the circulation and that apoA-I exhibits a specific binding site for MPO (Nicholls *et al.*, 2005; Zheng *et al.*, 2004). Additionally it was demonstrated that apoA-I isolated from patients with coronary artery disease is enriched in nitrotyrosine and 3-chlorotyrosine compared to apoA-I from healthy controls (Zheng *et al.*, 2004). Furthermore, HDL acts as a physiological carrier of MPO and MPO-mediated modification of HDL further increases its binding affinity for MPO which results in an elevated bioavailability of modified HDL within inflammatory regions (Marsche *et al.*, 2008). Comparable to modified LDL, modified HDL is also efficiently taken up and degraded by macrophages, which may develop into foam cells, an early hallmark in the development of atherosclerosis (Malle

et al., 2006). Moreover, MPO-mediated modification of HDL leads to a decrease in reverse cholesterol transport and to increased endothelial dysfunction by reducing expression and activity of eNOS (Marsche *et al.*, 2004; Nicholls *et al.*, 2005).

It was demonstrated that copper-oxidized LDL potently induces HO-1 in vascular endothelial cells, vascular smooth muscle cells and macrophages (Abraham *et al.*, 2008). Furthermore HO-1 expression was observable in endothelial cells, macrophages and foam cells in atherosclerotic lesions of humans and apoE$^{-/-}$ mice (Wang *et al.*, 1998). Ishikawa and colleagues (Ishikawa *et al.*, 2001a; Ishikawa *et al.*, 2001b) reported that induction of HO-1 leads to a reduction in atherosclerotic lesion size in LDL-receptor$^{-/-}$ mice and in Watanabe heritable hyperlipidemic rabbits. In line with these findings Juan and colleagues (Juan *et al.*, 2001) showed that adenovirus-mediated gene transfer of HO-1 caused a decrease in atherosclerotic lesion size in apoE$^{-/-}$ mice. Furthermore it was reported that apoE$^{-/-}$HO-1$^{-/-}$ double knockout mice, fed a Western type diet, were prone to formation of more advanced and larger atherosclerotic lesions compared to apoE$^{-/-}$ mice (Yet *et al.*, 2003).

These previous findings led to the suggestion that HO-1 is induced in response to oxidative stress and inflammation as a cellular rescue mechanism to prevent endothelial dysfunction. The present study aimed at investigating the signaling pathways involved in HOCl-HDL-mediated induction of HO-1 in human EA.hy926 endothelial cells. Furthermore we wanted to analyze the functional correlation between HO-1 and eNOS and to determine possible anti-proliferative and apoptotic effects in HOCl-HDL-treated cells.

4.1 HOCl-HDL-treated EA.hy926 Endothelial Cells as a Model System for Cardiovascular Disease

The human vascular endothelium accounts for about 1% of total body mass and for approximately 5,000 m^2. One layer of endothelial cells is lining the blood vessels thereby separating blood components from extravascular tissues. The main functions of endothelial cells are the regulation of vessel tone,

vascular permeability, coagulation, fibrinolysis and inflammation (Toborek *et al.*, 1999). It was reported that endothelial cell dysfunction caused by oxidative stress or mechanical injury is regarded as one of the initial events in the development of atherosclerosis due to its ability to stimulate smooth muscle cell proliferation and migration, leukocyte infiltration and foam cell formation (Toborek *et al.*, 1999). To mediate the recruitment, attachment and transmigration of leukocytes, endothelial cells express: (i) chemokines like IL-8 and MCP-1 to recruit leukocytes, (ii) P-, E-, and L-selectin to mediate the loose adherence of leukocytes (leukocyte rolling), (iii) ICAM-1 (intercellular adhesion molecule-1) and VCAM-1 to mediate firm adhesion and (iv) PCAM-1 (platelet-endothelial cell adhesion molecule-1) to mediate transmigration of leukocytes (Toborek *et al.*, 1999).

The human endothelial cell line EA.hy926, used within this project, was established by fusion of the permanent human lung epithelial cell line A549 with HUVECs (Edgell *et al.*, 1983). Immortalized endothelial cells, amongst them the well characterized EA.hy926 cell line, are widely used as an *in vitro* model to study various physiological and pathological conditions like inflammation, angiogenesis, tumor growth and atherosclerosis (Baranska *et al.*, 2005). Although differences exist between HUVECs and EA.hy926 cells, EA.hy926 cells exhibit significant similarities with HUVECs such as the expression of endothelial cell markers like ICAM-1, VCAM-1 and E-selectin as well as tube formation in matrigel and interaction with neutrophils upon cytokine stimulation (Baranska *et al.*, 2005).

HDL modified by HOCl, added as reagent or generated enzymatically by the MPO-H_2O_2-chloride system, is regarded as a pro-atherogenic lipoprotein due to its diminished capacity in “reverse cholesterol transport” and its uptake by macrophages which might develop into foam cells (Malle *et al.*, 2006). Previous reports demonstrated that plasma HDL concentrations range between 6 and 12 µM and that HOCl concentrations up to 340 µM might occur under acute inflammatory conditions; these findings let suggest an *in vivo* occurring HOCl-HDL ratio between 30:1 and 50:1 (Malle *et al.*, 2006; Panzenboeck *et al.*, 1997). Most of the experiments in the present study were performed with

HOCl-HDL (200:1), however, to ensure physiological significance, control experiments were performed using (i) HDL modified with a lower oxidant:lipoprotein molar ratio (50:1 and 100:1), and (ii) HDL modified by MPO in the absence (MPO-HDL) or presence of ascorbate (MPO-Asc-HDL) which results in an oxidant:lipoprotein molar ratio of approximately 25:1 to 50:1. Marquez and colleagues (Marquez *et al.*, 1990) reported that addition of ascorbate to the MPO-chlorination reaction leads to an increased regeneration of the native enzyme which should result in an enhanced chlorination reaction. Contrary to these findings we were not able to observe any differences between HDL modified by the MPO-H_2O_2-chloride system with our without ascorbate (Fig. 6, 8 and 19).

4.2 Impact of native HDL and HOCl-HDL on MAPK Signaling

MAPK signaling pathways represent one of the most widespread signaling cascades in mammals that participate in the regulation of proliferation, differentiation, apoptosis, cell cycle machinery and gene transcription (Raman *et al.*, 2007). There are three major groups of MAPKs characterized: (i) p42/44 MAPKs (ERK1/2 (extracellular signal-regulated kinases)), (ii) p38 MAPKs (α, β, γ, and δ), and (iii) SAPK/JNKs (SAPKα/JNK2, SAPKγ/JNK3, and SAPKβ/JNK1) (Raman *et al.*, 2007). The consecutive activation of three different kinases, namely the MAPK kinase kinase (MAPKKK), the MAPKK and the MAPK is required for the transmission of MAPK signaling (Hagemann *et al.*, 2001). Stimuli from a transmembrane receptor or binding of an activator protein activate the MAPKKK, which then phosphorylates serine and threonine residues of an MAPKK. The activated MAPKK, a threonine-tyrosine kinase, in turn phosphorylates its substrate, the MAPK. MAPKs are serine-threonine kinases that transmit the signal to target proteins on the one hand via phosphorylation of cytoplasmic proteins or by translocation to the nucleus and direct interaction with transcription factors (Hagemann *et al.*, 2001).

It was previously reported that MAPK signaling cascades are activated by various stimuli like growth factors, inflammatory cytokines, oxidative stress,

and DNA damage (Raman *et al.*, 2007). In line with previous findings that both copper-oxidized HDL, as well as native HDL induces phosphorylation of p42/44 and p38 MAPKs in HUVECs (Norata *et al.*, 2004a; Norata *et al.*, 2004b), we were able to show a time- and concentration-dependent phosphorylation of p42/44 and p38 MAPKs in native HDL- and HOCl-HDL-treated EA.hy926 cells (Fig. 3 and 4). Furthermore phosphorylation of p42/44 and p38 MAPKs was not only induced in native HDL- or HOCl-HDL-treated cells but also in cells treated with MPO-HDL (Fig. 6). Previous reports demonstrated that HOCl-HDL is able to bind to SR-BI (Marsche *et al.*, 2002; Marsche *et al.*, 2001) and that this binding might induce phosphorylation of p42/44 MAPK (Grewal *et al.*, 2003). Because of the fast phosphorylation of MAPKs upon HOCl-HDL or native HDL treatment (maximum phosphorylation was observed between 5 and 10 min incubation time) we suggest that binding of modified HDL to SR-BI might be one of the initial events in this activation cascade.

By testing the commonly used MAPK inhibitors PD98059 (p42/44 MAPKK inhibitor) and SB203580 (p38 MAPK inhibitor) we here observed that incubation of cells with SB203580 did not abolish lipoprotein-induced p38 MAPK phosphorylation but even increased the immunoreactive pp42/44 MAPK signal (Fig. 5). This unexpected observation was concordant with previous findings that SB203580 inhibits only the α- and β-isoform but not the γ- or δ-isoform of p38 MAPK (Ryter *et al.*, 2006). Furthermore it was reported that SB203580 has no effect on threonine or tyrosine phosphorylation of p38 MAPK itself but can potently inhibit the activity and downstream signaling of pp38 MAPK (Kumar *et al.*, 1999). In line with our observation other authors (Birkenkamp *et al.*, 2000; Schaefer *et al.*, 2004; Westermarck *et al.*, 2001; Zhang *et al.*, 2001a) previously reported that treatment of cells with SB203580 could lead to a further increase in p42/44 MAPK phosphorylation. Moreover it was shown that pp38α MAPK is able to interact with p42/44 MAPK thereby blocking its phosphorylation and therefore treatment of cells with SB203580 results in a more pronounced p42/44 MAPK phosphorylation (Westermarck *et al.*, 2001; Zhang *et al.*, 2001a).

4.3 Influence of native HDL and HOCl-HDL on Egr-1 and Nrf2 Expression

Nrf2 is one of the best characterized transcription factors regulating HO-1 expression and contributing to the induction of various antioxidant genes in cardiovascular diseases (Nguyen *et al.*, 2003). Leung and colleagues (Leung *et al.*, 2003) demonstrated that Nrf2 deficient mice exhibit diminished mRNA expression of HO-1, elevated ROS accumulation and increased apoptosis. Moreover previous reports showed that treatment of human endothelial cells with HOCl causes induction of HO-1 via Nrf2 activation that antagonizes mitochondrial dysfunction and cell death (Wei *et al.*, 2009). Furthermore, Calay and colleagues (Calay *et al.*, 2010) demonstrated that copper- and MPO-modified LDL induces expression of HO-1 via accumulating ROS and Nrf2 activation in murine macrophages. Contrary to these findings we were not able to observe HOCl-HDL-mediated induction of Nrf2 on mRNA and protein level (Fig. 7, 8 and 11B), nor nuclear translocation of Nrf2 upon HOCl-HDL treatment (Fig. 12). Due to these unexpected findings, we examined the contribution of an alternative transcription factor, Egr-1, in HOCl-HDL-mediated HO-1 expression.

Previous reports demonstrated an involvement of the transcription factor Egr-1 in the pathogenesis of atherosclerosis (Khachigian, 2006). McCaffrey and colleagues (McCaffrey *et al.*, 2000) reported that expression of Egr-1 is elevated in human and mice atherosclerotic lesions. Furthermore it was demonstrated that Egr-1$^{-/-}$/apoE$^{-/-}$ mice exhibit a reduced atherosclerotic lesion size compared to Egr-1$^{+/+}$/apoE$^{-/-}$ littermates, pointing to a pro-atherogenic role for Egr-1 (Harja *et al.*, 2004). Other reports, however, showed that the antioxidant gene HO-1 exhibits an Egr-1 consensus DNA-binding site and that Egr-1 is involved in the regulation of HO-1 expression in fibroblasts from mouse and hamster (Chen *et al.*, 2010; Yang *et al.*, 2001).

It was further demonstrated that native HDL induces Egr-1 mRNA expression in rat vascular smooth muscle cells (Sachinidis *et al.*, 1993) as well as enzymatically modified LDL elevates Egr-1 mRNA expression in human monocytes (Stoyanova *et al.*, 2001). In line with these findings we observed a time-dependent increase in Egr-1 mRNA expression as well as a time- and concentration-dependent induction of Egr-1 protein expression in HOCl-HDL-

treated cells, whereas incubation with native HDL caused only a minor induction of Egr-1 expression (Fig. 7 and 11A). Moreover, treatment of cells with MPO-HDL caused an induction of Egr-1 protein expression comparable to that induced by HOCl-HDL (Fig. 8). Furthermore HOCl-HDL-mediated nuclear translocation of Egr-1 was observed in Western Blot experiments using cytosolic and nuclear protein extracts and was confirmed by immunofluorescence microscopy (Fig. 12 and 13). Immunoreactive Egr-1 signal as well as staining for Egr-1 of native HDL-treated cells was predominantly observable in the cytosol.

Egr-1 transcription was reported to be regulated by various cellular signaling pathways including p42/44 and p38 MAPKs, PI3K and PLC respectively (Day *et al.*, 1999; Guha *et al.*, 2001; Heo *et al.*, 2008; Silverman *et al.*, 1999; Tai *et al.*, 2010). The usage of the well-characterized MAPKK inhibitor (PD98059) revealed that both the HOCl-HDL-mediated Egr-1 expression and the nuclear translocation of Egr-1 are pp42/44 MAPK dependent (Fig. 9, 11A and 14). Treatment of cells with SB203580 along with HOCl-HDL caused a more pronounced increase in Egr-1 mRNA and protein expression (Fig. 9 and 11A) and an elevated nuclear translocation (Fig. 14) compared to HOCl-HDL incubation alone. This finding might be expected due to our previous observations that SB203580 along with HOCl-HDL caused a further increase in p42/44 activation (Fig. 5) and that expression of Egr-1 is p42/44 MAPK dependent. Comparable observations were made by Schaefer and colleagues (Schaefer *et al.*, 2004) who reported that SB203580 enhanced p42/44 MAPK activation and Egr-1 expression. An unexpected observation was that treatment of cells with the PI3K inhibitor LY294002 along with HOCl-HDL caused an induction of Egr-1 mRNA and protein expression as well as an enhanced nuclear translocation of Egr-1 (Fig. 10, 11A and 14). Concordant with our findings Guha and colleagues (Guha *et al.*, 2002) reported that inhibition of the PI3K pathway using LY294002 might enhance p42/44 MAPK activation and Egr-1 mRNA and protein expression.

The functional significance of these results was confirmed by EMSA experiments that demonstrated an increase in the Egr-1 DNA-binding activity in HOCl-HDL-treated cells (Fig. 15), which led suggest that HOCl-HDL-induced Egr-1 protein is able to bind to the promoter region of target genes thereby regulating their transcription.

4.4 Influence of native HDL and HOCl-HDL on HO-1 Expression

The antioxidant protein HO-1 is reported to be expressed in atherosclerotic lesions (Wang *et al.*, 1998) and many observations let suggest a protective role for HO-1 in atherosclerotic lesion development and progression (Cheng *et al.*, 2009; Yet *et al.*, 2003). Furthermore it was reported that various stimuli related to oxidative stress like H_2O_2, oxidized phospholipids, metal ions, copper-oxidized LDL and reagent HOCl might induce HO-1 expression (Loboda *et al.*, 2008; Ryter *et al.*, 2006; Wei *et al.*, 2009).

Previous reports demonstrated that copper-oxidized LDL is able to induce mRNA expression of HO-1 compared to native LDL-treated cells in HUVECs (Agarwal *et al.*, 1996) as well as in human vascular smooth muscle cells (Anwar *et al.*, 2005). In accordance with these findings we observed a time-dependent increase in HOCl-HDL-mediated HO-1 mRNA expression, whereas native HDL did not induce HO-1 expression compared to non-stimulated cells (Fig. 23B). Moreover we were able to demonstrate a time- and concentration-dependent elevation in HO-1 protein expression in native HDL (Fig. 17), as well as in HOCl-HDL-treated cells (Fig. 18). However, treatment of cells with HOCl-HDL caused a much more pronounced increase in HO-1 protein expression compared to native HDL (Fig. 17A and 18A). Furthermore, we observed induction of HO-1 protein expression in MPO-HDL-treated cells (Fig. 19), as well as in cells incubated with HOCl-LDL and HOCl-BSA, respectively (Fig. 20). However, induction of HO-1 protein expression in response to MPO-HDL, HOCl-LDL and HOCl-BSA was less effective compared to HOCl-HDL.

It was previously reported that induction of HO-1 might be regulated via various signaling pathways including PI3K, p42/44 and p38 MAPKs (Anwar *et*

al., 2005; Li *et al.*, 2006). In line with these observations and our findings regarding Egr-1 expression we were able to show that HO-1 expression is p42/44 MAPK dependent (Fig. 21). Incubation of the MAPKK inhibitor PD98059 along with HOCl-HDL did not cause a reduction of immunoreactive HO-1 signal to the level of non-stimulated cells, which might point to the involvement of another signaling pathway. Since incubation of cells with the PI3K inhibitor LY294002 reduced the HOCl-HDL-mediated increase of HO-1 protein expression, PI3K might be involved in the induction of HO-1 in response to HOCl-HDL (Fig. 22). However, further investigations are required to clarify the involvement of PI3K in HO-1 regulation in HOCl-HDL-treated cells.

Although most reports upon HO-1 induction in response to oxidative stress focus on a contribution of the transcription factor Nrf2 (Anwar *et al.*, 2005; Nguyen *et al.*, 2003), some reports demonstrate that Egr-1 might mediate HO-1 induction (Chen *et al.*, 2010; Yang *et al.*, 2001). In line with our previous findings that HOCl-HDL-mediated Egr-1 and HO-1 expression is p42/44 MAPK dependent, silencing of Egr-1, using RNA interference, resulted in a reduced Egr-1 expression as well as nuclear translocation of Egr-1 (Fig. 29) and moreover in a decrease in HO-1 mRNA and protein expression in response to HOCl-HDL (Fig. 26 and 28). These observations let suggest that HOCl-HDL induces HO-1 expression via activation of p42/44 MAPK and transcription factor Egr-1 in EA.hy926 endothelial cells.

4.5 Impact of native HDL and HOCl-HDL on eNOS Expression

Previous reports demonstrated that treatment of endothelial cells with HOCl decreased eNOS activity and reduced eNOS dimer stability (Stocker *et al.*, 2004a). Furthermore, Marsche and colleagues (Marsche *et al.*, 2004) showed that HOCl-modified HDL leads to reduced eNOS mRNA and protein expression and decreased eNOS activity in HUVECs, which might be due to HOCl-HDL-induced translocation of eNOS from the plasma membrane. Moreover it was demonstrated that overexpression of HO-1 results in downregulation of eNOS expression and activity, which suggests a negative

feedback mechanism between HO-1 and eNOS in endothelial cells (Batzlsperger *et al.*, 2007). Comparable observations were made by Heiss and colleagues (Heiss *et al.*, 2009) who reported that downregulation of eNOS in response to HO-1 induction is due to a transient and local heme deficiency. In line with our observations that Egr-1 is involved in the induction of HO-1, Gotoh and colleagues (Gotoh *et al.*, 2011) have shown that Egr-1 represses the transcription of δ-aminolevulinic acid synthase 1, the first and rate limiting enzyme in heme biosynthesis. From these findings one may conclude a possible role of Egr-1 in the regulation of heme bioavailability in response to oxidative stress.

Taurine chloramine, generated within neutrophils by HOCl-mediated chlorination of taurine, has been found to induce HO-1 expression and, simultaneously, to decrease NO production in murine macrophages (Olszanecki *et al.*, 2004; Park *et al.*, 1993). Under inflammatory conditions, an overproduction of NO is likely to occur (Kim *et al.*, 2010), which unfortunately could result in enhanced peroxynitrite formation; thus induction of HO-1 is regarded as a protective feedback mechanism in murine macrophages. Furthermore, Kim and colleagues (Kim *et al.*, 2010) demonstrated that taurine chloramine may also enhance the production of ROS within murine macrophages; this mechanism may lead to activation of transcription factor Nrf2 and to subsequent induction of HO-1. Comparable observations were reported from Calay and colleagues (Calay *et al.*, 2010) who demonstrated that copper- and MPO-modified LDL induced ROS formation in murine macrophages. This group (Calay *et al.*, 2010) revealed that expression of HO-1 occurs via Nrf-2-mediated pathways.

We here demonstrate induction of HO-1 in human endothelial cells via activation of transcription factor Egr-1. Moreover, we observed a more pronounced induction of HO-1 expression in HOCl-HDL- than in HOCl-LDL-treated cells (Fig. 20A). Furthermore we were not able to observe any HOCl-HDL-mediated decrease in protein expression or activity of eNOS (Fig. 31 and 32). However, HOCl-HDL incubation decreased eNOS mRNA expression compared to native HDL in EA.hy926 endothelial cells (Fig. 30). These

unexpected results might be due to a decreased susceptibility of EA.hy926 cells to oxidative stress compared to primary HUVECs.

4.6 Impact of native HDL and HOCl-HDL on Cell Viability and Apoptosis

Vissers and colleagues (Vissers *et al.*, 1999) reported that low concentrations of HOCl induce apoptosis and growth arrest in HUVECs. Furthermore it was demonstrated that HOCl-LDL induces apoptosis in Jurkat T-cell lines (Resch *et al.*, 2011). Marsche and colleagues (Marsche *et al.*, 2004), however, reported that HOCl-HDL did not induce apoptosis or reduced cell viability in HUVECs. In line with these latter findings treatment of EA.hy926 cells with HOCl-HDL did not induce apoptosis or exhibit any detrimental effect on cell proliferation (Fig. 33 and 34).

4.7 Summary

We here demonstrate a novel compensatory pathway of EA.hy926 human endothelial cells to cope with oxidative stress and endothelial dysfunction induced by HOCl-modified HDL.

To better mimic *in vivo* conditions, HOCl-HDL generated not only by the addition of the reagent but also by the action of the MPO-H_2O_2-chloride system was used to assess phosphorylation of MAPKs and expression of Egr-1 and HO-1.

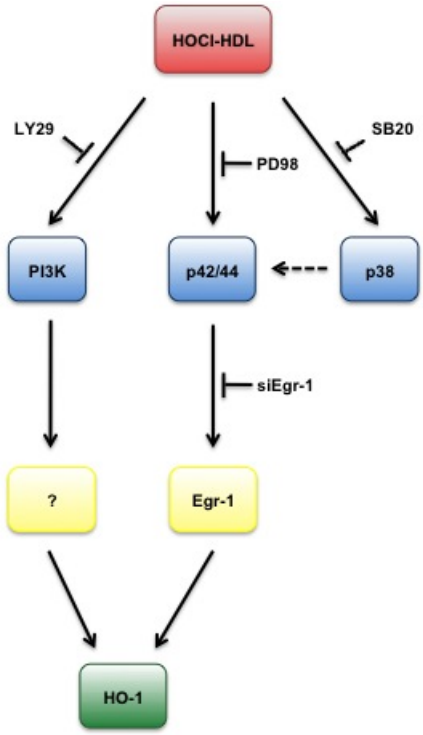

Figure 35: *Proposed scheme of HOCl-HDL-mediated HO-1 induction in EA.hy926 cells.* HOCl-HDL treatment induced phosphorylation of p42/44 and p38 MAPKs and induction of Egr-1 and HO-1 expression. MAPKK inhibitor (PD98059) blocked HOCl-HDL-mediated p42/44 MAPK phosphorylation and induction of Egr-1 and HO-1 expression. Since phosphorylated p38 MAPK could interact with p42/44 MAPK thereby inhibiting p42/44 MAPK phosphorylation, incubation of cells with the p38 MAPK inhibitor (SB203580) further increased p42/44 MAPK activation in response to HOCl-HDL. Silencing of Egr-1 (siEgr-1) resulted in decreased Egr-1 and HO-1 expression in HOCl-HDL stimulated cells. Inhibition of the PI3K pathway using a pharmacological inhibitor (LY294002) decreased HOCl-HDL-induced HO-1 expression.

We were able to demonstrate that HOCl-modified HDL, as well as native HDL induced phosphorylation of p42/44 and p38 MAPKs in a time- and concentration-dependent manner. However, treatment of cells with the p38

MAPK inhibitor (SB203580) along with HOCl-HDL further increased p42/44 phosphorylation and Egr-1 expression by reducing the inhibitory effect of p38α MAPK on p42/44 MAPK phosphorylation.

Furthermore, only treatment of cells with HOCl-HDL increased mRNA and protein expression of transcription factor Egr-1 whereas Nrf2 was not affected upon HOCl-HDL treatment. Moreover HOCl-HDL led to Egr-1 nuclear translocation as well as to an increased Egr-1 DNA-binding activity. Incubation of cells with a well-characterized pharmacological MAPKK inhibitor revealed that HOCl-HDL-mediated expression and nuclear translocation of Egr-1 is p42/44 MAPK dependent. Furthermore, we could show that mRNA and protein expression of HO-1 was induced upon HOCl-HDL-treatment. In line with findings regarding Egr-1 expression, HOCl-HDL-mediated HO-1 expression could be blocked by the MAPKK inhibitor, demonstrating that HO-1 expression is p42/44 MAPK dependent. Furthermore, treatment of cells with the PI3K inhibitor LY294002 along with HOCl-HDL decreased HO-1 protein expression. Silencing of Egr-1 using RNA interference decreased expression and nuclear translocation of Egr-1 as well as HO-1 mRNA and protein expression in response to HOCl-HDL. Furthermore, we here show that HOCl-HDL did not decrease eNOS activity or eNOS protein expression, whereas a slight reduction in HOCl-HDL-mediated eNOS mRNA expression could be observed. Moreover incubation with HOCl-HDL neither induced apoptosis nor caused any anti-proliferative effects.

From our findings one may conclude that HOCl-HDL-mediated induction of HO-1 in human EA.hy926 endothelial cells is dependent on subsequent activation of p42/44 MAPK and transcription factor Egr-1. The observation that inhibition of the PI3K pathway blocks HO-1 expression might indicate an alternative pathway for HOCl-HDL-induced HO-1 expression in endothelial cells. However, further studies are required to elucidate the contribution of PI3K in HOCl-HDL-mediated HO-1 expression.

5. References

Abraham, NG, Kappas, A (2008) Pharmacological and clinical aspects of heme oxygenase. *Pharmacol Rev* **60**(1)**:** 79-127.

Agarwal, A, Balla, J, Balla, G, Croatt, AJ, Vercellotti, GM, Nath, KA (1996) Renal tubular epithelial cells mimic endothelial cells upon exposure to oxidized LDL. *Am J Physiol* **271**(4 Pt 2)**:** F814-823.

Amersi, F, Shen, XD, Anselmo, D, Melinek, J, Iyer, S, Southard, DJ, Katori, M, Volk, HD, Busuttil, RW, Buelow, R, Kupiec-Weglinski, JW (2002) Ex vivo exposure to carbon monoxide prevents hepatic ischemia/reperfusion injury through p38 MAP kinase pathway. *Hepatology* **35**(4)**:** 815-823.

Anwar, AA, Li, FY, Leake, DS, Ishii, T, Mann, GE, Siow, RC (2005) Induction of heme oxygenase 1 by moderately oxidized low-density lipoproteins in human vascular smooth muscle cells: role of mitogen-activated protein kinases and Nrf2. *Free Radic Biol Med* **39**(2)**:** 227-236.

Balla, G, Jacob, HS, Balla, J, Rosenberg, M, Nath, K, Apple, F, Eaton, JW, Vercellotti, GM (1992) Ferritin: a cytoprotective antioxidant strategem of endothelium. *J Biol Chem* **267**(25)**:** 18148-18153.

Baranska, P, Jerczynska, H, Pawlowska, Z, Koziolkiewicz, W, Cierniewski, CS (2005) Expression of integrins and adhesive properties of human endothelial cell line EA.hy 926. *Cancer Genomics & Proteomics* **2**(5)**:** 265-269.

Batzlsperger, CA, Achatz, S, Spreng, J, Riegger, GA, Griese, DP (2007) Evidence for a possible inhibitory interaction between the HO-1/CO- and Akt/NO-pathways in human endothelial cells. *Cardiovasc Drugs Ther* **21**(5)**:** 347-355.

Berg, JM, Tymoczko, JL, Stryer, L (2002) *Biochemistry, 5th edition*. W H Freeman: New York.

Bergt, C, Pennathur, S, Fu, X, Byun, J, O'Brien, K, McDonald, TO, Singh, P, Anantharamaiah, GM, Chait, A, Brunzell, J, Geary, RL, Oram, JF, Heinecke, JW (2004) The myeloperoxidase product hypochlorous acid oxidizes HDL in the human artery wall and impairs ABCA1-dependent cholesterol transport. *Proc Natl Acad Sci U S A* **101**(35)**:** 13032-13037.

Bergt, C, Reicher, H, Malle, E, Sattler, W (1999) Hypochlorite modification of high density lipoprotein: effects on cholesterol efflux from J774 macrophages. *FEBS Lett* **452**(3)**:** 295-300.

Birkenkamp, KU, Tuyt, LM, Lummen, C, Wierenga, AT, Kruijer, W, Vellenga, E (2000) The p38 MAP kinase inhibitor SB203580 enhances nuclear factor-kappa B transcriptional activity by a non-specific effect upon the ERK pathway. *Br J Pharmacol* **131**(1)**:** 99-107.

Blaschke, F, Bruemmer, D, Law, RE (2004) Egr-1 is a major vascular pathogenic transcription factor in atherosclerosis and restenosis. *Rev Endocr Metab Disord* **5**(3)**:** 249-254.

Calay, D, Rousseau, A, Mattart, L, Nuyens, V, Delporte, C, Van Antwerpen, P, Moguilevsky, N, Arnould, T, Boudjeltia, KZ, Raes, M (2010) Copper and myeloperoxidase-modified LDLs activate Nrf2 through different pathways of ROS production in macrophages. *Antioxid Redox Signal* **13**(10)**:** 1491-1502.

Chen, H, Wang, L, Gong, T, Yu, Y, Zhu, C, Li, F, Li, C (2010) EGR-1 regulates Ho-1 expression induced by cigarette smoke. *Biochem Biophys Res Commun* **396**(2)**:** 388-393.

Cheng, C, Noordeloos, AM, Jeney, V, Soares, MP, Moll, F, Pasterkamp, G, Serruys, PW, Duckers, HJ (2009) Heme oxygenase 1 determines atherosclerotic lesion progression into a vulnerable plaque. *Circulation* **119**(23)**:** 3017-3027.

Clark, JE, Foresti, R, Sarathchandra, P, Kaur, H, Green, CJ, Motterlini, R (2000) Heme oxygenase-1-derived bilirubin ameliorates postischemic myocardial dysfunction. *Am J Physiol Heart Circ Physiol* **278**(2)**:** H643-651.

Cui, MZ, Penn, MS, Chisolm, GM (1999) Native and oxidized low density lipoprotein induction of tissue factor gene expression in smooth muscle cells is mediated by both Egr-1 and Sp1. *J Biol Chem* **274**(46)**:** 32795-32802.

Daugherty, A, Dunn, JL, Rateri, DL, Heinecke, JW (1994) Myeloperoxidase, a catalyst for lipoprotein oxidation, is expressed in human atherosclerotic lesions. *J Clin Invest* **94**(1)**:** 437-444.

Davidson, WS, Thompson, TB (2007) The structure of apolipoprotein A-I in high density lipoproteins. *J Biol Chem* **282**(31)**:** 22249-22253.

Day, FL, Rafty, LA, Chesterman, CN, Khachigian, LM (1999) Angiotensin II (ATII)-inducible platelet-derived growth factor A-chain gene expression is p42/44 extracellular signal-regulated kinase-1/2 and Egr-1-dependent and mediated via the ATII type 1 but not type 2 receptor. Induction by ATII antagonized by nitric oxide. *J Biol Chem* **274**(34)**:** 23726-23733.

Dignam, JD, Lebovitz, RM, Roeder, RG (1983) Accurate transcription initiation by RNA polymerase II in a soluble extract from isolated mammalian nuclei. *Nucleic Acids Res* **11**(5)**:** 1475-1489.

Edgell, CJ, McDonald, CC, Graham, JB (1983) Permanent cell line expressing human factor VIII-related antigen established by hybridization. *Proc Natl Acad Sci U S A* **80**(12)**:** 3734-3737.

Eisenstein, RS, Garcia-Mayol, D, Pettingell, W, Munro, HN (1991) Regulation of ferritin and heme oxygenase synthesis in rat fibroblasts by different forms of iron. *Proc Natl Acad Sci U S A* **88**(3)**:** 688-692.

Faour, WH, Alaaeddine, N, Mancini, A, He, QW, Jovanovic, D, Di Battista, JA (2005) Early growth response factor-1 mediates prostaglandin E2-dependent transcriptional suppression of cytokine-induced tumor necrosis factor-alpha gene expression in human macrophages and rheumatoid arthritis-affected synovial fibroblasts. *J Biol Chem* **280**(10)**:** 9536-9546.

Fogelman, AM (2004) When good cholesterol goes bad. *Nat Med* **10**(9)**:** 902-903.

Gerrity, RG (1981) The role of the monocyte in atherogenesis: I. Transition of blood-borne monocytes into foam cells in fatty lesions. *Am J Pathol* **103**(2)**:** 181-190.

Gordon, DJ, Rifkind, BM (1989) High-density lipoprotein--the clinical implications of recent studies. *N Engl J Med* **321**(19)**:** 1311-1316.

Gotoh, S, Nakamura, T, Kataoka, T, Taketani, S (2011) Egr-1 regulates the transcriptional repression of mouse delta-aminolevulinic acid synthase 1 by heme. *Gene* **472**(1-2)**:** 28-36.

Grewal, T, de Diego, I, Kirchhoff, MF, Tebar, F, Heeren, J, Rinninger, F, Enrich, C (2003) High density lipoprotein-induced signaling of the MAPK pathway involves scavenger receptor type BI-mediated activation of Ras. *J Biol Chem* **278**(19)**:** 16478-16481.

Guha, M, Mackman, N (2002) The phosphatidylinositol 3-kinase-Akt pathway limits lipopolysaccharide activation of signaling pathways and expression of inflammatory mediators in human monocytic cells. *J Biol Chem* **277**(35)**:** 32124-32132.

Guha, M, O'Connell, MA, Pawlinski, R, Hollis, A, McGovern, P, Yan, SF, Stern, D, Mackman, N (2001) Lipopolysaccharide activation of the MEK-ERK1/2 pathway in human monocytic cells mediates tissue factor and tumor necrosis factor alpha expression by inducing Elk-1 phosphorylation and Egr-1 expression. *Blood* **98**(5)**:** 1429-1439.

Hagemann, C, Blank, JL (2001) The ups and downs of MEK kinase interactions. *Cell Signal* **13**(12)**:** 863-875.

Harja, E, Bucciarelli, LG, Lu, Y, Stern, DM, Zou, YS, Schmidt, AM, Yan, SF (2004) Early growth response-1 promotes atherogenesis: mice deficient in early growth response-1 and apolipoprotein E display decreased atherosclerosis and vascular inflammation. *Circ Res* **94**(3)**:** 333-339.

Hayashi, S, Omata, Y, Sakamoto, H, Higashimoto, Y, Hara, T, Sagara, Y, Noguchi, M (2004) Characterization of rat heme oxygenase-3 gene. Implication of processed pseudogenes derived from heme oxygenase-2 gene. *Gene* **336**(2)**:** 241-250.

Heiss, EH, Schachner, D, Werner, ER, Dirsch, VM (2009) Active NF-E2-related factor (Nrf2) contributes to keep endothelial NO synthase (eNOS) in the coupled state: the role of reactive oxygen species (ROS)-, eNOS- and heme oxygenase (HO-1) levels. *J Biol Chem*.

Heo, KS, Ryoo, SW, Kim, L, Nam, M, Baek, ST, Lee, H, Lee, AR, Park, SK, Park, Y, Myung, CS, Kim, DU, Hoe, KL (2008) Cl- -channel is essential for LDL-induced cell proliferation via the activation of Erk1/2 and PI3k/Akt and the upregulation of Egr-1 in human aortic smooth muscle cells. *Mol Cells* **26**(5)**:** 468-473.

Ishikawa, K, Sugawara, D, Goto, J, Watanabe, Y, Kawamura, K, Shiomi, M, Itabe, H, Maruyama, Y (2001a) Heme oxygenase-1 inhibits atherogenesis in Watanabe heritable hyperlipidemic rabbits. *Circulation* **104**(15)**:** 1831-1836.

Ishikawa, K, Sugawara, D, Wang, X, Suzuki, K, Itabe, H, Maruyama, Y, Lusis, AJ (2001b) Heme oxygenase-1 inhibits atherosclerotic lesion formation in ldl-receptor knockout mice. *Circ Res* **88**(5)**:** 506-512.

Itoh, K, Chiba, T, Takahashi, S, Ishii, T, Igarashi, K, Katoh, Y, Oyake, T, Hayashi, N, Satoh, K, Hatayama, I, Yamamoto, M, Nabeshima, Y (1997) An Nrf2/small Maf heterodimer mediates the induction of phase II detoxifying enzyme genes through antioxidant response elements. *Biochem Biophys Res Commun* **236**(2)**:** 313-322.

Itoh, K, Wakabayashi, N, Katoh, Y, Ishii, T, Igarashi, K, Engel, JD, Yamamoto, M (1999) Keap1 represses nuclear activation of antioxidant responsive elements by Nrf2 through binding to the amino-terminal Neh2 domain. *Genes Dev* **13**(1)**:** 76-86.

Juan, SH, Lee, TS, Tseng, KW, Liou, JY, Shyue, SK, Wu, KK, Chau, LY (2001) Adenovirus-mediated heme oxygenase-1 gene transfer inhibits the development of atherosclerosis in apolipoprotein E-deficient mice. *Circulation* **104**(13)**:** 1519-1525.

Kajimura, M, Goda, N, Suematsu, M (2002) Organ design for generation and reception of CO: lessons from the liver. *Antioxid Redox Signal* **4**(4)**:** 633-637.

Kaspar, JW, Niture, SK, Jaiswal, AK (2009) Nrf2:INrf2 (Keap1) signaling in oxidative stress. *Free Radic Biol Med* **47**(9)**:** 1304-1309.

Kawamura, K, Ishikawa, K, Wada, Y, Kimura, S, Matsumoto, H, Kohro, T, Itabe, H, Kodama, T, Maruyama, Y (2005) Bilirubin from heme oxygenase-1 attenuates vascular endothelial activation and dysfunction. *Arterioscler Thromb Vasc Biol* **25**(1)**:** 155-160.

Khachigian, LM (2006) Early growth response-1 in cardiovascular pathobiology. *Circ Res* **98**(2)**:** 186-191.

Kim, C, Jang, JS, Cho, MR, Agarawal, SR, Cha, YN (2010) Taurine chloramine induces heme oxygenase-1 expression via Nrf2 activation in murine macrophages. *Int Immunopharmacol* **10**(4)**:** 440-446.

Kirkby, KA, Adin, CA (2006) Products of heme oxygenase and their potential therapeutic applications. *Am J Physiol Renal Physiol* **290**(3)**:** F563-571.

Klebanoff, SJ (2005) Myeloperoxidase: friend and foe. *J Leukoc Biol* **77**(5)**:** 598-625.

Kontush, A, Chapman, MJ (2006) Functionally defective high-density lipoprotein: a new therapeutic target at the crossroads of dyslipidemia, inflammation, and atherosclerosis. *Pharmacol Rev* **58**(3)**:** 342-374.

Kumar, S, Jiang, MS, Adams, JL, Lee, JC (1999) Pyridinylimidazole compound SB 203580 inhibits the activity but not the activation of p38 mitogen-activated protein kinase. *Biochem Biophys Res Commun* **263**(3)**:** 825-831.

Kwak, JY, Takeshige, K, Cheung, BS, Minakami, S (1991) Bilirubin inhibits the activation of superoxide-producing NADPH oxidase in a neutrophil cell-free system. *Biochim Biophys Acta* **1076**(3)**:** 369-373.

Leung, L, Kwong, M, Hou, S, Lee, C, Chan, JY (2003) Deficiency of the Nrf1 and Nrf2 transcription factors results in early embryonic lethality and severe oxidative stress. *J Biol Chem* **278**(48)**:** 48021-48029.

Li, MH, Cha, YN, Surh, YJ (2006) Peroxynitrite induces HO-1 expression via PI3K/Akt-dependent activation of NF-E2-related factor 2 in PC12 cells. *Free Radic Biol Med* **41**(7)**:** 1079-1091.

Libby, P (2002) Inflammation in atherosclerosis. *Nature* **420**(6917)**:** 868-874.

Lim, CP, Jain, N, Cao, X (1998) Stress-induced immediate-early gene, egr-1, involves activation of p38/JNK1. *Oncogene* **16**(22)**:** 2915-2926.

Lin, CC, Chiang, LL, Lin, CH, Shih, CH, Liao, YT, Hsu, MJ, Chen, BC (2007) Transforming growth factor-beta1 stimulates heme oxygenase-1 expression via the PI3K/Akt and NF-kappaB pathways in human lung epithelial cells. *Eur J Pharmacol* **560**(2-3)**:** 101-109.

Linsel-Nitschke, P, Tall, AR (2005) HDL as a target in the treatment of atherosclerotic cardiovascular disease. *Nat Rev Drug Discov* **4**(3)**:** 193-205.

Loboda, A, Jazwa, A, Grochot-Przeczek, A, Rutkowski, AJ, Cisowski, J, Agarwal, A, Jozkowicz, A, Dulak, J (2008) Heme oxygenase-1 and the vascular bed: from molecular mechanisms to therapeutic opportunities. *Antioxid Redox Signal* **10**(10)**:** 1767-1812.

Lowry, OH, Rosebrough, NJ, Farr, AL, Randall, RJ (1951) Protein measurement with the Folin phenol reagent. *J Biol Chem* **193**(1)**:** 265-275.

Lusis, AJ (2000) Atherosclerosis. *Nature* **407**(6801)**:** 233-241.

Malle, E, Hazell, L, Stocker, R, Sattler, W, Esterbauer, H, Waeg, G (1995a) Immunologic detection and measurement of hypochlorite-modified LDL with specific monoclonal antibodies. *Arterioscler Thromb Vasc Biol* **15**(7)**:** 982-989.

Malle, E, Ibovnik, A, Leis, HJ, Kostner, GM, Verhallen, PF, Sattler, W (1995b) Lysine modification of LDL or lipoprotein(a) by 4-hydroxynonenal or malondialdehyde decreases platelet serotonin secretion without affecting platelet aggregability and eicosanoid formation. *Arterioscler Thromb Vasc Biol* **15**(3)**:** 377-384.

Malle, E, Ibovnik, A, Steinmetz, A, Kostner, GM, Sattler, W (1994) Identification of glycoprotein IIb as the lipoprotein(a)-binding protein on platelets. Lipoprotein(a) binding is independent of an arginyl-glycyl-aspartate tripeptide located in apolipoprotein(a). *Arterioscler Thromb* **14**(3)**:** 345-352.

Malle, E, Marsche, G, Panzenboeck, U, Sattler, W (2006) Myeloperoxidase-mediated oxidation of high-density lipoproteins: fingerprints of newly recognized potential proatherogenic lipoproteins. *Arch Biochem Biophys* **445**(2)**:** 245-255.

Malle, E, Waeg, G, Schreiber, R, Grone, EF, Sattler, W, Grone, HJ (2000) Immunohistochemical evidence for the myeloperoxidase/H2O2/halide system in human atherosclerotic lesions: colocalization of myeloperoxidase and hypochlorite-modified proteins. *Eur J Biochem* **267**(14)**:** 4495-4503.

Marquez, LA, Dunford, HB, Van Wart, H (1990) Kinetic studies on the reaction of compound II of myeloperoxidase with ascorbic acid. Role of ascorbic acid in myeloperoxidase function. *J Biol Chem* **265**(10)**:** 5666-5670.

Marsche, G, Furtmuller, PG, Obinger, C, Sattler, W, Malle, E (2008) Hypochlorite-modified high-density lipoprotein acts as a sink for myeloperoxidase in vitro. *Cardiovasc Res* **79**(1)**:** 187-194.

Marsche, G, Hammer, A, Oskolkova, O, Kozarsky, KF, Sattler, W, Malle, E (2002) Hypochlorite-modified high density lipoprotein, a high affinity ligand to scavenger receptor class B, type I, impairs high density lipoprotein-dependent selective lipid uptake and reverse cholesterol transport. *J Biol Chem* **277**(35)**:** 32172-32179.

Marsche, G, Heller, R, Fauler, G, Kovacevic, A, Nuszkowski, A, Graier, W, Sattler, W, Malle, E (2004) 2-chlorohexadecanal derived from hypochlorite-modified high-density lipoprotein-associated plasmalogen is a natural inhibitor of endothelial nitric oxide biosynthesis. *Arterioscler Thromb Vasc Biol* **24**(12)**:** 2302-2306.

Marsche, G, Levak-Frank, S, Quehenberger, O, Heller, R, Sattler, W, Malle, E (2001) Identification of the human analog of SR-BI and LOX-1 as receptors for hypochlorite-modified high density lipoprotein on human umbilical venous endothelial cells. *FASEB J* **15**(6)**:** 1095-1097.

Martin, D, Rojo, AI, Salinas, M, Diaz, R, Gallardo, G, Alam, J, De Galarreta, CM, Cuadrado, A (2004) Regulation of heme oxygenase-1 expression through the phosphatidylinositol 3-kinase/Akt pathway and the Nrf2 transcription factor in response to the antioxidant phytochemical carnosol. *J Biol Chem* **279**(10)**:** 8919-8929.

McCaffrey, TA, Fu, C, Du, B, Eksinar, S, Kent, KC, Bush, H, Jr., Kreiger, K, Rosengart, T, Cybulsky, MI, Silverman, ES, Collins, T (2000) High-level expression of Egr-1 and Egr-1-inducible genes in mouse and human atherosclerosis. *J Clin Invest* **105**(5)**:** 653-662.

McCoubrey, WK, Jr., Huang, TJ, Maines, MD (1997) Isolation and characterization of a cDNA from the rat brain that encodes hemoprotein heme oxygenase-3. *Eur J Biochem* **247**(2)**:** 725-732.

Moi, P, Chan, K, Asunis, I, Cao, A, Kan, YW (1994) Isolation of NF-E2-related factor 2 (Nrf2), a NF-E2-like basic leucine zipper transcriptional activator that binds to the tandem NF-E2/AP1 repeat of the beta-globin locus control region. *Proc Natl Acad Sci U S A* **91**(21)**:** 9926-9930.

Morita, T (2005) Heme oxygenase and atherosclerosis. *Arterioscler Thromb Vasc Biol* **25**(9)**:** 1786-1795.

Morsi, WG, Shaker, OG, Ismail, EF, Ahmed, HH, El-Serafi, TI, Maklady, FA, Abdel-Aziz, MT, El-Asmar, MF, Atta, HM (2006) HO-1 and VGEF gene expression in human arteries with advanced atherosclerosis. *Clin Biochem* **39**(11)**:** 1057-1062.

Muller, RM, Taguchi, H, Shibahara, S (1987) Nucleotide sequence and organization of the rat heme oxygenase gene. *J Biol Chem* **262**(14)**:** 6795-6802.

Nakayama, M, Takahashi, K, Komaru, T, Fukuchi, M, Shioiri, H, Sato, K, Kitamuro, T, Shirato, K, Yamaguchi, T, Suematsu, M, Shibahara, S (2001) Increased expression of heme oxygenase-1 and bilirubin accumulation in foam cells of rabbit atherosclerotic lesions. *Arterioscler Thromb Vasc Biol* **21**(8)**:** 1373-1377.

Navab, M, Fogelman, AM, Berliner, JA, Territo, MC, Demer, LL, Frank, JS, Watson, AD, Edwards, PA, Lusis, AJ (1995) Pathogenesis of atherosclerosis. *Am J Cardiol* **76**(9)**:** 18C-23C.

Nguyen, T, Sherratt, PJ, Pickett, CB (2003) Regulatory mechanisms controlling gene expression mediated by the antioxidant response element. *Annu Rev Pharmacol Toxicol* **43:** 233-260.

Nicholls, SJ, Zheng, L, Hazen, SL (2005) Formation of dysfunctional high-density lipoprotein by myeloperoxidase. *Trends Cardiovasc Med* **15**(6)**:** 212-219.

Norata, GD, Banfi, C, Pirillo, A, Tremoli, E, Hamsten, A, Catapano, AL, Eriksson, P (2004a) Oxidised-HDL3 induces the expression of PAI-1 in human endothelial cells. Role of p38MAPK activation and mRNA stabilization. *Br J Haematol* **127**(1)**:** 97-104.

Norata, GD, Callegari, E, Inoue, H, Catapano, AL (2004b) HDL3 induces cyclooxygenase-2 expression and prostacyclin release in human endothelial cells via a p38 MAPK/CRE-dependent pathway: effects on COX-2/PGI-synthase coupling. *Arterioscler Thromb Vasc Biol* **24**(5)**:** 871-877.

Nuszkowski, A, Grabner, R, Marsche, G, Unbehaun, A, Malle, E, Heller, R (2001) Hypochlorite-modified low density lipoprotein inhibits nitric oxide synthesis in endothelial cells via an intracellular dislocalization of endothelial nitric-oxide synthase. *J Biol Chem* **276**(17)**:** 14212-14221.

Ollinger, R, Bilban, M, Erat, A, Froio, A, McDaid, J, Tyagi, S, Csizmadia, E, Graca-Souza, AV, Liloia, A, Soares, MP, Otterbein, LE, Usheva, A, Yamashita, K, Bach, FH (2005) Bilirubin: a natural inhibitor of vascular smooth muscle cell proliferation. *Circulation* **112**(7)**:** 1030-1039.

Ollinger, R, Yamashita, K, Bilban, M, Erat, A, Kogler, P, Thomas, M, Csizmadia, E, Usheva, A, Margreiter, R, Bach, FH (2007) Bilirubin and biliverdin treatment of atherosclerotic diseases. *Cell Cycle* **6**(1)**:** 39-43.

Olszanecki, R, Marcinkiewicz, J (2004) Taurine chloramine and taurine bromamine induce heme oxygenase-1 in resting and LPS-stimulated J774.2 macrophages. *Amino Acids* **27**(1)**:** 29-35.

Orozco, LD, Kapturczak, MH, Barajas, B, Wang, X, Weinstein, MM, Wong, J, Deshane, J, Bolisetty, S, Shaposhnik, Z, Shih, DM, Agarwal, A, Lusis, AJ, Araujo, JA (2007) Heme oxygenase-1 expression in macrophages plays a beneficial role in atherosclerosis. *Circ Res* **100**(12)**:** 1703-1711.

Otterbein, LE, Otterbein, SL, Ifedigbo, E, Liu, F, Morse, DE, Fearns, C, Ulevitch, RJ, Knickelbein, R, Flavell, RA, Choi, AM (2003) MKK3 mitogen-activated protein kinase pathway mediates carbon monoxide-induced protection against oxidant-induced lung injury. *Am J Pathol* **163**(6)**:** 2555-2563.

Panzenboeck, U, Raitmayer, S, Reicher, H, Lindner, H, Glatter, O, Malle, E, Sattler, W (1997) Effects of reagent and enzymatically generated hypochlorite on physicochemical and metabolic properties of high density lipoproteins. *J Biol Chem* **272**(47)**:** 29711-29720.

Park, E, Quinn, MR, Wright, CE, Schuller-Levis, G (1993) Taurine chloramine inhibits the synthesis of nitric oxide and the release of tumor necrosis factor in activated RAW 264.7 cells. *J Leukoc Biol* **54**(2)**:** 119-124.

Ponka, P, Beaumont, C, Richardson, DR (1998) Function and regulation of transferrin and ferritin. *Semin Hematol* **35**(1)**:** 35-54.

Raman, M, Chen, W, Cobb, MH (2007) Differential regulation and properties of MAPKs. *Oncogene* **26**(22)**:** 3100-3112.

Resch, U, Semlitsch, M, Hammer, A, Susani-Etzerodt, H, Walczak, H, Sattler, W, Malle, E (2011) Hypochlorite-modified low-density lipoprotein induces the apoptotic machinery in Jurkat T-cell lines. *Biochem Biophys Res Commun* **410**(4)**:** 895-900.

Rothblat, GH, Phillips, MC (2010) High-density lipoprotein heterogeneity and function in reverse cholesterol transport. *Curr Opin Lipidol* **21**(3)**:** 229-238.

Ryter, SW, Alam, J, Choi, AM (2006) Heme oxygenase-1/carbon monoxide: from basic science to therapeutic applications. *Physiol Rev* **86**(2)**:** 583-650.

Ryter, SW, Otterbein, LE (2004) Carbon monoxide in biology and medicine. *Bioessays* **26**(3)**:** 270-280.

Sachinidis, A, Ko, Y, Wieczorek, A, Weisser, B, Locher, R, Vetter, W, Vetter, H (1993) Lipoproteins induce expression of the early growth response gene-1 in vascular smooth muscle cells from rat. *Biochem Biophys Res Commun* **192**(2)**:** 794-799.

Schaefer, A, Kosa, F, Bittorf, T, Magocsi, M, Rosche, A, Ramirez-Chavez, Y, Marotzki, S, Marquardt, H (2004) Opposite effects of inhibitors of mitogen-activated protein kinase pathways on the egr-1 and beta-globin expression in erythropoietin-responsive murine erythroleukemia cells. *Cell Signal* **16**(2)**:** 223-234.

Schmidt, K, Rehn, M, Stessel, H, Wolkart, G, Mayer, B (2010) Evidence against tetrahydrobiopterin depletion of vascular tissue exposed to nitric oxide/superoxide or nitroglycerin. *Free Radic Biol Med* **48**(1)**:** 145-152.

Schmidt, K, Werner-felmayer, G, Mayer, B, Werner, ER (1999) Preferential inhibition of inducible nitric oxide synthase in intact cells by the 4-amino analogue of tetrahydrobiopterin. *Eur J Biochem* **259**(1-2)**:** 25-31.

Shibahara, S, Sato, M, Muller, RM, Yoshida, T (1989) Structural organization of the human heme oxygenase gene and the function of its promoter. *Eur J Biochem* **179**(3)**:** 557-563.

Silverman, ES, Collins, T (1999) Pathways of Egr-1-mediated gene transcription in vascular biology. *Am J Pathol* **154**(3)**:** 665-670.

Solan, NJ, Miyoshi, H, Carmona, EM, Bren, GD, Paya, CV (2002) RelB cellular regulation and transcriptional activity are regulated by p100. *J Biol Chem* **277**(2)**:** 1405-1418.

Spagnoli, LG, Bonanno, E, Sangiorgi, G, Mauriello, A (2007) Role of inflammation in atherosclerosis. *J Nucl Med* **48**(11)**:** 1800-1815.

Stary, HC, Chandler, AB, Dinsmore, RE, Fuster, V, Glagov, S, Insull, W, Jr., Rosenfeld, ME, Schwartz, CJ, Wagner, WD, Wissler, RW (1995) A definition of advanced types of atherosclerotic lesions and a histological classification of atherosclerosis. A report from the Committee on Vascular Lesions of the Council on Arteriosclerosis, American Heart Association. *Circulation* **92**(5)**:** 1355-1374.

Steinberg, D, Parthasarathy, S, Carew, TE, Khoo, JC, Witztum, JL (1989) Beyond cholesterol. Modifications of low-density lipoprotein that increase its atherogenicity. *N Engl J Med* **320**(14)**:** 915-924.

Stocker, R, Huang, A, Jeranian, E, Hou, JY, Wu, TT, Thomas, SR, Keaney, JF, Jr. (2004a) Hypochlorous acid impairs endothelium-derived nitric oxide bioactivity through a superoxide-dependent mechanism. *Arterioscler Thromb Vasc Biol* **24**(11)**:** 2028-2033.

Stocker, R, Keaney, JF, Jr. (2004b) Role of oxidative modifications in atherosclerosis. *Physiol Rev* **84**(4)**:** 1381-1478.

Stocker, R, Yamamoto, Y, McDonagh, AF, Glazer, AN, Ames, BN (1987) Bilirubin is an antioxidant of possible physiological importance. *Science* **235**(4792)**:** 1043-1046.

Stoyanova, E, Tesch, A, Armstrong, VW, Wieland, E (2001) Enzymatically degraded low density lipoproteins are more potent inducers of egr-1 mRNA than oxidized or native low density lipoproteins. *Clin Biochem* **34**(6)**:** 483-490.

Tai, TC, Wong-Faull, DC, Claycomb, R, Wong, DL (2010) Hypoxia and adrenergic function: molecular mechanisms related to Egr-1 and Sp1 activation. *Brain Res* **1353:** 14-27.

Tenhunen, R, Marver, HS, Schmid, R (1969) Microsomal heme oxygenase. Characterization of the enzyme. *J Biol Chem* **244**(23)**:** 6388-6394.

Tenhunen, R, Marver, HS, Schmid, R (1968) The enzymatic conversion of heme to bilirubin by microsomal heme oxygenase. *Proc Natl Acad Sci U S A* **61**(2)**:** 748-755.

Thukkani, AK, McHowat, J, Hsu, FF, Brennan, ML, Hazen, SL, Ford, DA (2003) Identification of alpha-chloro fatty aldehydes and unsaturated lysophosphatidylcholine molecular species in human atherosclerotic lesions. *Circulation* **108**(25)**:** 3128-3133.

Toborek, M, Kaiser, S (1999) Endothelial cell functions. Relationship to atherogenesis. *Basic Res Cardiol* **94**(5)**:** 295-314.

Venugopal, R, Jaiswal, AK (1998) Nrf2 and Nrf1 in association with Jun proteins regulate antioxidant response element-mediated expression and coordinated induction of genes encoding detoxifying enzymes. *Oncogene* **17**(24)**:** 3145-3156.

Vissers, MC, Pullar, JM, Hampton, MB (1999) Hypochlorous acid causes caspase activation and apoptosis or growth arrest in human endothelial cells. *Biochem J* **344** (2)**:** 443-449.

von Eckardstein, A, Nofer, JR, Assmann, G (2001) High density lipoproteins and arteriosclerosis. Role of cholesterol efflux and reverse cholesterol transport. *Arterioscler Thromb Vasc Biol* **21**(1)**:** 13-27.

Wang, LJ, Lee, TS, Lee, FY, Pai, RC, Chau, LY (1998) Expression of heme oxygenase-1 in atherosclerotic lesions. *Am J Pathol* **152**(3)**:** 711-720.

Wei, Y, Liu, XM, Peyton, KJ, Wang, H, Johnson, FK, Johnson, RA, Durante, W (2009) Hypochlorous acid-induced heme oxygenase-1 gene expression promotes human endothelial cell survival. *Am J Physiol Cell Physiol* **297**(4)**:** C907-915.

Westermarck, J, Li, SP, Kallunki, T, Han, J, Kahari, VM (2001) p38 mitogen-activated protein kinase-dependent activation of protein phosphatases 1 and 2A inhibits MEK1 and MEK2 activity and collagenase 1 (MMP-1) gene expression. *Mol Cell Biol* **21**(7)**:** 2373-2383.

Winterbourn, CC, Kettle, AJ (2000) Biomarkers of myeloperoxidase-derived hypochlorous acid. *Free Radic Biol Med* **29**(5)**:** 403-409.

Yachie, A, Niida, Y, Wada, T, Igarashi, N, Kaneda, H, Toma, T, Ohta, K, Kasahara, Y, Koizumi, S (1999) Oxidative stress causes enhanced endothelial cell injury in human heme oxygenase-1 deficiency. *J Clin Invest* **103**(1)**:** 129-135.

Yang, G, Nguyen, X, Ou, J, Rekulapelli, P, Stevenson, DK, Dennery, PA (2001) Unique effects of zinc protoporphyrin on HO-1 induction and apoptosis. *Blood* **97**(5)**:** 1306-1313.

Yet, SF, Layne, MD, Liu, X, Chen, YH, Ith, B, Sibinga, NE, Perrella, MA (2003) Absence of heme oxygenase-1 exacerbates atherosclerotic lesion formation and vascular remodeling. *FASEB J* **17**(12)**:** 1759-1761.

Yokoyama, S (2006) Assembly of high-density lipoprotein. *Arterioscler Thromb Vasc Biol* **26**(1)**:** 20-27.

Yoshida, T, Biro, P, Cohen, T, Muller, RM, Shibahara, S (1988) Human heme oxygenase cDNA and induction of its mRNA by hemin. *Eur J Biochem* **171**(3)**:** 457-461.

Zannis, VI, Chroni, A, Krieger, M (2006) Role of apoA-I, ABCA1, LCAT, and SR-BI in the biogenesis of HDL. *J Mol Med* **84**(4)**:** 276-294.

Zhang, H, Shi, X, Hampong, M, Blanis, L, Pelech, S (2001a) Stress-induced inhibition of ERK1 and ERK2 by direct interaction with p38 MAP kinase. *J Biol Chem* **276**(10)**:** 6905-6908.

Zhang, P, Tchou-Wong, KM, Costa, M (2007) Egr-1 mediates hypoxia-inducible transcription of the NDRG1 gene through an overlapping Egr-1/Sp1 binding site in the promoter. *Cancer Res* **67**(19)**:** 9125-9133.

Zhang, R, Brennan, ML, Fu, X, Aviles, RJ, Pearce, GL, Penn, MS, Topol, EJ, Sprecher, DL, Hazen, SL (2001b) Association between myeloperoxidase levels and risk of coronary artery disease. *JAMA* **286**(17)**:** 2136-2142.

Zhang, X, Shan, P, Otterbein, LE, Alam, J, Flavell, RA, Davis, RJ, Choi, AM, Lee, PJ (2003) Carbon monoxide inhibition of apoptosis during ischemia-reperfusion lung injury is dependent on the p38 mitogen-activated protein kinase pathway and involves caspase 3. *J Biol Chem* **278**(2)**:** 1248-1258.

Zheng, L, Nukuna, B, Brennan, ML, Sun, M, Goormastic, M, Settle, M, Schmitt, D, Fu, X, Thomson, L, Fox, PL, Ischiropoulos, H, Smith, JD, Kinter, M, Hazen, SL (2004) Apolipoprotein A-I is a selective target for myeloperoxidase-catalyzed oxidation and functional impairment in subjects with cardiovascular disease. *J Clin Invest* **114**(4)**:** 529-541.

6. Supplement

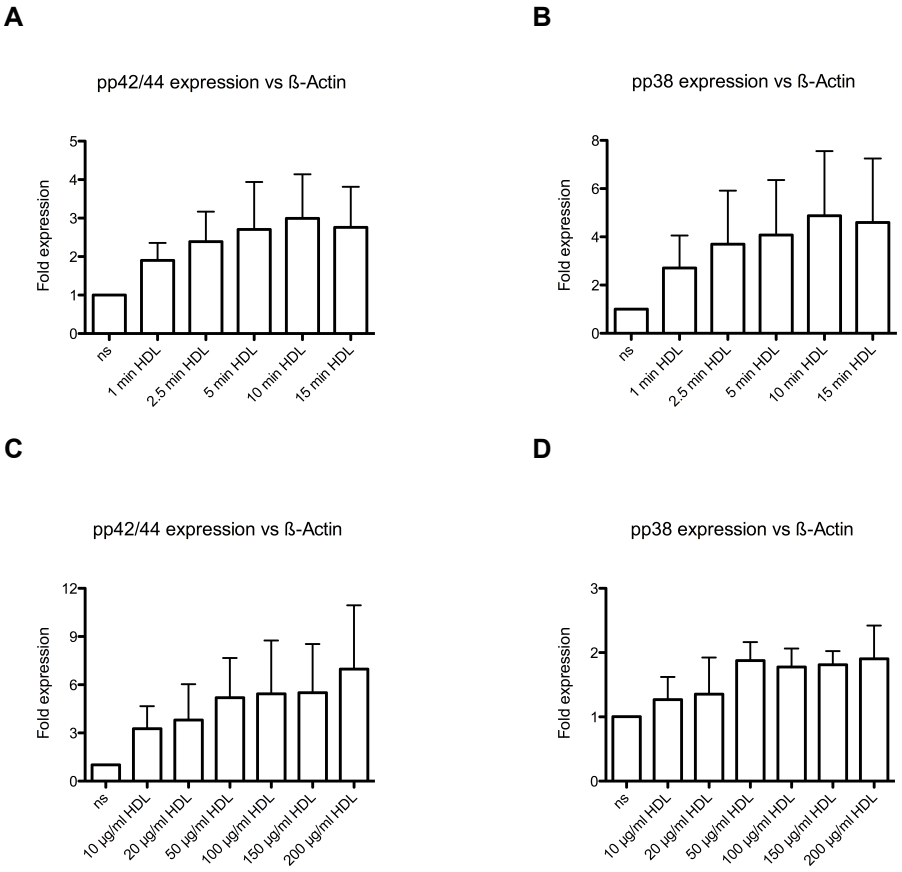

Supplement Figure I: *Densitometric evaluation of Figure 3: Western blot analysis of HDL-induced MAPK activation in EA.hy926 cells.* **A-B** Cells were incubated with 100 µg/ml HDL for indicated times (1-15 min). **C-D** Cells were incubated with indicated concentrations of HDL (10–200 µg/ml) for 5 min. **A-D** Western blot analysis was performed for pp42/44 (**A, C**) and pp38 (**B, D**) MAPKs. β-Actin was used as a loading control. Lane 1 represents non-stimulated cells (ns). Results were obtained from 3 independent experiments and are expressed as means ± SD.

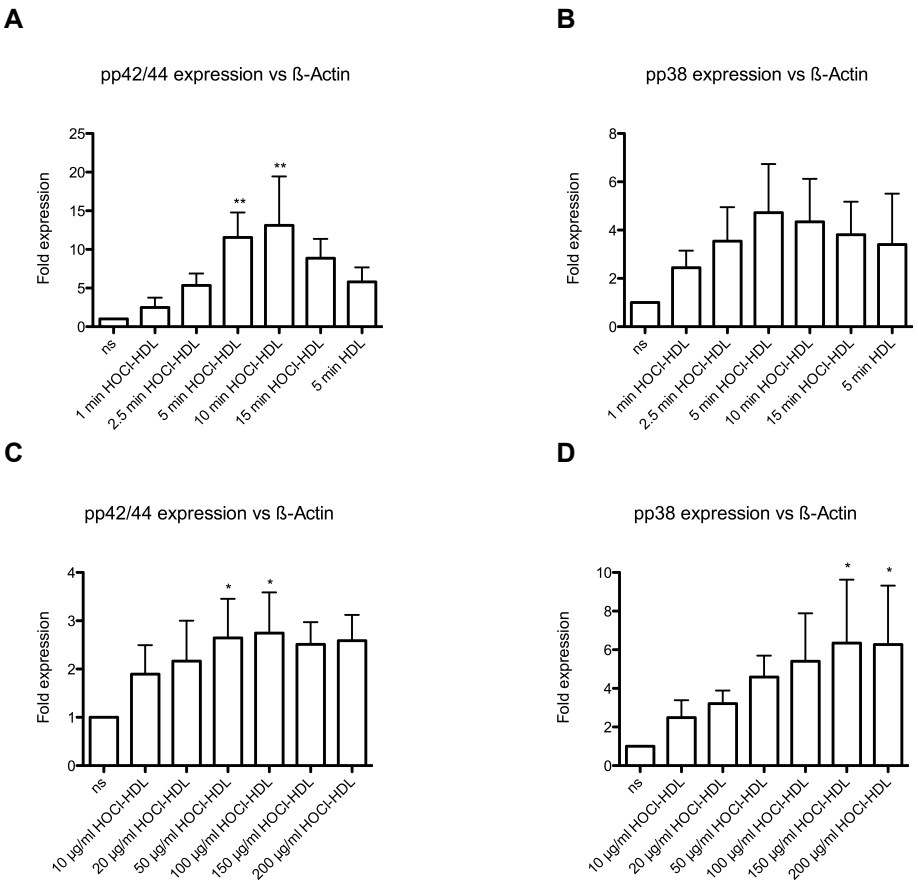

Supplement Figure II: *Densitometric evaluation of Figure 4: Western blot analysis of HOCl-HDL-induced MAPK activation in EA.hy926 cells.* **A-B** Cells were incubated with 100 µg/ml HOCl-HDL or HDL for indicated time points (1-15 min). **C-D** Cells were incubated with indicated concentrations of HOCl-HDL (10–200 µg/ml) for 5 min. **A-D** Western blot analysis was performed for pp42/44 (**A, C**) and pp38 MAPKs (**B, D**). β-Actin was used as a loading control. Lane 1 represents non-stimulated cells (ns). Results were obtained from 3 independent experiments and are expressed as means ± SD. (* $p<0.05$, ** $p<0.01$ versus non-stimulated cells).

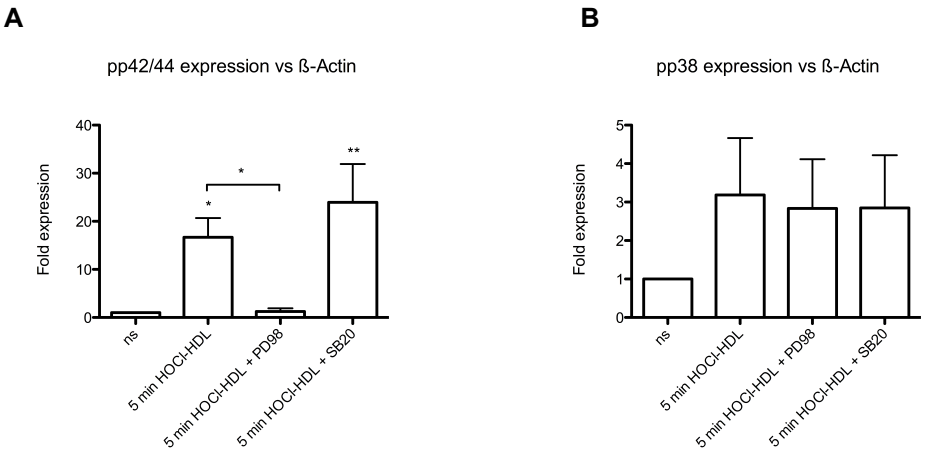

Supplement Figure III: *Densitometric evaluation of Figure 5: Western blot analysis of HOCl-HDL-induced MAPK activation in EA.hy926 cells in the absence or presence of MAPK inhibitors.* **A-B** Cells were incubated for 30 min with 25 µM PD98059 or 10 µM SB203580 prior to stimulation with 100 µg/ml HOCl-HDL for 5 min. Western blot analysis was performed for pp42/44 (**A**) and pp38 MAPKs (**B**). β-Actin was used as a loading control. Lane 1 represents non-stimulated cells (ns). Results were obtained from 3 independent experiments and are expressed as means ± SD. (* $p<0.05$, ** $p<0.01$ versus non-stimulated cells).

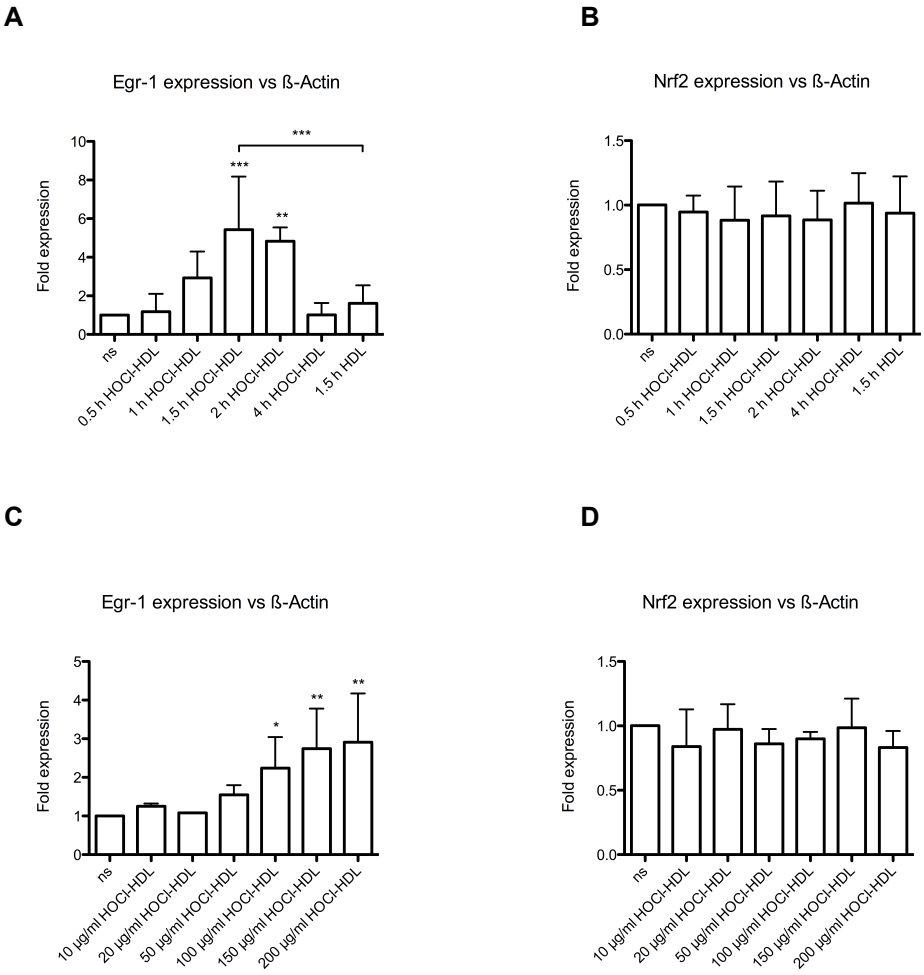

Supplement Figure IV: *Densitometric evaluation of Figure 7: Western blot analysis of HOCl-HDL-induced Egr-1 and Nrf2 expression in EA.hy926 cells.* **A-B** Cells were incubated with 100 µg/ml HOCl-HDL or HDL for indicated time points (0.5-4 h). **C-D** Cells were incubated with indicated concentrations of HOCl-HDL (10–200 µg/ml) for 1.5 h. **A-D** Western blot analysis was performed for Egr-1 (**A, C**) and Nrf2 (**B, D**). β-Actin was used as a loading control. Lane 1 represents non-stimulated cells (ns). Results were obtained from 3 independent experiments and are expressed as means ± SD. (* $p<0.05$, ** $p<0.01$, *** $p<0.001$ versus non-stimulated cells).

7. Publication

Rossmann C, Rauh A, Hammer A, Windischhofer W, Zirkl S, Sattler W, Malle E.
Hypochlorite-modified high-density lipoprotein promotes induction of HO-1 in endothelial cells via activation of p42/44 MAPK and zinc finger transcription factor Egr-1.
Arch Biochem Biophys. 2011 May 1;509(1):16-25.